

PDF hosted at the Radboud Repository of the Radboud University Nijmegen

The following full text is a publisher's version.

For additional information about this publication click this link.

<http://hdl.handle.net/2066/19594>

Please be advised that this information was generated on 2017-12-05 and may be subject to change.

**Rhodopsin mechanism probed by
cysteine scanning mutagenesis in
combination with FT-IR difference
spectroscopy**

Githa Breikers

**Rhodopsin mechanism probed by cysteine scanning
mutagenesis in combination with FT-IR difference
spectroscopy**

een wetenschappelijke proeve op het gebied van de Medische
Wetenschappen

Proefschrift

ter verkrijging van de graad van doctor
aan de Radboud Universiteit Nijmegen
op gezag van de Rector Magnificus prof. dr. C.W.P.M. Blom,
volgens besluit van het College van Decanen
in het openbaar te verdedigen op donderdag 24 februari 2005
des namiddags om 1.30 uur precies

door

Githa Breikers

geboren op 9 november 1972
te Geleen

Promotor:

Prof. dr. W.J. de Grip

Co-promotor:

Dr. G.J.C.G.M. Bosman

Manuscriptcommissie:

Prof. dr. F. Russell

Prof. dr. W.W. de Jong

Prof. dr. J. Lugtenburg (Universiteit Leiden)

Cover design: Ellie Breikers

ISBN 90-9018964-5

Printed by Datawyse, Maastricht

The work presented in this thesis was financially supported by the Council of Chemical Sciences of the Netherlands Organization for Scientific Research (CW-NWO: CW-05309 to W.J.DG)

Contents

Chapter 1: General introduction	7
1.1 Vision: rods and cones	8
1.2 Structure and function of rhodopsin	9
1.2.1 General features of rhodopsin	9
1.2.2 Crystal structure of rhodopsin	11
1.2.3 Photocascade	12
1.2.4 Phototransduction	14
1.3 Cysteine scanning mutagenesis	17
1.3.1 Site-directed spin labeling	17
1.3.2 Site-directed chemical labeling	18
1.3.3 FT-IR difference spectroscopy	19
1.4 Aim and outline of this thesis	20
Chapter 2: A structural role for Asp83 in the photoactivation of rhodopsin	27
2.1 Introduction	28
2.2 Materials and methods	30
2.2.1 Cloning and expression of rhodopsin mutants	30
2.2.2 Analysis of recombinant rhodopsins	30
2.3 Results and discussion	30
2.3.1 Expression and spectral properties of D83 mutants	30
2.3.2 Meta I \leftrightarrow Meta II equilibrium	32
2.3.3 G-protein activation	33
2.3.4 Structural studies using FT-IR difference spectroscopy	33
2.3.5 Conclusions	36
Chapter 3: Development of a base-mutant for cysteine scanning mutagenesis in rhodopsin	41
3.1 Introduction	42
3.2 Materials and methods	43
3.2.1 Cloning and expression	43
3.2.2 Analysis of recombinant rhodopsins	47
3.3 Results	48
3.4 Discussion	51
3.4.1 Novel application of cysteine scanning mutagenesis: combination with FT-IR difference spectroscopy	51
3.4.2 Base-mutant	52
Chapter 4: Cysteine scanning mutagenesis in rhodopsin on a cysteine-free background	57
4.1 Introduction	58
4.2 Materials and methods	59
4.2.1 Cloning and expression	59
4.2.2 Analysis of recombinant rhodopsins	62
4.3 Results	64
4.3.1 Protein production	64

4.3.2	Purification and reconstitution	66
4.3.3	Functional analysis	67
4.4	Discussion	69
4.4.1	Expression of single TM II cysteine mutants	69
4.4.2	Functional properties of single TM II cysteine mutants	70

Chapter 5: Cysteine scanning mutagenesis in rhodopsin on a wild type background **77**

5.1	Introduction	78
5.2	Materials and methods	79
5.2.1	Cloning and expression	79
5.2.2	Analysis of recombinant rhodopsins	80
5.3	Results	80
5.3.1	Protein production	80
5.3.2	Purification and reconstitution	82
5.3.3	Functional analysis	83
5.4	Discussion	87
5.4.1	Expression and purification of single TM II cysteine mutants	87
5.4.2	Functional properties of single TM II cysteine mutants	87

Chapter 6: Retinitis pigmentosa associated rhodopsin mutations in three membrane-located cysteine residues present three different biochemical phenotypes **93**

6.1	Introduction	94
6.2	Materials and methods	96
6.2.1	Cloning and expression of rhodopsin mutants	96
6.2.2	Analysis of recombinant rhodopsins	96
6.3	Results and discussion	96
6.3.1	C222R	97
6.3.2	C167R	99
6.3.3	C264del	100
6.3.4	Conclusions	101

Chapter 7: Summary and general discussion **105**

Samenvatting **115**

List of abbreviations **121**

Dankwoord **123**

Publications **124**

Curriculum vitae **125**



Chapter 1

General introduction

1.1 Vision: rods and cones

Vision is mediated by the eye and is one of the five sense perceptions that evolved to receive and respond to environmental signals. The vertebrate eye primarily consists of the cornea, sclera, lens, retinal pigment epithelium and retina (Fig.1). Although all parts of the eye are important for generating a good image, the most vital layer for vision is the retina. The retina lines the posterior of the eye and contains the photoreceptors, which are highly specialized neuronal cells. There are two types of photoreceptors, rods and cones. They differ both in physiology and in morphology [1]. Rods mediate dim light or scotopic vision. Their detection threshold is about three orders of magnitude lower than that of cones, while cones have more rapid photoresponses and adaptation kinetics [2,3]. All rods in the retina have the same spectral sensitivity and the rod system therefore reports only in “grey levels”, so called "black and white" or scotopic vision. In contrast, three types of cones are present in the retina; blue, green and red light-sensitive cones, the spectral sensitivity of which lies at respectively 425 nm, 530 nm and 560 nm [4-6]. The cone system therefore allows wavelength discrimination (so called colour or photopic vision).

The spectral sensitivity is based on the presence of distinctive visual pigments in the retina, one rod pigment (rhodopsin) and three cone pigments. The cone pigments evolved long before the rod pigment [7-9]. The ancient photoreceptor thus probably was some type of cone from which the rods evolved. The photoreceptor cells consist of three cellular substructures: the outer segment, the inner segment and a synaptic region (Fig. 2). The inner and outer segment are connected by a cilium. The gross anatomy of rods and cones is very similar except for the outer segment (Fig. 2). Rod outer segments have intracellular disks. These are flattened membranes which contain the photoreceptor protein rhodopsin. Cones have so called sacs, infoldings of the plasma membrane, instead of disks. The rationale for this difference is not yet understood [10]. The disks and sacs are tightly packed and a parallel array serves to align for optimal absorption of light. New disks/sacs are inserted from the ciliary region during the outer segment renewal process [11], in which old disks/sacs are daily removed from the tip of the outer

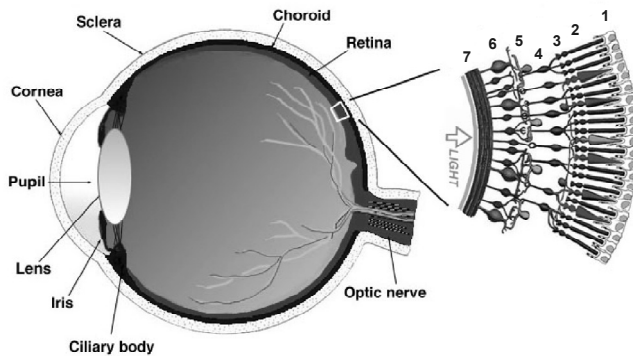


Fig. 1: The vertebrate eye. Schematic presentation of the eye. The inset shows a detailed view of the retina. 1: pigment epithelium, 2: rod and cones outer and inner segment, 3: rod and cone nuclei, 4: bipolar cells and horizontal cells, 5: amacrine cells, 6: ganglion cells, 7: ganglion axons; optic nerve. Adapted from: Webvision (<http://retina.umh.es/webvision>).

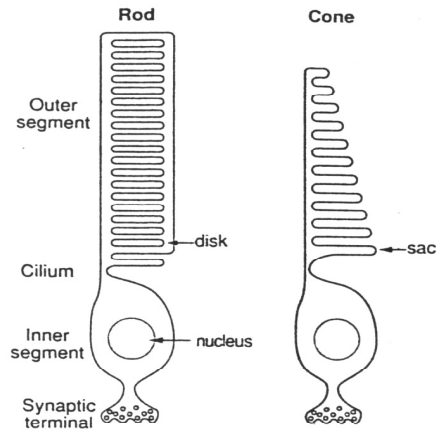


Fig. 2: The photoreceptor cells. Schematic presentation of a rod and a cone from the vertebrate retina. The outer segment is specialized for visual transduction. Cone photopigment molecules are located on infoldings of the plasma membrane, called sacs, rather than in the membrane of intracellular discs as in rods. From: Zimmerman (1995) [10].

segment through phagocytosis by the pigment epithelial cells. The inner segment contains the nucleus, mitochondria and other intracellular organelles that are involved in cellular homeostasis. In the synaptic region, neurotransmitter release is modulated for transduction of the signal to second-order retinal neurons (bipolar cells) and eventually via the optic nerve to the brain.

1.2 Structure and function of rhodopsin

1.2.1 General features of rhodopsin

Rhodopsin is a membrane-spanning protein containing seven transmembrane (TM) segments that belongs to the family of G protein-coupled receptors (GPCRs; Fig. 3). Rhodopsin is a special GPCR in that it consists of a protein, opsin and a covalently bound ligand, 11-*cis* retinal, that is responsible for the spectral properties of the pigment. Because 11-*cis* retinal is present in situ, photoactivation can occur very rapidly. 11-*Cis* retinal is bound to lysine 296 of opsin via a protonated Schiff base linkage. The counterion stabilizing the protonated Schiff base is provided by Glu113, which is highly conserved among all known vertebrate visual pigments [12-14]. Upon photoactivation, the retinal ligand isomerizes to the all-*trans* form and drives the protein through a series of transient photointermediates (Rhodopsin \rightarrow Bathorhodopsin (Batho) \leftrightarrow Blue-shifted intermediate (BSI) \rightarrow Lumirhodopsin (Lumi) \rightarrow Metarhodopsin I (Meta I) \leftrightarrow Metarhodopsin II (Meta II) \rightarrow Metarhodopsin III (Meta III)) that within milliseconds leads to the generation of the active state (Meta II), which binds and activates the G protein transducin (G_T ; Fig. 4) [15].

Rhodopsin is synthesized on membrane-associated ribosomes and cotranslationally inserted into the endoplasmic reticulum (E.R.) membrane in the inner segment of the photoreceptor. Rhodopsin requires posttranslational modification (thiopalmitoylation,

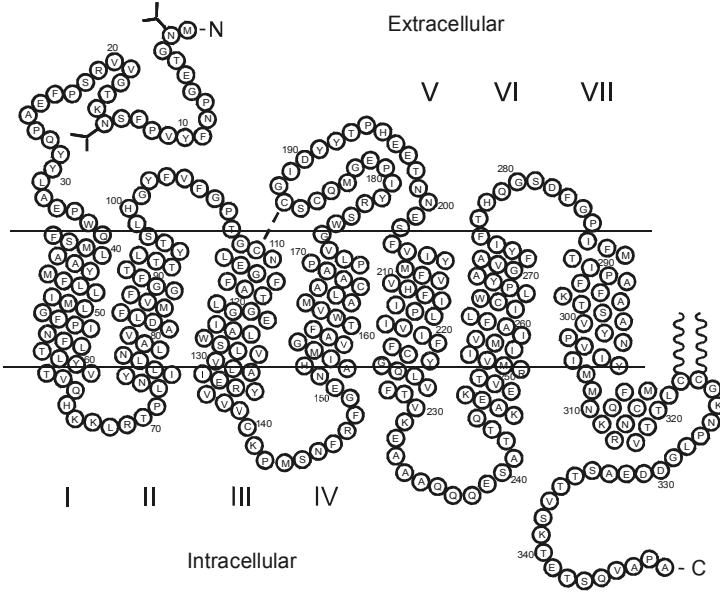


Fig. 3: Schematic representation of the two-dimensional structure of rhodopsin. The transmembrane segments are numbered. Modified from Hargrave and McDowell (1992) [17] and Palczewski et al. (2000) [18].

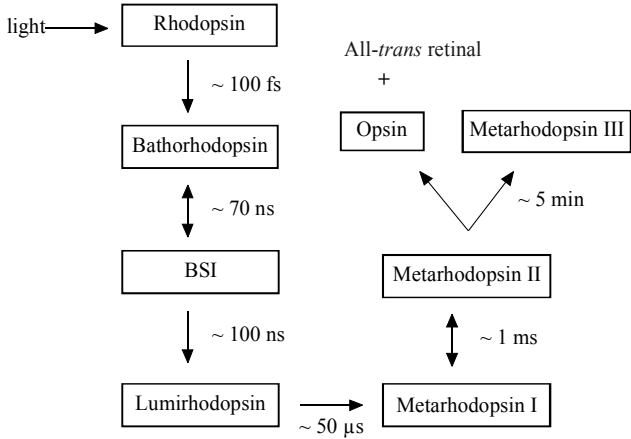


Fig. 4: The photocascade of rhodopsin.

disulfide bridge formation, glycosylation) and subsequently targeting to the rod outer segment membrane to fulfil its structural and functional tasks. These modifications take place in the E.R. and during passage through the Golgi membranes. In the Golgi membranes rhodopsin is sorted into distinct transport vesicles for transport through the trans-Golgi network [16]. After its passage through the Golgi, rhodopsin-containing vesicles move to the outer segment where they fuse to generate the disk membrane. Rhodopsin comprises more than 90% of the intrinsic protein content of the disk membranes.

1.2.2. Crystal structure of rhodopsin

Rhodopsin is one of the best studied GPCRs [17]. Recently, a 2.8 Å-resolution crystal structure of bovine rhodopsin finally provided a more detailed three-dimensional structure for rhodopsin (Fig. 5) [18]. About 97% of the whole opsin molecule could be identified in the electron density profile and the current structure lacks only part of the intracellular loops and the COOH-terminal region, but includes all 194 protein residues that form the seven transmembrane helices (Fig. 3) [18]. These are residue 35 to 64 for helix I, 71 to 100 for helix II, 107 to 139 for helix III, 151 to 173 for helix IV, 200 to 225 for helix V, 247 to 277 for helix VI and 286 to 306 for helix VII. Helices I, IV, VI and VII are bent at proline residues, whereas helix V is almost straight. It is proposed that helix IV is involved in the stabilization of the dark-state rhodopsin through hydrophobic interactions with helices II, III and V [19]. The chromophore is bound via a protonated Schiff base linkage to Lys296 in helix VII. Glu113 in helix III forms a salt bridge with the protonated Schiff base of the chromophore which keeps the protein constrained in its inactive conformation. Helix II is kinked around Gly89 and Gly90 placing Gly90 close to Glu113, the residue that interacts with the protonated Schiff base. Helix III is the longest helix and the helix that is most tilted away from the membrane normal. The highly conserved sequence Glu134-Arg135-Tyr136 (E/(D)RY

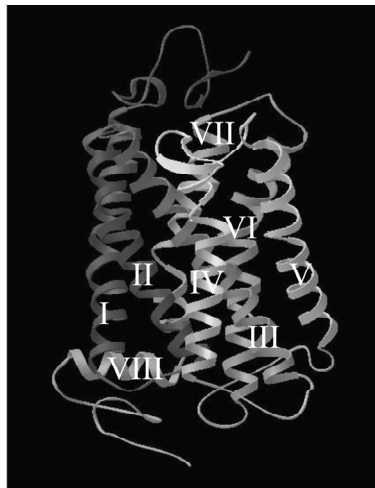


Fig. 5: The three-dimensional structure of rhodopsin. The helices are numbered. Modified from Palczewski et al. [18].

motif) that forms a potential binding site for a G protein, is located in the cytoplasmic terminal region of helix III surrounded by hydrophobic residues from helix II, cytoplasmic loop II (C-II), helix V and helix VI [18].

The extracellular region starts with residues 1-34 which are considered to form the N-terminal tail. Residues 101 to 106 represent the extracellular loop I (E-I) which connects helix II and III, 174 to 199 form E-II which connects helix IV and V, and 278 to 285 form E-III which connects helix VI and VII. The N-terminal tail is glycosylated at Asn2 and Asn15. Glycosylation plays a role in the folding and maturation of rhodopsin [20,21]. The oligosaccharides probably extend away from the extracellular domain and do not seem to interact with any part of the molecule [22]. Cys187 forms a disulfide bond with Cys110 at the extracellular end of helix III. Residues Cys110 and Cys187 are conserved in all known visual pigments [23] and many transmembrane receptors that are coupled to G proteins [23-26]. The disulfide bond forms an important determinant in the thermal stability of rhodopsin as well as its photointermediates and in coupling to G protein activation [27].

The cytoplasmic region is formed by residue 65 to 70 for cytoplasmic loop I (C-I) which connects helix I and II, 140 to 150 for C-II which connects helix III and IV, 226 to 235 and 240 to 246 have been assigned to C-III which connects helix V and VI and 307 to 327 and 334 to 348 to the COOH-terminal region. The missing residues have not yet been determined in the 3D crystal structure but form part of the cytoplasmic loops. C-II and C-III are known to participate in the interaction with the G protein transducin [28-30]. Residue 310 to 323 of the cytoplasmic domain appear to form a helix (helix VIII or C-IV). This eighth helix is of particular interest because of its putative interaction with G_T [31]. This short amphipathic helix is clearly distinct from TM helix VII and lies nearly perpendicular to it. Rhodopsin undergoes palmitoylation at residues Cys322 and Cys323 [32,33] and these acyl chains provide anchor sites to the membrane [34]. Sequence conservation implies a similar structure in most other seven transmembrane receptors of the rhodopsin-like family [35]. The amino-terminal part of the C-IV loop contributes to the binding site for the carboxyl terminus of the α -subunit of G_T and plays a role in the regulation of $\beta\gamma$ -subunit binding [31,36]. Studies using transgenic animals show that the carboxyl-terminal domain is necessary for vectorial transport of rhodopsin from the inner to the outer segment of the rod photoreceptor cell [37]. The highly conserved C-terminal sequence QV(S)APA is thought to be critical in this rhodopsin trafficking [38].

Since this detailed crystal structure of rhodopsin has become available, directed and systematic efforts can be designed, using a combination of recombinant DNA, biochemical, cell biological and biophysical approaches, to unravel the receptor mechanism of rhodopsin leading to activation of the G protein, i.e. to map the underlying conformational changes and to understand the structural and/or functional role of contributing protein residues and motifs.

1.2.3 Photocascade

As was already described in paragraph 1.2.1. the photoactivation of rhodopsin leads to a cascade of photo-induced transitions including the Batho \leftrightarrow BSI \rightarrow Lumi \rightarrow Meta I \leftrightarrow Meta II \rightarrow Meta III transitions [39,40]. Fourier Transform Infrared (FT-IR) difference spectroscopy (see paragraph 1.3.3) can be used to study the structural changes that occur during these major steps in photoactivation. FT-IR difference spectroscopy can measure small structural changes; it detects transitions between molecular rotational or

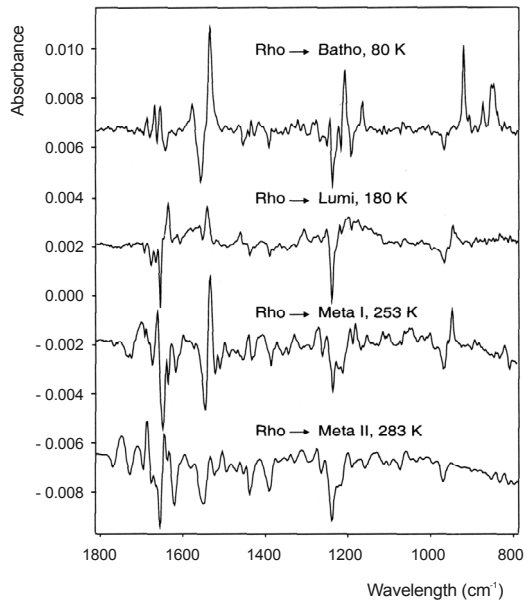


Fig. 6: FT-IR difference spectra of the various transitions in the rhodopsin photocascade. The spectra were taken at the indicated temperature to arrest the cascade at that specific intermediate. The rhodopsin spectrum was subtracted from the photoproduct spectrum and negative bands thus represent vibrational bands originally present in rhodopsin and positive peaks represent bands originating from the photointermediate. FT-IR difference spectroscopy data are not yet available for BSI.

vibrational energy levels. Such data can provide direct information about the structural changes that occur during the individual steps of the photocascade (Fig. 6).

Rhodopsin → Batho(rhodopsin)

The first reaction in the photoactivation of visual pigments, the photo-induced isomerization of the ligand, triggers the cascade of structural transitions eventually producing the active receptor conformation Meta II (Fig. 6). Only the first step in the photocascade is light-dependent: the subsequent steps are thermodynamically driven. Hydrogen-out-of plane (HOOP) bands at 853, 877 and 921 cm^{-1} in the FT-IR difference spectrum are characteristic for the highly strained all-*trans* chromophore in Batho. Strong FT-IR difference bands near 1560 and 1535 cm^{-1} mainly reflect the changing electronic structure of the chromophore due to photoisomerization. The peptide backbone only undergoes small structural changes, reflected in small bands in the Amide I region (1620-1680 cm^{-1}), that are restricted to protein residues lining the chromophore binding site [41,42]. The very small bands in the 1730-1775 cm^{-1} region have been assigned to Asp/Glu carboxyl group stretch modes [43].

Blue-shifted -intermediate (BSI)

Although low temperature data do not provide clear evidence for the existence of an intermediate between Batho and Lumi in native rhodopsin, time-resolved studies suggest that the formation of BSI involves the first structural rearrangements in the protein and the initial relaxation of the all-*trans* chromophore [44]. Batho and BSI form an equilibrium, with BSI decaying to Lumi [45,46]. This equilibrium is strongly

temperature dependent and at the low temperatures where Batho is trapped, the BSI component fraction is very small. Structural information is therefore very limited [44].

Lumi(rhodopsin)

The retinal chromophore shows relatively large conformational changes upon the formation of Lumi as a result of major relaxation of the chromophore strain [42,44]. This is supported by the disappearance of the intense bathorhodopsin HOOP modes at 921, 874 and 851 cm^{-1} and the appearance of a new band at 946 cm^{-1} in the FT-IR difference spectrum [39]. The first significant protein changes also occur upon Lumi formation. This is indicated by the appearance of prominent new bands near 1655 and 1635 cm^{-1} in the amide I region (1600-1700 cm^{-1}) [39].

Meta(rhodopsin) I

Upon formation of the Meta I intermediate, additional changes occur in the protein structure as indicated by peaks that appear in the amide I region in the FT-IR difference spectrum [39]. Most prominent is a positive peak at 1664 cm^{-1} , consistent with alterations in α -helical structure or orientation. New bands also appear above 1700 cm^{-1} , representing alterations in the carboxyl groups of Asp and/or Glu residues [40,47,48]. Chromophore bands characteristic of Meta I appear at 950 cm^{-1} and 1537 cm^{-1} .

Meta(rhodopsin) II

The Meta I \rightarrow Meta II transition is accompanied by deprotonation of the Schiff base and uptake of a proton from the cytosol [49]. The Schiff base deprotonation is accompanied by protonation of its counterion Glu113 [50,51]. The major conformational changes occur in the protein upon formation of meta II [39,48]. An intense band appears at 1686 cm^{-1} , characteristic of β -turns [52]. Several bands appear in the region above 1700 cm^{-1} , most prominently at 1767 (-)/1748 (+), 1729 and near 1710 cm^{-1} which have been assigned to Asp83, Glu122 and Glu113 respectively [43,53].

Meta(rhodopsin) III and opsin

Decay of Meta II is accompanied by a nearly complete loss of signaling activity. The protein largely refolds into a conformation resembling that of rhodopsin as indicated by the decay of bands assigned to protein backbone and carboxyl group C=O stretch [54]. During the meta II decay the retinal is released from its binding pocket and opsin can bind 11-*cis* retinal to form a pigment with spectral properties identical to rhodopsin [55,56]. FT-IR studies also showed that Meta III and opsin share very similar protein structures distinct from both the Meta II and the rhodopsin state [54,57].

1.2.4 Phototransduction

In the present model of vertebrate phototransduction, a dark current carried by Na^+ and Ca^{2+} ions maintains the cytoplasmic membrane of the rod photoreceptor in a depolarized state (-35 mV). A cGMP-gated channel plays a central role in phototransduction by controlling the flow of Na^+ and Ca^{2+} ions into the outer segment in response to light-induced changes in intracellular cGMP concentrations [2,58,59]. Briefly, in dark-adapted rod cells, Na^+ and Ca^{2+} ions flow into the rod outer segment through cGMP-gated channels maintained in their open state by a relatively high concentration of cGMP. The balanced efflux of Ca^{2+} through the $\text{Na}^+/\text{Ca}^{2+}$ exchanger in

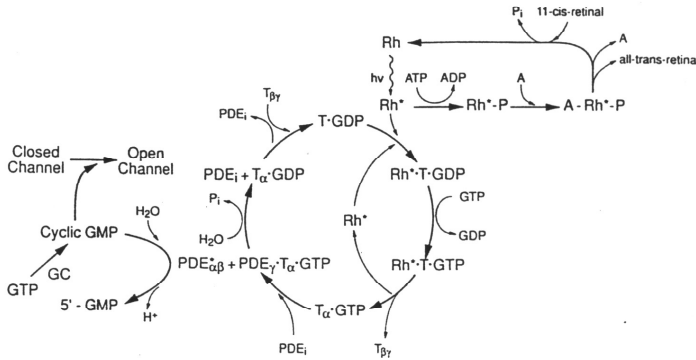


Fig. 7: The cyclic nucleotide cascade. The enzyme cascade controlling visual transduction in rods. Abbreviations: A: arrestin, channel: cGMP-gated channel, GC: guanylate cyclase, PDE: cGMP-specific phosphodiesterase (*, active form), Rh: rhodopsin (*, photoexcited, active form), T: G-protein transducin. From: Zimmerman (1995) [10].

the plasma membrane of the outer segment maintains an intracellular Ca^{2+} concentration of ~ 400 nM. Na^+ ions flow out of the inner segment through a Na^+-K^+ ATPase, thereby completing a dark current loop. In dark there is a constant release of neurotransmitter from the synaptic region of the photoreceptor cell [60].

Upon photoactivation, the 11-*cis* retinal chromophore of rhodopsin is converted to its all-*trans* isomer and this isomerization leads to the formation of the active form of rhodopsin (Meta II) [61-63]. The probability for the photoreceptor rod cell to catch a photon is very high due to the density of the rhodopsin molecules embedded in the disk membranes, which is about 10^6 molecules per disk [64]. Meta II catalyses the activation of the GTP-binding protein transducin via the exchange of GDP for GTP on its α -subunit ($G_{T,\alpha}$). The high rate of the interaction between Meta II and transducin is explained by the high mobility of the rhodopsin molecule in the plane of the disk membrane. Within a fraction of a second, one molecule of Meta II is able to contact hundreds of transducins. GTP- $G_{T,\alpha}$ on its turn activates a phosphodiesterase (PDE) to hydrolyse cGMP to 5'-GMP (Fig. 7). One molecule of the complex GTP- $G_{T,\alpha}$ activates one PDE molecule by removing its inhibitory γ -subunits. PDE can catalyse the hydrolysis of about 1000 molecules of cGMP per second [65,66]. The decrease in intracellular cGMP causes the cGMP-gated channels to close and the rod cell to become hyperpolarized. Under this condition, neurotransmitter release at the synaptic region of the rod cell is inhibited and this signal is eventually processed to the brain.

After photoactivation, the photoreceptor cell returns to its dark state by the shutdown of the visual cascade and resynthesis of cGMP [61,67]. The decrease of the calcium level due to the closure of the cGMP-gated channels and the ongoing extruding of Ca^{2+} ions by the $\text{Na}^+/\text{Ca}^{2+}$ exchanger stimulates the activity of guanylate cyclase which synthesizes cGMP for the reopening of the cationic channels. This causes the decrease of the electrical signal and the dark current is restored. In the same time, different shutoff reactions contribute to the recovery of the dark conditions. The shutdown of the visual cascade already starts when the first rhodopsin molecule is activated. Meta II is inactivated by ATP-dependent phosphorylation by rhodopsin kinase at its C-terminus, first predominantly at Ser334, Ser338 and Ser343 [68] and next on threonine residues

such as Thr335, Thr336, Thr340 and Thr342 [68-71]. The major role of rhodopsin phosphorylation is to promote high affinity binding of arrestin and inhibit transducin binding [72]. Arrestin binds to the C-terminal region (residue 331-348) of phosphorylated Meta II [73] to inactivate Meta II. By binding to the phosphorylated region arrestin becomes "activated" and next binds to residues in the cytoplasmic loops C-1, C-II and C-III [74,75]. Meta II phosphorylation is regulated by recoverin, a calcium sensitive protein that decreases the catalytic activity of rhodopsin kinase [76,77]. Phosphorylated opsin will be recycled to opsin by a phosphatase [78,79]. Active T_{α} is shut off by its own GTPase activity, accelerated by PDE γ en RGS9 [80,81], while PDE activity returns to dark state levels when it recombines with its inhibitory γ subunits.

Finally, in order to regain photosensitivity opsin needs to be regenerated with 11-*cis* retinal. Exposure to light eventually results in hydrolysis of the Schiff base linkage between retinal and opsin and release of all-*trans* retinal. Regeneration requires isomerization of all-*trans* retinal to generate 11-*cis* retinal (visual cycle). The visual cycle takes place in the photoreceptors and in the adjacent retinal pigment epithelium (RPE; Fig. 8). In short, all-*trans* retinal released from activated rhodopsin is converted in the rod outer segment into all-*trans* retinol [82]. In the main pathway all-*trans* retinol is transported by the interphotoreceptor retinoid-binding protein (IRBP) to the RPE where it is isomerized to 11-*cis*-retinol by a retinol isomerase [83-87]. An alcohol dehydrogenase in the RPE is then required in order to produce 11-*cis* retinal [88-91] which is temporarily stored bound to the cellular retinal binding protein (CRALBP) [92]. In addition, there is evidence that the rhodopsin-like retinal G protein-coupled

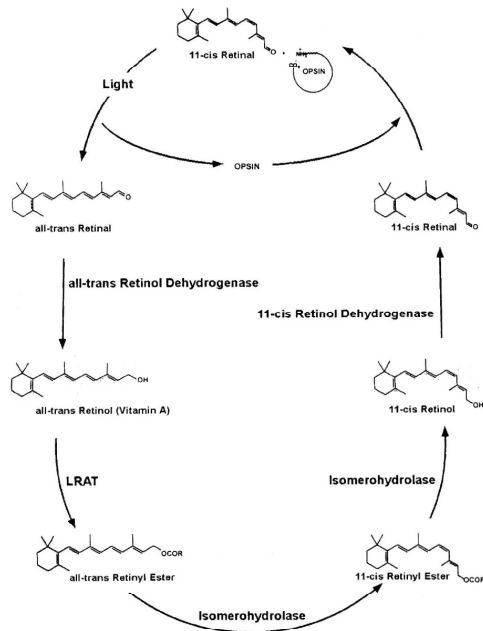


Fig. 8: The visual cycle. Schematic model of the visual cycle which takes place in the photoreceptor cell and the RPE. LRAT: lecithin:retinol acyltransferase. Adapted from: Driessen (1999) [119].

receptor (RGR) plays a role in the visual cycle. RGR has been shown to bind all-*trans* retinal and to function as a photoisomerase to produce 11-*cis*-retinal [93,94]. From transgenic studies it is indicated that RGR contributes by light-dependent synthesis of 11-*cis*-retinal but is not necessary for maintaining normal state levels of both 11-*cis* retinal and rhodopsin in the visual cycle [95]. Once 11-*cis*-retinol is formed it is esterified to generate a retinyl ester stock of the 11-*cis* isomers in the RPE or it is transported back as 11-*cis* retinal from the RPE to the rod outer segment with help of IRBP for regeneration with opsin to form rhodopsin [88-91].

1.3 Cysteine scanning mutagenesis

Since the publication of the 2.8 Å resolution crystal structure of rhodopsin by Palczewski and coworkers in 2000 [18], a wealth of information has been revealed on the structure of rhodopsin. However, the role of individual protein residues in the photoactivation cannot be deduced from this structural model, since the crystal structure was obtained in the dark configuration and is difficult to extrapolate to rhodopsin in the activated state. There are several techniques which can be used to study the function of individual protein residues in the photoactivation of rhodopsin. One of these techniques is cysteine scanning mutagenesis and this approach will be further discussed in this thesis.

Cysteine scanning mutagenesis is a technique which uses cysteine as a reporter group to study the structural and functional properties of a protein. Single amino acids are replaced by a cysteine residue. This is used to analyse structural and functional properties for which a variety of methods is available. Site-directed spin labeling is a technique that uses nitroxide spin labels to study the mobility and accessibility of individual protein residues and their environment. Site-directed chemical labeling is based on the chemical reaction of cysteines with a sulfhydryl reagent. Both techniques have been applied to rhodopsin and will be discussed in short in paragraph 1.3.1 and 1.3.2. In paragraph 1.3.3. the combination of cysteine scanning mutagenesis and FT-IR spectroscopy will be discussed as a novel approach to map conformational changes.

1.3.1 Site-directed spin labeling

The general strategy of site-directed spin labeling (SDSL) is to introduce a nitroxide side chain at selected sites created by site-directed mutagenesis. First, a cysteine is introduced by means of cysteine-substitution mutagenesis in a base mutant in which all reactive native cysteines have been replaced by a suitable non-reactive residue. This is followed by derivatization of the reactive cysteine with a sulfhydryl-selective nitroxide reagent [96]. Next, an electron paramagnetic resonance (EPR) spectrum of the nitroxide is recorded to study the local environment of the nitroxide side chain [97].

In the last decade site-directed spin labeling has revealed information on the cytoplasmic loops of rhodopsin concerning accessibility and mobility of residues, loop structure and conformational changes upon photoactivation, and distances between residues. Due to the sterical constraints of the nitroxide label, mainly residues outside the transmembrane domain have been studied [98]. The hydrophobic-water interfaces of the cytoplasmic loops have been determined using SDSL and appear to agree very well with the crystal structure of rhodopsin [18,99-101]. According to SDSL the structure of loops C-I, C-II and C-IV displays a more ordered loop structure than C-III which forms

an extended, mobile loop [102]. The C-terminus (residue 324-348) is a highly disordered and dynamic structure [103]. From the crystal structure of rhodopsin, the structure of the cytoplasmic loops could only partly be determined because the cytoplasmic loops are almost certainly flexible and mobile in the physiological environment [103,104]. In addition, the crystal structure is based upon a non-natural conformation and thus may provide inaccurate information about the structure of the cytoplasmic loops. So far, the secondary structure of the cytoplasmic loops C-I and C-III and the C-terminus predicted from SDSL experiments correspond very well with the crystal structure of rhodopsin [18]. SDSL has also been used to probe conformational changes upon photoactivation. Meta II formation results in conformational changes in cytoplasmic loops C-I, C-II, C-IV and the N-terminal region of C-III [99-102,105,106]. In addition to structural information about the cytoplasmic loops, the EPR-spectra of labeled cytoplasmic residues can be extrapolated to the conformational changes of the transmembrane helices upon photoactivation of rhodopsin. Measurements using nitroxide labeled cysteines 140 and 316 located at the cytoplasmic termination of helix III and VII respectively indicate that Helix III and VII show conformational changes upon photoactivation [102]. Labels at residue 65 in Helix I and varying residues in Helix VII show that the cytoplasmic portion of helix VII moves away from helix I upon photoactivation [107,108]. Helix III contains the Glu113 counterion that forms a salt bridge with the protonated Schiff base of retinal. Upon Meta II formation, the salt bridge is broken and this might cause the movement of helices III and VII [102,106,109]. Helix II moves away from C-IV and toward helix IV due to backbone rotations at the Gly89/Gly90 pair. Helix VI displays a robust displacement outward toward helix V, probably caused by rotation at Pro267 [105]. Helix VI and III that are located close to each other seem to be the most mobile helices in the rhodopsin structure. After photoactivation helix III displays an outward movement relative to helix II, IV, V, VI and VII. This is thought to be the result of a rigid body movement [106,110]. Helix V shows no detectable movement upon stimulation of rhodopsin by light [101].

1.3.2 Site-directed chemical labeling

Relative comparable structural information, as achieved with site-directed spin labeling, can also be obtained using site-directed chemical labeling [104,111-113]. In site-directed modification the structure of proteins can be studied by measuring the reactivity and accessibility of amino acids by chemically labeling cysteines with a (fluorescent) sulfhydryl reagent. Again a cysteine is introduced by means of cysteine-substitution mutagenesis in a base-mutant in which all reactive native cysteines have been replaced by a suitable non-reactive amino acid. The sulfhydryl reagents can be either membrane-permeant or membrane-impermeant and provide a handle to study the cysteine environment. The reactivity of the sulfhydryl reagent is determined by the accessibility of the residue and hence by the local structure of the protein. Using two labeled cysteines the spatial proximity of two residues can be measured by energy transfer. In contrast to site-directed spin labeling it is possible to label amino acids located in the transmembrane domain provided that the amino acid is not buried too deep inside the protein [112,113]. While e.g. for transporter proteins this approach has been quite successful [114], it has offered only limited information on rhodopsin. Residues 136-150 of the intracellular C-II loop were found to be located in an ordered and sterically restricted environment [115] which indicates that the C-II loop has an ordered structure. This is in agreement with SDSL experiments (see § 1.3.1). Part of the

C-III loop (residue 240-250) is considered to be α -helical [104] in contrast to the crystal structure which indicates that only residue 243-246 exhibit helical structure [18].

1.3.3 FT-IR difference spectroscopy

The nature of the above discussed techniques implies that preferentially protein residues of the intracellular and extracellular loops can be properly addressed. In addition, in site-directed chemical or spin labeling the dynamics of the label have to be taken into account which need to be extrapolated to structure or structural changes of the protein, and this technique thus only indirectly reports on the dynamics of the residue they probe. Since nitroxide and chemical labels are invasive, the labels may perturb the tertiary structure of the protein studied and thus provide inaccurate information. On the other hand, Fourier transform infrared (FT-IR) spectroscopy does not need any labels and therefore this approach does not disturb the structure of the protein. It is a non-invasive technique and can address both the protein residues located in the intracellular and extracellular loops and those that are located in the transmembrane domain.

FT-IR spectroscopy is a very sensitive technique that can measure small structural changes. It detects transitions between molecular rotational or vibrational energy levels [116] during which the electrical dipole moment changes. In the spectrum of electromagnetic radiation, the infrared region begins at about 800 nm (the near infrared region), followed by the mid infrared region (between 2500 and 25000 nm) and the far infrared (> 25000 nm). Usually, frequencies are expressed in wavenumbers, i.e. reciprocal wavelengths (cm^{-1}). Thus the mid infrared region, which in practice is the most important, lies between 4000 and 400 cm^{-1} . Most absorption bands, associated with stretching and bending vibrations, occur in the mid infrared region. Of particular importance are the amide I and amide II vibrations in the $1700\text{-}1500 \text{ cm}^{-1}$ region representing the amide backbone of peptides and proteins. They are sensitive to hydrogen bonding and thus to the secondary structure of the protein. Hydrogen bonding causes a down-shift in frequency and broadening of the stretching bands. Bands around 2900, 1740, 1400 and 1230 cm^{-1} represent (phospho)lipids and several bands around 1100 and below 1000 cm^{-1} can be attributed to carbohydrates or nucleic acids.

Infrared spectra of biomolecules consist of many bands which contain information about structural aspects of the molecule under study. The band positions are highly sensitive to molecular structure as well as to the micro-environment. The observed spectral bands have to be assigned to distinct components of the molecule. In many cases, comparison with infrared spectra of analogues is necessary but often not sufficient to assign the spectral features. Site-directed mutagenesis or stable-isotope labeling can help in the assignment of the spectral features. The combined efforts of both techniques might eventually result in detailed knowledge of structure-function relationships of the protein under study.

In the work presented in this thesis, we aim to use cysteine scanning mutagenesis in combination with FT-IR difference spectroscopy to study the structural and functional role of residues located in the second transmembrane domain in the photoactivation of rhodopsin. Activation of rhodopsin often involves small structural rearrangements in the active site(s) that will be accompanied by changes in vibrational band position, width or intensity. These structural changes can be visualized in infrared difference spectra. In earlier experiments it was shown that vibrational changes in cysteine sulfhydryl groups (-SH) can be detected in the FT-IR difference spectrum around 2550 cm^{-1} [117,118]. The -SH group is very sensitive to changes in local structure and polarity and small structural changes can be observed. Furthermore, the $2500\text{-}2600 \text{ cm}^{-1}$ region is an

isolated region in the FT-IR difference spectrum without interference from other biomembrane components. Hence, local protein conformational changes are reflected in small changes in -SH vibrational activity which makes the sulfhydryl group an excellent reporter group. The background of native cysteines should preferentially be eliminated and a base mutant created in which all native cysteines are replaced by a suitable amino acid, except for Cys110 and Cys187 that form the disulfide bridge. Subsequently, single residues can be mutated into a cysteine and -SH vibrational activity in the photocascade measured by means of FT-IR difference spectroscopy. In this way the role of individual residues in the photoactivation of rhodopsin can be studied.

1.4 Aim and outline of this thesis

Rhodopsin is a complex integral membrane protein and a member of the large family of G protein-coupled receptors. The recently determined 3-D crystal structure of ground-state rhodopsin gives detailed information on the structure of rhodopsin and its three-dimensional arrangement. However, it does not show which elements of the protein are involved in its photoactivation. The role of most individual protein residues during the photoactivation of rhodopsin, including the residues located in the transmembrane domain, has not yet been elucidated. From earlier experiments it is known that Asp83 participates in the formation of Meta II. Since Asp83 is located in the second transmembrane helix of rhodopsin the aim of the work presented in this thesis was to study the role of the protein residues located in the second transmembrane helix in the photoactivation of rhodopsin.

Chapter 2 investigates the contribution of Asp83 to structure and function of rhodopsin in more detail. It shows that the function of Asp83 can be largely maintained by a cysteine residue. The H-bonding changes involving Asp83 upon Meta II formation can also be probed by Cys83 as changes in the vibrational activity of its -SH group. This provides an experimental validation for mapping residues participating in photoactivation of rhodopsin by cysteine scanning mutagenesis. Chapter 3 describes the development of a cysteine-free base-mutant that can be used in cysteine scanning mutagenesis to study single protein residues of the second transmembrane helix of rhodopsin. Chapter 4 describes the construction, production and analysis of single cysteine mutants in the second transmembrane domain of rhodopsin on the background of a cysteine-free base-mutant. Serious production problems were encountered with production of sufficient quantities of functional mutants. In chapter 2 it was shown that changes in sulfhydryl vibrations of an introduced cysteine residue can be measured on a background of native cysteines. To allow purification and further study we constructed the same mutant rhodopsins as studied in chapter 4 in wild type rhodopsin. The results of this approach are described in chapter 5.

Rhodopsin contains three native transmembrane domain located cysteines. Single mutations of these cysteines (C167R, C222R, C264del) result in a retinitis pigmentosa phenotype. Chapter 6 provides a biochemical characterization of these three retinitis pigmentosa prone cysteine mutants.

The work presented in this thesis is summarized and discussed in chapter 7.

References

1. Wald, G. (1968). The molecular basis of visual excitation. *Nature*, 219, 800 - 807.
2. Yau, K.-W. (1994). Phototransduction mechanism in retinal rods and cones - The Friedenwald lecture. *Invest. Ophthalmol. Visual Sci.*, 35, 9 - 32.
3. Baylor, D. A. (1996). How photons start vision. *Proc. Nat. Acad. Sci. USA*, 93, 560 - 565.
4. Nathans, J. (1989). The genes for color vision. *Sci. Amer.*, 260(2), 28 - 35.
5. Oprian, D. D., Asenjo, A. B., Lee, N., and Pelletier, S. L. (1991). Design, chemical synthesis, and expression of genes for the three human color vision pigments. *Biochemistry-USA*, 30, 11367 - 11372.
6. Merbs, S. L. and Nathans, J. (1992). Absorption spectra of human cone pigments. *Nature*, 356, 433 - 435.
7. Okano, T., Kojima, D., Fukada, Y., Shichida, Y., and Yoshizawa, T. (1992). Primary structures of chicken cone visual pigments - Vertebrate rhodopsins have evolved out of cone visual pigments. *Proc. Nat. Acad. Sci. USA*, 89, 5932 - 5936.
8. Jacobs, G. H. (1993). The distribution and nature of colour vision among the mammals. *Biol. Rev.*, 68, 413 - 471.
9. Johnson, R. L., Grant, K. B., Zankel, T. C., Boehm, M. F., Merbs, S. L., Nathans, J., and Nakanishi, K. (1993). Cloning and expression of goldfish opsin sequences. *Biochemistry-USA*, 32, 208 - 214.
10. Zimmerman, A. L. (1995). Visual transduction in: *Cell Physiology Source Book* (Academic Press, New York, U.S.A.).
11. Young, R. W. (1976). Visual cells and the concept of renewal. *Invest. Ophthalmol. Visual Sci.*, 15, 700 - 725.
12. Nathans, J. (1990). Determinants of visual pigment absorbance: Identification of the retinylidene Schiff's base counterion in bovine rhodopsin. *Biochemistry-USA*, 29, 9746 - 9752.
13. Zhukovsky, E. A. and Oprian, D. D. (1989). Effect of carboxylic acid side chains on the absorption maximum of visual pigments. *Science*, 246, 928 - 930.
14. Sakmar, T. P., Franke, R. R., and Khorana, H. G. (1989). Glutamic acid-113 serves as the retinylidene Schiff base counterion in bovine rhodopsin. *Proc. Nat. Acad. Sci. USA*, 86, 8309 - 8313.
15. Okada, T., Ernst, O. P., Palczewski, K., and Hofmann, K. P. (2001). Activation of rhodopsin: New insights from structural and biochemical studies. *Trends Biochem. Sci.*, 26, 318 - 324.
16. Wandinger-Ness, A., Bennett, M. K., Antony, C., and Simons, K. (1990). Distinct transport vesicles mediate the delivery of plasma membrane proteins to the apical and basolateral domains of MDCK cells. *J Cell Biol.*, 111, 987 - 1000.
17. Hargrave, P. A. and McDowell, J. H. (1992). Rhodopsin and phototransduction - A model system for G-protein-linked receptors. *FASEB J.*, 6, 2323 - 2331.
18. Palczewski, K., Kumasaka, T., Hori, T., Behnke, C. A., Motoshima, H., Fox, B. A., LeTrong, I., Teller, D. C., Okada, T., Stenkamp, R. E., Yamamoto, M., and Miyano, M. (2000). Crystal structure of rhodopsin: A G protein-coupled receptor. *Science*, 289, 739 - 745.
19. Teller, D. C., Okada, T., Behnke, C. A., Palczewski, K., and Stenkamp, R. E. (2001). Advances in determination of a high-resolution three-dimensional structure of rhodopsin, a model of G-protein-coupled receptors (GPCRs). *Biochemistry-USA*, 40, 7761 - 7772.
20. Sung, C.-H., Schneider, B. G., Agarwal, N., Papermaster, D. S., and Nathans, J. (1991). Functional heterogeneity of mutant rhodopsins responsible for autosomal dominant retinitis-pigmentosa. *Proc. Nat. Acad. Sci. USA*, 88, 8840 - 8844.
21. Kaushal, S., Ridge, K. D., and Khorana, H. G. (1994). Structure and function in rhodopsin: The role of asparagine-linked glycosylation. *Proc. Nat. Acad. Sci. USA*, 91, 4024 - 4028.
22. Menon, S. T., Han, M., and Sakmar, T. P. (2001). Rhodopsin: Structural basis of molecular physiology. *Physiol. Rev.*, 81, 1659 - 1688.
23. Applebury, M. L. and Hargrave, P. A. (1986). Molecular biology of the visual pigments. *Vision Res.*, 26, 1881 - 1895.
24. Dixon, R. A., Kobilka, B. K., Strader, D. J., Benovic, J. L., Dohlman, H. G., Frielle, T., Bolanowski, M. A., Bennett, C. D., Rands, E., Diehl, R. E., Mumford, R. A., Slater, E. E., Sigal, E. S., Caron, M. G., Lefkowitz, R. J., and Strader, C. D. (1986). Cloning of the gene and cDNA for mammalian β -adrenergic receptor and homology with rhodopsin. *Nature*, 321, 75 - 79.
25. Julius, D., MacDermott, A. B., Jessel, T. M., Huang, K., Molineaux, S., Schieren, I., and Axel, R. (1988). Functional expression of the 5-HT_{1c} receptor in neuronal and nonneuronal cells. *Cold Spring Harb. Symp. Quant. Biol.*, 53, 385 - 393.
26. Krause, J. E., Hershey, A. D., Dykema, P. E., and Takeda, Y. (1990). Molecular biological studies on the diversity of chemical signalling in tachykinin peptidergic neurons. *Ann. N. Y. Acad. Sci.*, 579, 254 - 272.

27. Davidson, F. F., Loewen, P. C., and Khorana, H. G. (1994). Structure and function in rhodopsin: Replacement by alanine of cysteine residues 110 and 187, components of a conserved disulfide bond in rhodopsin, affects the light-activated metarhodopsin II state. *Proc. Nat. Acad. Sci. USA*, 91, 4029 - 4033.
28. Franke, R. R., König, B., Sakmar, T. P., Khorana, H. G., and Hofmann, K. P. (1990). Rhodopsin mutants that bind but fail to activate transducin. *Science*, 250, 123 - 125.
29. Franke, R. R., Sakmar, T. P., Graham, R. M., and Khorana, H. G. (1992). Structure and function in rhodopsin: studies of the interaction between the rhodopsin cytoplasmic domain and transducin. *J. Biol. Chem.*, 267, 14767 - 14774.
30. Borjigin, J. and Nathans, J. (1994). Insertional mutagenesis as a probe of rhodopsin's topography, stability, and activity. *J. Biol. Chem.*, 269, 14715 - 14722.
31. König, B., Arendt, A., McDowell, J. H., Kahlert, M., Hargrave, P. A., and Hofmann, K. P. (1989). Three cytoplasmic loops of rhodopsin interact with transducin. *Proc. Nat. Acad. Sci. USA*, 86, 6878 - 6882.
32. Ovchinnikov, Y. A., Abdulaev, N. G., and Bogachuk, A. S. (1988). Two adjacent cysteine residues in the C-terminal cytoplasmic fragment of bovine rhodopsin are palmitylated. *FEBS Lett.*, 230, 1 - 5.
33. Papac, D. I., Thornburg, K. R., Büllesbach, E. E., Crouch, R. K., and Knapp, D. R. (1992). Palmitylation of a G-protein coupled receptor - Direct analysis by tandem mass spectrometry. *J. Biol. Chem.*, 267, 16889 - 16894.
34. Moench, S. J., Moreland, J., Stewart, D. H., and Dewey, T. G. (1994). Fluorescence studies of the location and membrane accessibility of the palmitoylation sites of rhodopsin. *Biochemistry-USA*, 33, 5791 - 5796.
35. Probst, W. C., Snyder, L. A., Schuster, D. I., Brosius, J., and Sealfon, S. C. (1992). Sequence alignment of the G-protein coupled receptor superfamily. *DNA Cell Biol.*, 11, 1 - 20.
36. Ernst, O. P., Meyer, C. K., Marin, E. P., Henklein, P., Fu, W.-Y., Sakmar, T. P., and Hofmann, K. P. (2000). Mutation of the fourth cytoplasmic loop of rhodopsin affects binding of transducin and peptides derived from the carboxyl-terminal sequences of transducin α and γ subunits. *J. Biol. Chem.*, 275, 1937 - 1943.
37. Concepcion, F., Mendez, A., and Chen, J. (2002). The carboxyl-terminal domain is essential for rhodopsin transport in rod photoreceptors. *Vision Res.*, 42, 417 - 426.
38. Deretic, D., Schmerl, S., Hargrave, P. A., Arendt, A., and McDowell, J. H. (1998). Regulation of sorting and post-Golgi trafficking of rhodopsin by its C-terminal sequence QVS(A)PA. *Proc. Nat. Acad. Sci. USA*, 95, 10620 - 10625.
39. DeGrip, W. J., Gray, D., Gillespie, J., Bovee-Geurts, P. H. M., VanDenBerg, E. M. M., Lugtenburg, J., and Rothschild, K. J. (1988). Photoexcitation of rhodopsin: Conformation changes in the chromophore, protein and associated lipid, as determined by FTIR difference spectroscopy. *Photochem. Photobiol.*, 48, 497 - 504.
40. Rothschild, K. J. and DeGrip, W. J. (1986). FTIR studies of the rhodopsin transduction mechanism. *Photobiochem. Photobiophys.*, 13, 245 - 258.
41. Yoshizawa, T., Shichida, Y., and Matuoka, S. (1984). Primary intermediates of rhodopsin studied by low temperature spectrophotometry and laser photolysis. Bathorhodopsin, hypsorhodopsin and photorhodopsin. *Vision Res.*, 24, 1455 - 1463.
42. Ujj, L., Jäger, F., and Atkinson, G. H. (1998). Vibrational spectrum of the lumi intermediate in the room temperature rhodopsin photo-reaction. *Biophys. J.*, 74, 1492 - 1501.
43. Rath, P., DeCaluwé, G. L. J., Bovee-Geurts, P. H. M., DeGrip, W. J., and Rothschild, K. J. (1993). Fourier transform infrared difference spectroscopy of rhodopsin mutants: Light activation of rhodopsin causes hydrogen-bonding changes in residue aspartic acid-83 during meta II formation. *Biochemistry-USA*, 32, 10277 - 10282.
44. DeGrip, W. J. and Rothschild, K. J. (2000). Structure and mechanism of vertebrate visual pigments in: *Molecular Mechanisms in Visual Transduction*, Stavenga, D. G., DeGrip, W. J., and Pugh, E. N., Jr., eds. (Elsevier Science Pub., Amsterdam, The Netherlands).
45. Randall, C. E., Lewis, J. W., Hug, S. J., Bjorling, S. C., Eisnershanas, I., Friedman, N., Ottolenghi, M., Sheves, M., and Kliger, D. S. (1991). A new photolysis intermediate in artificial and native visual pigments. *J. Amer. Chem. Soc.*, 113, 3473 - 3485.
46. Hug, S. J., Lewis, J. W., Einterz, C. M., Thorgeirsson, T. E., and Kliger, D. S. (1990). Nanosecond photolysis of rhodopsin: Evidence for a new, blue-shifted intermediate. *Biochemistry-USA*, 29, 1475 - 1485.
47. Siebert, F., Mäntele, W., and Gerwert, K. (1983). Fourier-transform infrared spectroscopy applied to rhodopsin. The problem of the protonation state of the retinylidene Schiff base re-investigated. *Eur. J. Biochem.*, 136, 119 - 127.
48. DeGrip, W. J., Gillespie, J., and Rothschild, K. J. (1985). Carboxyl group involvement in the meta I and meta II stages in rhodopsin bleaching. A Fourier transform infra-red spectroscopic study. *Biochim. Biophys. Acta*, 809, 97 - 106.

49. Hofmann, K. P. (1986). Photoproducts of rhodopsin in the disc membrane. *Photobiochem. Photobiophys.*, 13, 309 - 327.
50. Nishimura, S., Kandori, H., and Maeda, A. (1997). Transmembrane signaling mediated by water in bovine rhodopsin. *Photochem. Photobiol.*, 66, 796 - 801.
51. Jäger, F., Fahmy, K., Sakmar, T. P., and Siebert, F. (1994). Identification of glutamic acid 113 as the Schiff base proton acceptor in the metarhodopsin II photointermediate of rhodopsin. *Biochemistry-USA*, 33, 10878 - 10882.
52. Parker, F. S. (1983). Applications of infrared, Raman and resonance Raman spectroscopy in biochemistry (Plenum Press, New York, USA).
53. Fahmy, K., Jäger, F., Beck, M., Zvyaga, T. A., Sakmar, T. P., and Siebert, F. (1993). Protonation states of membrane-embedded carboxylic acid groups in rhodopsin and metarhodopsin II: A Fourier-transform infrared spectroscopy study of site-directed mutants. *Proc. Nat. Acad. Sci. USA*, 90, 10206 - 10210.
54. Rothschild, K. J., Gillespie, J., and DeGrip, W. J. (1987). Evidence for rhodopsin refolding during the decay of meta II. *Biophys. J.*, 51, 345 - 350.
55. VanBreugel, P. J. G. M., Bovee-Geurts, P. H. M., Bonting, S. L., and Daemen, F. J. M. (1979). Biochemical Aspects of the Visual Process XL. Spectral and chemical analysis of metarhodopsin III in photoreceptor membrane suspensions. *Biochim. Biophys. Acta*, 557, 188 - 198.
56. Rotmans, J. P., Daemen, F. J. M., and Bonting, S. L. (1974). Binding site and migration of retinaldehyde during rhodopsin photolysis. *Biochim. Biophys. Acta*, 357, 151 - 158.
57. Klinger, A. L. and Braiman, M. S. (1992). Structural comparison of metarhodopsin II, metarhodopsin III, and opsin based on kinetic analysis of Fourier transform infrared difference spectra. *Biophys. J.*, 63, 1244 - 1255.
58. Yau, K.-W. and Baylor, D. A. (1989). Cyclic GMP-activated conductance of retinal photoreceptor cells. *Annu. Rev. Neurosci.*, 12, 289 - 327.
59. Lagnado, L. and Baylor, D. A. (1992). Signal flow in visual transduction. *Neuron*, 8, 995 - 1002.
60. Copenhagen, D. R. and Jahr, C. E. (1989). Release of endogenous excitatory amino acids from turtle photoreceptors. *Nature*, 341, 536 - 539.
61. Stryer, L. (1991). Visual excitation and recovery. *J. Biol. Chem.*, 266, 10711 - 10714.
62. Pugh, E. N., Jr. and Lamb, T. D. (1993). Amplification and kinetics of the activation steps in phototransduction. *Biochim. Biophys. Acta*, 1141, 111 - 149.
63. Liebman, P. A., Parker, K. R., and Dratz, E. A. (1987). The molecular mechanism of visual excitation and its relation to the structure and composition of the rod outer segment. *Annu. Rev. Physiol.*, 49, 765 - 791.
64. Pepe, I. M. (1999). Rhodopsin and phototransduction. *J. Photochem. Photobiol. B-Biol.*, 48, 1 - 10.
65. Miki, N., Keirns, J. J., Marcus, F. R., Freeman, J., and Bitensky, M. W. (1973). Regulation of cyclic nucleotide concentrations in photoreceptors: An ATP-dependent stimulation of cyclic nucleotide phosphodiesterase by light. *Proc. Natl. Acad. Sci. U. S. A.*, 70, 3820 - 3824.
66. Lamb, T. D. (1996). Gain and kinetics of activation in the G-protein cascade of phototransduction. *Proc. Nat. Acad. Sci. USA*, 93, 566 - 570.
67. Kaupp, U. B. and Koch, K.-W. (1992). Role of cGMP and Ca²⁺ in vertebrate photoreceptor excitation and adaptation. *Annu. Rev. Physiol.*, 54, 153 - 175.
68. Ohguro, H., Rudnicka-Nawrot, M., Buczylo, J., Zhao, X. Y., Taylor, J. A., Walsh, K. A., and Palczewski, K. (1996). Structural and enzymatic aspects of rhodopsin phosphorylation. *J. Biol. Chem.*, 271, 5215 - 5224.
69. Ohguro, H., Palczewski, K., Ericsson, L. H., Walsh, K. A., and Johnson, R. S. (1993). Sequential phosphorylation of rhodopsin at multiple sites. *Biochemistry-USA*, 32, 5718 - 5724.
70. McDowell, J. H., Nawrocki, J. P., and Hargrave, P. A. (1993). Phosphorylation sites in bovine rhodopsin. *Biochemistry-USA*, 32, 4968 - 4974.
71. Zhang, L. R., Sports, C. D., Osawa, S., and Weiss, E. R. (1997). Rhodopsin phosphorylation sites and their role in arrestin binding. *J. Biol. Chem.*, 272, 14762 - 14768.
72. Palczewski, K., Rispoli, G., and Detwiler, P. B. (1992). The influence of arrestin (48K protein) and rhodopsin kinase on visual transduction. *Neuron*, 8, 117 - 126.
73. Kühn, H., Hall, S. W., and Wilden, U. (1984). Light-induced binding of 48-kDa protein to photoreceptor membranes is highly enhanced by phosphorylation of rhodopsin. *FEBS Lett.*, 176, 473 - 478.
74. Raman, D., Osawa, S., and Weiss, E. R. (1999). Binding of arrestin to cytoplasmic loop mutants of bovine rhodopsin. *Biochemistry-USA*, 38, 5117 - 5123.
75. Krupnick, J. G., Gurevich, V. V., Schepers, T., Hamm, H. E., and Benovic, J. L. (1994). Arrestin-rhodopsin interaction - Multi-site binding delineated by peptide inhibition. *J. Biol. Chem.*, 269, 3226 - 3232.

76. Klenchin, V. A., Calvert, P. D., and Bownds, M. D. (1995). Inhibition of rhodopsin kinase by recoverin - Further evidence for a negative feedback system in phototransduction. *J. Biol. Chem.*, 270, 16147 - 16152.
77. Chen, C.-K., Inglese, J., Lefkowitz, R. J., and Hurley, J. B. (1995). Ca^{2+} -dependent interaction of recoverin with rhodopsin kinase. *J. Biol. Chem.*, 270, 18060 - 18066.
78. Pepe, I. M. (2001). Recent advances in our understanding of rhodopsin and phototransduction. *Prog. Retin. Eye Res.*, 20, 733 - 759.
79. King, A. J., Andjelkovic, N., Hemmings, B. A., and Akhtar, M. (1994). The phospho-opsin phosphatase from bovine rod outer segments - An insight into the mechanism of stimulation of type-2A protein phosphatase activity by protamine. *Eur. J. Biochem.*, 225, 383 - 394.
80. Tsang, S. H., Burns, M. E., Calvert, P. D., Gouras, P., Baylor, D. A., Goff, S. P., and Arshavsky, V. Y. (1998). Role for the target enzyme in deactivation of photoreceptor G protein *in vivo*. *Science*, 282, 117 - 121.
81. Cowan, C. W., Fariss, R. N., Sokal, I., Palczewski, K., and Wensel, T. G. (1998). High expression levels in cones of RGS9, the predominant GTPase accelerating protein of rods. *Proc. Nat. Acad. Sci. USA*, 95, 5351 - 5356.
82. Rattner, A., Smallwood, P. M., and Nathans, J. (2000). Identification and characterization of all-*trans*-retinol dehydrogenase from photoreceptor outer segments, the visual cycle enzyme that reduces all-*trans*-retinal to all-*trans*-retinol. *J. Biol. Chem.*, 275, 11034 - 11043.
83. Bernstein, P. S., Law, W. C., and Rando, R. R. (1987). Isomerization of all-*trans*-retinoids to 11-*cis*-retinoids *in vitro*. *Proc. Natl. Acad. Sci. U. S. A.*, 84, 1849 - 1853.
84. Bridges, C. D. B. and Alvarez, R. A. (1987). The visual cycle operates via an isomerase acting on all-*trans* retinol in the pigment epithelium. *Science*, 236, 1678 - 1680.
85. Deigner, P. S., Law, W. C., Canada, F. J., and Rando, R. R. (1989). Membranes as the energy source in the endergonic transformation of vitamin A to 11-*cis*-retinol. *Science*, 244, 968 - 971.
86. Stecher, H., Gelb, M. H., Saari, J. C., and Palczewski, K. (1999). Preferential release of 11-*cis*-retinol from retinal pigment epithelial cells in the presence of cellular retinaldehyde-binding protein. *J. Biol. Chem.*, 274, 8577 - 8585.
87. Ho, M. T., Massey, J. B., Pownall, H. J., Anderson, R. E., and Hollyfield, J. G. (1989). Mechanism of vitamin A movement between rod outer segments, interphotoreceptor retinoid-binding protein, and liposomes. *J. Biol. Chem.*, 264, 928 - 935.
88. Futterman, S. and Saslaw, L. D. (1961). The estimation of vitamin A aldehyde with thiobarbituric acid. *J. Biol. Chem.*, 236, 1652 - 1657.
89. Nicotra, C. M. A. and Livrea, M. A. (1982). Retinol dehydrogenase from bovine retinal rod outer segments. Kinetic mechanism of the solubilized enzyme. *J. Biol. Chem.*, 257, 11836 - 11841.
90. Zimmerman, W. F., Lion, F., Daemen, F. J. M., and Bonting, S. L. (1975). Biochemical aspects of the visual process. XXX. Distribution of stereospecific retinol dehydrogenase activities in subcellular fractions of bovine retina and pigment epithelium. *Exp. Eye Res.*, 21, 325 - 332.
91. Simon, A., Hellman, U., Wernstedt, C., and Eriksson, U. (1995). The retinal pigment epithelial-specific 11-*cis* retinol dehydrogenase belongs to the family of short chain alcohol dehydrogenases. *J. Biol. Chem.*, 270, 1107 - 1112.
92. Crabb, J. W., Goldflam, S., Harris, S. E., and Saari, J. C. (1988). Cloning of the cDNAs encoding the cellular retinaldehyde-binding protein from bovine and human retina and comparison of the protein structures. *J. Biol. Chem.*, 263, 18688 - 18692.
93. Hao, W. S., Chen, P., and Fong, H. K. W. (2000). Analysis of chromophore of RGR: retinal G-protein-coupled receptor from pigment epithelium. *Meth. Enzymology*, 316, 413 - 422.
94. Chen, P., Lee, T. D., and Fong, H. K. W. (2001). Interaction of 11-*cis*-retinol dehydrogenase with the chromophore of retinal G protein-coupled receptor opsin. *J. Biol. Chem.*, 276, 21098 - 21104.
95. Maeda, T., VanHooser, J. P., Driessen, C. A. G. G., Filipek, S., Janssen, J. J. M., and Palczewski, K. (2003). Evaluation of the role of the retinal G protein-coupled receptor (RGR) in the vertebrate retina *in vivo*. *J. Neurochem.*, 85, 944 - 956.
96. Newman, E. A. and Reichenbach, A. (1996). The Müller cell: A functional element of the retina. *Trends Neurosci.*, 19, 307 - 312.
97. Hubbell, W. L., Mchaourab, H. S., Altenbach, C. A., and Lietzow, M. A. (1996). Watching proteins move using site-directed spin labeling. *Structure*, 4, 779 - 783.
98. Hubbell, W. L., Cafiso, D. S., and Altenbach, C. A. (2000). Identifying conformational changes with site-directed spin labeling. *Nature Struct. Biology*, 7, 735 - 739.
99. Altenbach, C. A., Cai, K. W., Khorana, H. G., and Hubbell, W. L. (1999). Structural features and light-dependent changes in the sequence 306-322 extending from helix VII to the palmitoylation sites in rhodopsin: A site-directed spin-labeling study. *Biochemistry-USA*, 38, 7931 - 7937.

100. Altenbach, C. A., Klein-Seetharaman, J., Hwa, J., Khorana, H. G., and Hubbell, W. L. (1999). Structural features and light-dependent changes in the sequence 59-75 connecting helices I and II in rhodopsin: A site-directed spin-labeling study. *Biochemistry-USA*, 38, 7945 - 7949.
101. Altenbach, C. A., Yang, K., Farrens, D. L., Farahbakhsh, Z. T., Khorana, H. G., and Hubbell, W. L. (1996). Structural features and light-dependent changes in the cytoplasmic interhelical E-F loop region of rhodopsin: A site-directed spin-labeling study. *Biochemistry-USA*, 35, 12470 - 12478.
102. Resek, J. F., Farahbakhsh, Z. T., Hubbell, W. L., and Khorana, H. G. (1993). Formation of the meta II photointermediate is accompanied by conformational changes in the cytoplasmic surface of rhodopsin. *Biochemistry-USA*, 32, 12025 - 12032.
103. Langen, R., Cai, K. W., Altenbach, C. A., Khorana, H. G., and Hubbell, W. L. (1999). Structural features of the C-terminal domain of bovine rhodopsin: A site-directed spin-labeling study. *Biochemistry-USA*, 38, 7918 - 7924.
104. Cai, K. W., Langen, R., Hubbell, W. L., and Khorana, H. G. (1997). Structure and function in rhodopsin: Topology of the c-terminal polypeptide chain in relation to the cytoplasmic loops. *Proc. Nat. Acad. Sci. USA*, 94, 14267 - 14272.
105. Altenbach, C. A., Klein-Seetharaman, J., Cai, K. W., Khorana, H. G., and Hubbell, W. L. (2001). Structure and function in rhodopsin: Mapping light-dependent changes in distance between residue 316 in helix 8 and residues in the sequence 60-75, covering the cytoplasmic end of helices TM1 and TM2 and their connection loop CL1. *Biochemistry-USA*, 40, 15493 - 15500.
106. Farahbakhsh, Z. T., Ridge, K. D., Khorana, H. G., and Hubbell, W. L. (1995). Mapping light-dependent structural changes in the cytoplasmic loop connecting helices C and D in rhodopsin: A site-directed spin labeling study. *Biochemistry-USA*, 34, 8812 - 8819.
107. Yang, K., Farrens, D. L., Altenbach, C. A., Farahbakhsh, Z. T., Hubbell, W. L., and Khorana, H. G. (1996). Structure and function in rhodopsin. Cysteines 65 and 316 are in proximity in a rhodopsin mutant as indicated by disulfide formation and interactions between attached spin labels. *Biochemistry-USA*, 35, 14040 - 14046.
108. Altenbach, C. A., Cai, K. W., Klein-Seetharaman, J., Khorana, H. G., and Hubbell, W. L. (2001). Structure and function in rhodopsin: Mapping light-dependent changes in distance between residue 65 in helix TM1 and residues in the sequence 306-319 at the cytoplasmic end of helix TM7 and in helix H8. *Biochemistry-USA*, 40, 15483 - 15492.
109. Farahbakhsh, Z. T., Hideg, K., and Hubbell, W. L. (1993). Photoactivated conformational changes in rhodopsin: A time-resolved spin label study. *Science*, 262, 1416 - 1419.
110. Farrens, D. L., Altenbach, C. A., Yang, K., Hubbell, W. L., and Khorana, H. G. (1996). Requirement of rigid-body motion of transmembrane helices for light activation of rhodopsin. *Science*, 274, 768 - 770.
111. Cai, K. W., Klein-Seetharaman, J., Farrens, D. L., Zhang, C.-F., Altenbach, C. A., Hubbell, W. L., and Khorana, H. G. (1999). Single-cysteine substitution mutants at amino acid positions 306-321 in rhodopsin, the sequence between the cytoplasmic end of helix VII and the palmitoylation sites: Sulfhydryl reactivity and transducin activation reveal a tertiary structure. *Biochemistry-USA*, 38, 7925 - 7930.
112. Ridge, K. D., Zhang, C.-F., and Khorana, H. G. (1995). Mapping of the amino acids in the cytoplasmic loop connecting helices C and D in rhodopsin. Chemical reactivity in the dark state following single cysteine replacements. *Biochemistry-USA*, 34, 8804 - 8811.
113. Dunham, T. D. and Farrens, D. L. (1999). Conformational changes in rhodopsin - Movement of helix F detected by site-specific chemical labeling and fluorescence spectroscopy. *J. Biol. Chem.*, 274, 1683 - 1690.
114. Frillingos, S., Sahin-Tóth, M., Wu, J. H., and Kaback, H. R. (1998). Cys-scanning mutagenesis: A novel approach to structure-function relationships in polytopic membrane proteins. *FASEB J.*, 12, 1281 - 1299.
115. Barclay, L. R. C., Artz, J. D., and Mowat, J. J. (1995). Partitioning and antioxidant action of the water-soluble antioxidant, Trolox, between the aqueous and lipid phases of phosphatidylcholine membranes: ¹⁴C tracer and product studies. *BBA-Biomembranes*, 1237, 77 - 85.
116. Wallach, D. F., Verma, S. P., and Fookson, J. (1979). Application of laser Raman and infrared spectroscopy to the analysis of membrane structure. *Biochim. Biophys. Acta*, 559, 153 - 208.
117. Rath, P., Bovee-Geurts, P. H. M., DeGrip, W. J., and Rothschild, K. J. (1994). Photoactivation of rhodopsin involves alterations in cysteine side chains: Detection of an S-H band in the meta I → meta II FTIR difference spectrum. *Biophys. J.*, 66, 2085 - 2091.
118. Breikers, G., Bovee-Geurts, P. H. M., DeCaluwé, G. L. J., and DeGrip, W. J. (2001). A structural role for Asp83 in the photoactivation of rhodopsin. *Biol. Chem.*, 382, 1263 - 1270.
119. Driessen, C. A. G. G. (1999). Visual cycle retinol dehydrogenase: molecular and biochemical aspects. Thesis, University of Nijmegen, The Netherlands.



Chapter 2

A structural role for Asp83 in the photoactivation of rhodopsin

Breikers, G., Bovee-Geurts, P.H.M., DeCaluwé, G.L.J. and DeGrip, W.J.
(2001). *Biol. Chem.*, 382, 1263-1270.

Abstract

Asp83 is a highly conserved residue in the second transmembrane domain of visual pigments and many members of other G protein-coupled receptor subfamilies. Upon illumination, the rod visual pigment rhodopsin proceeds through various intermediate states (Batho \leftrightarrow BSI \rightarrow Lumi \rightarrow Meta I \leftrightarrow Meta II \rightarrow Meta III). Meta II represents the active state of rhodopsin, which binds and activates the G protein transducin. Evidence has been presented that Asp83 participates in the formation of Meta II and undergoes a change in H-bonding. To investigate whether this role of Asp83 requires its proton-donating capacity and/or its H-bonding capability, we constructed the mutants D83C and D83N. Both mutants appear to effectively activate transducin, indicating that Asp83 is not essential for signal transduction. Differential effects of the mutations D83C and D83N are observed in the spectral properties and the pH sensitivity of the Meta I \rightarrow Meta II transition. In general, D83C behaves much more like wild-type than D83N. We conclude that the structural role of Asp83 also involves the acidic nature of its carboxyl group. In addition, the participation in Meta II formation of Cys83 in D83C manifests itself as a change in the vibrational properties of the sulfhydryl group, demonstrating that the $-SH$ group can be used as a non-invasive probe for local structural changes.

2.1 Introduction

Rhodopsin, the rod visual pigment of the vertebrate eye, belongs to the super-family of G protein-coupled receptors (GPCRs) [1]. Members of this membrane protein family all contain seven transmembrane spanning segments (Fig. 1). Rhodopsin consists of a protein, opsin, and a light-sensitive ligand or chromophore, 11-*cis* retinal. The chromophore is covalently linked through a Schiff base to lysine residue 296 of opsin [2-4]. Absorption of a photon by the chromophore induces a conformational change of the 11-*cis* to the all-*trans* configuration. This photo-isomerization triggers a cascade of distinct conformational steps (photointermediates: Batho \leftrightarrow BSI \rightarrow Lumi \rightarrow Meta I \leftrightarrow Meta II \rightarrow Meta III), eventually generating Meta II, the active intermediate that can bind and activate the G protein transducin [5]. Meta II exists in a pH-dependent equilibrium with Meta I [6-10].

Rhodopsin is one of the best studied GPCRs and represents a paradigm for this ubiquitous protein family [11]. Recently, a 2.8 Å-resolution crystal structure of bovine rhodopsin has become available [12], that displays the major structural features of the protein. An important task now has become to unravel the receptor mechanism of rhodopsin leading to activation of the G protein, e.g. to map the underlying conformational changes and to understand the structural and/or functional role of contributing protein residues and motifs [13]. In this report we further investigate the role of D83, a residue, that by a combination of site-specific mutagenesis and FT-IR spectroscopy has been shown to participate in the formation of Meta II [14-16] and that also seems to play a functional role in G protein activation by other aminergic GPCRs [1].

The aspartic acid at position 83 is a highly conserved residue located in the second transmembrane domain. The crystal structure of rhodopsin [12] suggests potential H-bond interaction with residues in the seventh transmembrane domain, with putative involvement of H₂O molecules. On basis of FT-IR studies H-bonded coupling, possibly

also through H₂O molecules, of Asp83 to residues in the third transmembrane segment has been proposed [17]. Evidence has been presented that Asp83 is active during formation of Meta II and undergoes a change in H-bonding [14,16,17]. In addition, preliminary data indicated that the mutation D83N results in a change in the pK_a of the Meta I ↔ Meta II equilibrium [15,18]. Presently it is completely unclear whether this role of Asp83 depends on the acidic nature (proton donating capacity) of its carboxyl group, and/or on its potential to donate or accept H-bonding interactions, or whether a structural size factor comes into play as well. We have further addressed this question in a detailed investigation of the mutants D83N (the side-chain of Asn is non-acidic, a good H-bond acceptor, strong H-bond donor) and D83C (the side-chain of Cys is weakly acidic and a weak H-bond donor and acceptor).

In this report we present conclusive evidence that the mutant D83C much more closely resembles wild-type rhodopsin than D83N, suggesting that for wild-type rhodopsin function the acidic nature of the side-chain at position 83 is an important supplement to its H-bonding potential. Quite interestingly, the participation of Cys83 in Meta II formation also manifests itself in a change in the vibrational properties of the sulfhydryl group, demonstrating that the -SH group indeed can be used in FT-IR studies as a sensitive non-invasive probe for local structural changes [19]. Our results also clearly

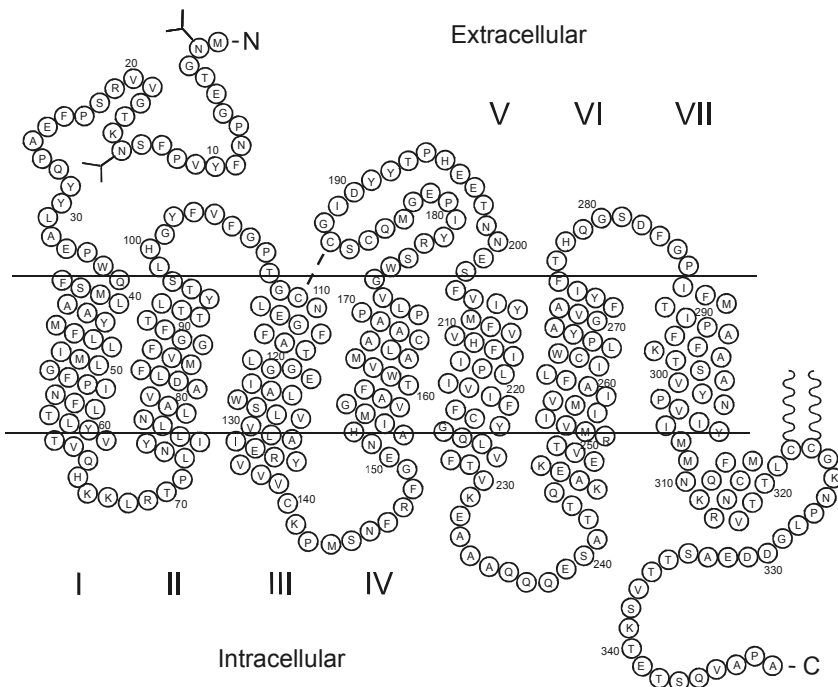


Fig. 1: Schematic representation of the two-dimensional structure of rhodopsin. The transmembrane segments are numbered. Modified from Hargrave and McDowell [1] and Palczewski et al. [2].

confirm that Asp83 participates in the determination of the pKa of the Meta I \leftrightarrow Meta II equilibrium. This suggests that the pKa of this transition is not determined by a single residue, but rather by a complex of several residues, possibly interacting through a H-bonded network.

2.2 Materials and methods

2.2.1 Cloning and expression of rhodopsin mutants

The rhodopsin mutants D83N and D83C were constructed by means of site-directed mutagenesis using the approach developed by Kunkel [20], incorporated into the BioRad Mutagene kit (BioRad Laboratories, Veenendaal, The Netherlands). All constructs were extended with a 6x his-tag to allow rapid purification by immobilized metal affinity chromatography (IMAC) [21]. Cloning, isolation and propagation of recombinant baculovirus were performed as described before [22,23]. D83C was directionally subcloned from the pAcRP23 vector [24] into the transfer vector pFastbacdual (Life Technologies, Inc., Breda, The Netherlands) with help of *Bam*HI and *Not*I (Promega, Leiden, The Netherlands). This transfer vector was used to generate recombinant baculovirus in the *Spodoptera frugiperda* derived cell line (IPLB-Sf9) as described before [25]. Recombinant virus was checked for the presence of the correct mutation by cycle-sequencing using appropriate rhodopsin primers [23,26]. Sf9 cell culture, expression and purification of recombinant protein were performed as described before [26,27].

2.2.2 Analysis of recombinant rhodopsins

Recombinant protein was regenerated into photosensitive pigment by incubation of total cellular membrane preparations with a five-fold excess of 11-*cis* retinal, as described before [27], and was subsequently purified by means of IMAC [21,27]. For analysis of photointermediates by UV-VIS or FT-IR spectroscopy, the purified pigments were reconstituted into retina lipids as described previously [28]. PH-dependence of the Meta I - Meta II transition was measured according to DeLange *et al.* [29]. Fourier transform infrared difference spectra of the Rho \rightarrow Meta I and the Rho \rightarrow Meta II transition were recorded on a Mattson Cygnus 100 FT-IR spectrometer, using set-up and settings similar to those previously reported [30]. Activation of the bovine G protein transducin (G_T) by recombinant rhodopsin was measured by the intrinsic fluorescence enhancement of the G protein α -subunit upon binding of GTP γ S (Roche, Almere, The Netherlands) as earlier described [25,31]. Initial rates were determined to assess activation capacity of the mutants relative to wild type (wt) rhodopsin.

2.3 Results and discussion

2.3.1 Expression and spectral properties of D83 mutants

The his-tagged single mutants D83N and D83C were produced in Sf9 insect cells at functional levels comparable to his-tagged wt rhodopsin (12-16 pmol/10⁶ cells, versus 15-20 pmol/10⁶ cells). Purification of the mutants was achieved through immobilized metal chromatography over Ni²⁺-agarose with a similar efficiency as wt rhodopsin

Rhodopsin	λ_{\max} (nm)		Meta I \rightarrow Meta II transition		Transducin activation (wt \equiv 1)	Half-life Meta II (min) (10 °C, pH 6.5)
	pH 5-11 (isotonic)	pH 11 (4 M KCl)	pKa	Relative area -SH vibration		
wt	498 \pm 1	493 \pm 2	6.5 \pm 0.2	100	1	33 \pm 4
D83N	492 \pm 1	492 \pm 2	7.3 \pm 0.3	95 \pm 15	0.8 \pm 0.3	28 \pm 4
D83C	495 \pm 2	495 \pm 2	6.6 \pm 0.3	170 \pm 20	1.0 \pm 0.1	27 \pm 3

Table 1: Spectral, photochemical and functional properties of wt rhodopsin and D83 mutants. The area of the -SH vibration was ratioed relative to the chromophore vibration at 1230 cm^{-1} , and this ratio was set at 100 for wt rhodopsin. The transducin activation rate was calculated from the initial velocity from curves as presented in Figure 4. The activation rate for wt rhodopsin was set at 1. N = 2-5.

[21,27]. The profile of the absorbance bands of D83C and D83N is very similar to that of wt rhodopsin, as is obvious from the difference spectra (dark minus illuminated; Fig. 2). However, their λ_{\max} show a blue-shift (Table 1) relative to wt rhodopsin (λ_{\max} : 498 \pm 1 nm), that is smaller in D83C (λ_{\max} : 495 \pm 2 nm) than in D83N (λ_{\max} : 492 \pm 1 nm). The small downshift of D83C suggests that the cysteine side-chain affects the electronic properties of the chromophore not much different from the wt Asp side chain. Apparently, the substitution of Asp at position 83 by Cys causes little structural and electronic perturbation of the chromophore.

It has been reported, that at high pH (11) and ionic strength (4M KCl) the λ_{\max} of bovine rhodopsin exhibits a blue-shift of 5-6 nm, while that of frog rhodopsin is not affected [32]. Since frog rhodopsin carries an asparagine residue at the equivalent position of 83 [33], we investigated the behaviour of the three position 83 variants up to pH 11.5 and up to 4 M KCl. Indeed, wild-type D83 showed the expected blue-shift at pH 11 and 4 M KCl (Table 1). No shift was observed, however, for D83N and D83C. This demonstrates, that an Asp residue at position 83 is essential for this phenomenon. As an

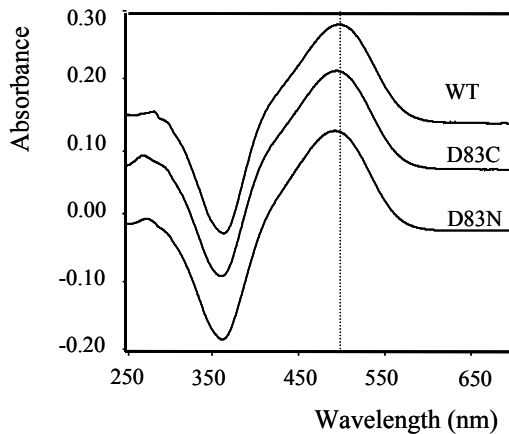


Fig. 2: Absorbance dark-minus-light difference spectra of wt rhodopsin, D83N and D83C. Spectra were obtained by subtracting a spectrum obtained after illumination in the presence of 50 mM hydroxylamine from the original spectrum before illumination. Illumination then produces the all-*trans*-retinoxime absorbing at 365 nm. The dotted line indicates the position of the λ_{\max} of wt rhodopsin.

increase in ionic strength also has a dramatic effect on the pKa of the Meta I \leftrightarrow Meta II equilibrium [29,34] and this pKa also shifts upon substitution of D83 (see below), we assume that these phenomena are connected through an extended H-bonded network in which Asp83 participates, as will be discussed below.

2.3.2 Meta I \leftrightarrow Meta II equilibrium

The late photointermediates Meta I and Meta II are in a pH-dependent equilibrium [6-10] and hence determine the level of activated receptor (Meta II state). The Meta I \leftrightarrow Meta II equilibrium was analyzed for the three position 83 variants at the pH range 5.2 – 8.8. (Fig. 3). At higher pH values Meta I becomes very unstable and cannot be reliably determined. The assay was performed at 10 °C, where Meta II is sufficiently stable. The half life of Meta II at pH 6.5 and 10 °C was slightly, but not significantly lower in the mutants compared to wt rhodopsin (Table 1). The resulting data are fit with a Michaelis-Menten equation and the apparent pKa is determined from the mid-transition (Fig. 3). Evidently, the D83C mutation does not significantly affect the pKa of the Meta I \leftrightarrow Meta II equilibrium (6.6 ± 0.3 in D83C versus 6.5 ± 0.2 in wt). However, a significant upshift was observed for this pKa in the D83N mutant (Table 1), where it shifts to a value of 7.3 ± 0.3 . This agrees with earlier reports, that the mutation D83N produces less Meta I than wild-type [15,18].

The pKa of the Meta I \leftrightarrow Meta II equilibrium is also markedly upshifted by an increase in bulk ionic strength, with the strongest effects induced by ions with more lipophilic character [29]. This suggests a connection between this phenomenon and the high pH/KCl effect on the λ_{\max} . Since the D83N mutant mimicks the effects of high KCl on pKa and of high pH/KCl on λ_{\max} , we propose, that in this mutant the side chain of residue 83 is uncoupled from an extended H-bonded network, that contributes to wavelength regulation and Meta I \rightarrow Meta II transition. In our view, extreme conditions of pH and ionic strength will induce proton loss and/or transfer in this network, leading to deprotonation of the Asp83 carboxyl group. This would uncouple the latter from the network, accompanied by a blue-shift similar to that observed for the D83N mutant. In this view, we would also expect a high pH/KCl effect on the D83C mutant. Due to the much lower acidity of the -SH group as compared to a carboxyl group it might however

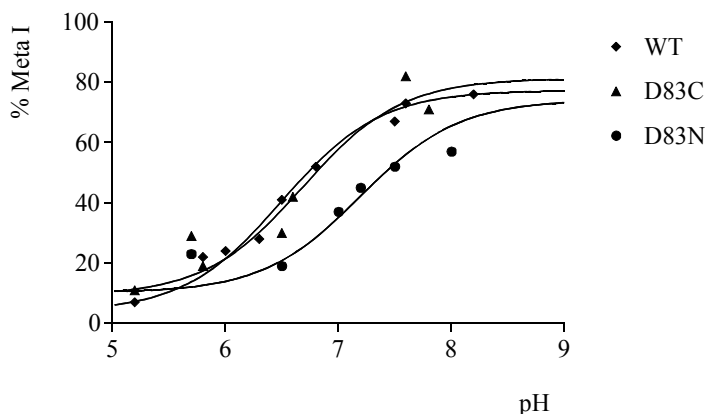


Fig. 3: pH-Dependence of the Meta I \leftrightarrow Meta II equilibrium of wt rhodopsin (\blacklozenge), D83N (\bullet) and D83C (\blacktriangle). Solid lines represent best fits with a Michaelis-Menten equation.

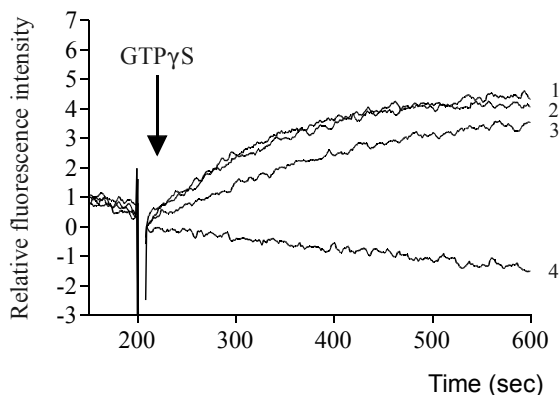


Fig. 4: G protein activation capability of wt rhodopsin and D83 mutants. Intrinsic fluorescence enhancement (excitation: 295 nm; emission: 337 nm) of the G protein α -subunit upon GTP binding was used to monitor activation by either wild-type rhodopsin (trace 1) or mutants D83C (trace 2) and D83N (trace 3). As a control the activation rate in the presence of the apoprotein opsin was measured (trace 4). The measuring sample contained 100 nM of transducin and 5 nM of pigment. The sample was illuminated and after an equilibration period the reaction was initiated by the addition of guanosine 5'-O-(3-thiotriphosphate) (GTP γ S) to a concentration of 2.5 μ M (arrow).

require an even higher bulk pH to achieve this. Such conditions are not experimentally accessible, since rhodopsin rapidly denatures at a pH above 11.5.

The participation of a larger network of residues controlling the Meta I \rightarrow Meta II transition would also explain earlier reports, that mutation of a variety of residues does affect the pH dependence of this transition [15,18,35,36].

2.3.3 G protein activation

The signaling activity of the Asp83 mutants was compared with the wild type by the kinetics of GTP exchange in the α -subunit of transducin, that can be monitored as an increase in the fluorescence quantum yield of an intrinsic Trp residue [31,37,38]. Again the D83C mutant is very similar to wt rhodopsin, while D83N exhibits slightly reduced activity (Fig. 4, Table 1). Apparently, the presence of an Asp residue at this position is less critical for the signaling activity of rhodopsin than reported for other GPCRs [1]. This also explains, why the substitution D83N is a natural variant in aquatic animals, and appears to be exploited to blue-shift the absorbance spectrum of visual pigments in adaptation to the spectral profile of the ecotope [39-42].

2.3.4 Structural studies using FT-IR difference spectroscopy

FT-IR difference spectroscopy is very sensitive to changes in protein structure, even at a very local level. We have used this technique to probe whether mutation of Asp83 leads to long-range structural perturbation. In addition, we have shown previously that vibrational changes in cysteine sulfhydryl (-SH) groups can be detected in the FT-IR difference spectrum around 2550 cm^{-1} [19]. This is an isolated region in the FT-IR difference spectrum that would allow to detect small changes in -SH vibrational activity, which is quite sensitive to changes in local structure or polarity. Since the

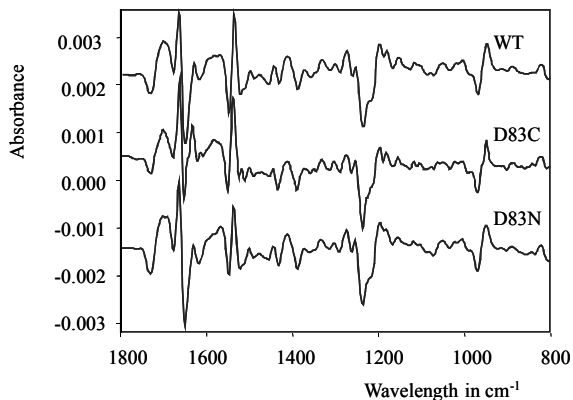


Fig. 5: FT-IR difference spectra of the Rho \rightarrow Meta I transition of wt rhodopsin, D83N and D83C. The 1800 - 800 cm^{-1} region is shown, where the major changes occur. Spectra were taken at -20°C , where the Meta I intermediate is stable.

carboxyl group of Asp83 reports local changes upon Meta II formation [14,16], we would expect that these changes would also be reflected in the Cys83 -SH vibration.

The FT-IR difference spectra of the Rho \rightarrow Meta I transition of the D83 mutants are nearly identical to wt rhodopsin (Fig. 5). The FT-IR difference spectra of the Rho \rightarrow Meta II transition of both mutants also are highly similar to wt rhodopsin (Fig. 6 and [14], accurately copying all positive and negative peaks in the 1700-800 cm^{-1} range. This is conclusive evidence that these Asp83 mutations do not induce long-range structural perturbation, and presents a structural basis for our observation that these mutations do not significantly affect receptor activity.

In addition, the Rho \rightarrow Meta II difference spectra present a highly reproducible pattern

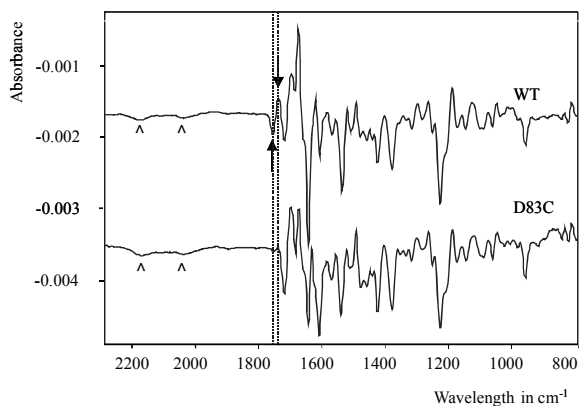


Fig. 6: FT-IR difference spectra of the Rho \rightarrow Meta II transition of wt rhodopsin and D83C. The 2300 - 800 cm^{-1} region is shown. The 2300 - 1900 cm^{-1} region shows band shifts (arrow heads), that indicate changes in proton continua, typical for H-bonded networks. Arrows point at the bilobal bands of the Asp83 carboxyl group, that are absent in the Asp83 mutants. Spectra were taken at 10°C and pH 6.0 and within 5 minutes of illumination, so as to minimize interference by the slow decay of Meta II (half life of ca 30 min under these conditions).

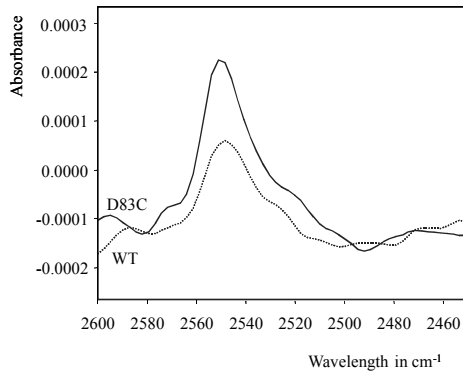


Fig. 7: FT-IR difference spectra of the Rho \rightarrow Meta II transition of wt rhodopsin and D83C. The 2600 - 2500 cm^{-1} region is shown where the stretch vibration of the sulfhydryl group absorbs. Spectra were scaled on the chromophore peaks at 1230 and 970 cm^{-1} (cf. Figure 6). The -SH band of the D83N mutant is very similar to wt and left out for clarity. The -SH band peaks at 2548 cm^{-1} (wt) and 2550 cm^{-1} (D83C), respectively.

of relatively weak, broad bandshifts in the 2300-1900 cm^{-1} region (Fig. 6, arrowheads). Such broad changes typically reflect rearrangements in extended H-bonded networks, that include water molecules (“proton continua”) [43-45]. This will be discussed elsewhere in more detail, but these data provide independent evidence for the presence of such networks in rhodopsin. The bandshifts are accurately reproduced in the D83C mutant, demonstrating that this mutation does not significantly affect the network rearrangements accompanying formation of Meta II.

Changes in the Rho \rightarrow Meta II difference spectrum of the mutants in comparison to the wt are obvious in the 1800-1700 cm^{-1} range (Fig. 6, arrows) and the 2600-2500 cm^{-1} range (Fig. 7). As reported previously [14,16], mutation of the Asp83 residue abolishes the corresponding carbonyl (C=O) stretch vibration of its β -carboxyl (COOH) group (arrows in Fig. 6, wt spectrum). This vibration exhibits bilobal bands, representing a significant frequency shift between rhodopsin (1767 cm^{-1}) and Meta II (1748 cm^{-1}), that can be interpreted as an increase in H-bonding interaction. The cysteine -SH group of course lacks carbonyl vibrations, explaining why these bilobal bands are absent from the D83C spectrum. The asparagine carboxamide group (CONH₂) does contain a carbonyl group, but its stretch vibration is shifted into the 1700-1600 cm^{-1} region [46]. However, new bands representing this carboxamide group are not apparent in the D83N spectrum [14]. This supports our view, that the side chain of Asn83 does not participate in a H-bonded network, and is not structurally involved in Meta II formation.

In the 2600-2500 cm^{-1} range, the mutants do contain a distinct band near 2550 cm^{-1} that can be assigned to -SH stretch vibrations [19]. However, the difference spectrum of the D83C mutant presents a significant increase in the sulfhydryl peak, with a slight shift in frequency (Fig. 7, Table 1). These effects can only be produced by the additional sulfhydryl group of Cys83. Hence, similar to the Asp83 carboxyl group, the Cys83 -SH group also reports on the local changes occurring upon formation of Meta II. Because the -SH peak is located in a very uncrowded spectral region and vibrational changes of a single residue can be measured on a background of native cysteines, the -SH peak reporter group can be exploited as a very sensitive, non-invasive reporter group for the analysis of local conformational changes using FT-IR difference spectroscopy .

Obviously, the spectral region between 1800 and 1740 cm^{-1} is nearly flat in the absence of the bilobal Asp83 bands (Fig. 6, and [14]). This contrasts recent results reported by Siebert and coworkers [47,48] which show a distinct bandshift in the Rho \rightarrow Meta II transition (1727 \rightarrow 1743 cm^{-1}) in rhodopsin reconstituted in dioleoyl-PC. This bilobal pair is insensitive to H- 2 H exchange, but does shift in dioleoyl-PC ^{13}C -labeled in the ester group. The authors conclude that these bands reflect a structural change in one strongly bound lipid residue upon Meta II formation. Remarkably, we have never observed these bands in Asp83 or Glu122 mutants prepared in our laboratory (Fig. 6 and [14,15]). Since we routinely reconstitute our recombinant rhodopsin preparations in retina lipid extracts that closely resemble the native rod outer segment lipids in composition and degree of unsaturation, we assume that this lipid interaction is much weaker in a highly unsaturated lipid environment. This might relate to an abundance of observations, that a less unsaturated lipid environment affects several rhodopsin properties, including the kinetics of Meta II formation and the equilibrium of the Meta I \leftrightarrow Meta II transition [13].

2.3.5 Conclusions

In order to investigate the role of aspartic acid 83 in the photoactivation of rhodopsin, we constructed the mutants D83C and D83N. The λ_{max} and the pH dependence of the MI \leftrightarrow MII equilibrium of D83C (495 nm; pKa = 6.6) are very close to those of wt rhodopsin (498 nm; pKa = 6.5). However, D83N shows a significant blueshift (492 nm) and the corresponding pKa is strongly upshifted. This agrees with earlier observations that Asp83 contributes to spectral tuning [39-42]. Our observation that at high pH and ionic strength the λ_{max} of wt (Asp83) downshifts to that of D83N suggests that the carboxyl proton of Asp83 is involved in wavelength regulation, and that this effect is uncoupled by deprotonation. Uncoupling is also effectuated by the D83N mutation which abolishes the acidic nature of the side chain. The D83N mutation likewise provokes a strong upshift of the pKa of the Meta I \rightarrow Meta II transition, suggesting that both phenomena are mediated by the same mechanism. FT-IR data [14,16] indicate that in rhodopsin the Asp83 carboxyl group (absorbing at 1767 cm^{-1}) is weakly H-bonded, and that this H-bond interaction becomes stronger in Meta II (1748 cm^{-1}). Furthermore, Asp83 may have H-bonding interaction probably through intermediate water molecules with Gly120, and possibly Glu113, in TM III [17]. In addition, the crystal structure of rhodopsin [12] suggests weak H-bonding interaction of Asp83 with residues in TM VII. Finally, the FT-IR data provide direct evidence for the presence of extended H-bonded networks in rhodopsin.

On basis of these data, we propose that Asp83 participates, through its β -carboxyl proton, in an extended H-bonding network that contributes to spectral tuning as well as to setting the pKa of the Meta I \leftrightarrow Meta II equilibrium. These effects are based upon long-range interactions and represent global protein properties. Hence, this cannot only involve local H-bonding interaction, but requires the contribution of a larger network. The D83N mutation, which abolishes the acidic nature of the side-chain, uncouples residue 83 from this network, leading to shifts in λ_{max} and pKa that in wt can only be effectuated by high pH and/or ionic strength [29,32]. Our FT-IR results show that in the mutant D83C, on the other hand, the still weakly acidic sulfhydryl group of Cys83 does participate in the H-bonding network, and apparently is able to largely maintain its wild-type properties. The acidic nature of the side-chain at position 83 might for instance be

required to allow partial deprotonation, or to allow rapid proton-transfer with a transient, deprotonated state.

The FT-IR difference spectra of the Rho → Meta I transition of both mutants are nearly identical to that of wt rhodopsin. The FT-IR difference spectra of the Rho → Meta II transition are also very similar to wt rhodopsin except for the bilobal Asp83 carboxyl peaks which disappear upon mutation of this residue. These structural observations agree with the functional analyses, showing that the mutations do not significantly affect receptor activity.

The participation of the sulfhydryl group in Meta II formation of D83C also manifests itself in a change in the vibrational properties of the sulfhydryl group, demonstrating that the -SH group can be used as a sensitive, non-invasive probe for local structural changes.

In summary, our results demonstrate that Asp83 does not play an essential role in signal transduction of rhodopsin, but provides a more structural contribution involving spectral tuning and photointermediate propagation. This requires participation in an extended H-bonded network where the proton-donating capacity of its side-chain are an important supplement to its H-bonding capacity.

References

1. Iismaa, T. P., Biden, T. J., and Shine, J. (1995). *G Protein-Coupled Receptors*. R.G. Landes company, Austin, USA.
2. Bownds, M. D. (1967). Site of attachment of retinal in rhodopsin. *Nature*, 216, 1178 - 1181.
3. Wang, K., McDowell, J. H., and Hargrave, P. A. (1980). Site of attachment of 11-*cis*-retinal in bovine rhodopsin. *Biochemistry-USA*, 19, 5111 - 5117.
4. Ovchinnikov, Y. A. (1982). Rhodopsin and bacteriorhodopsin: Structure-function relationships. *FEBS Lett.*, 148, 179 - 191.
5. Hofmann, K. P. (2000). Late photoproducts and signaling states of bovine rhodopsin in: *Molecular Mechanisms in Visual Transduction*, Stavenga, D. G., DeGrip, W. J., and Pugh, E. N., Jr., eds. (Elsevier Science Pub., Amsterdam, The Netherlands).
6. Emeis, D., Kühn, H., Reichert, J., and Hofmann, K. P. (1982). Complex formation between metarhodopsin II and GTP-binding protein in bovine photoreceptor membranes leads to a shift of the photoproduct equilibrium. *FEBS Lett.*, 143, 29 - 34.
7. Matthews, R. G., Hubbard, R., Brown, P. K., and Wald, G. (1963). Tautomeric forms of metarhodopsin. *J. Gen. Physiol.*, 47, 215 - 240.
8. Ostroy, S. E., Erhardt, F., and Abrahamson, E. W. (1966). Protein configuration changes in the photolysis of rhodopsin. II. The sequence of intermediates in thermal decay of cattle metarhodopsin in vitro. *Biochim. Biophys. Acta*, 112, 265 - 277.
9. Parkes, J. H. and Liebman, P. A. (1984). Temperature and pH dependence of the metarhodopsin I-Metarhodopsin II kinetics and equilibria in de bovine rod disk membrane suspensions. *Biochemistry-USA*, 23, 5054 - 5061.
10. Parkes, J. H., Gibson, S. K., and Liebman, P. A. (1999). Temperature and pH dependence of the metarhodopsin I - metarhodopsin II equilibrium and the binding of metarhodopsin II to G protein in rod disk membranes. *Biochemistry-USA*, 38, 6862 - 6878.
11. Hargrave, P. A. and McDowell, J. H. (1992). Rhodopsin and phototransduction - A model system for G-protein-linked receptors. *FASEB J.*, 6, 2323 - 2331.
12. Palczewski, K., Kumasaka, T., Hori, T., Behnke, C. A., Motoshima, H., Fox, B. A., LeTrong, I., Teller, D. C., Okada, T., Stenkamp, R. E., Yamamoto, M., and Miyano, M. (2000). Crystal structure of rhodopsin: A G protein-coupled receptor. *Science*, 289, 739 - 745.
13. DeGrip, W. J. and Rothschild, K. J. (2000). Structure and mechanism of vertebrate visual pigments in: *Molecular Mechanisms in Visual Transduction*, Stavenga, D. G., DeGrip, W. J., and Pugh, E. N., Jr., eds. (Elsevier Science Pub., Amsterdam, The Netherlands).
14. Rath, P., DeCaluwé, G. L. J., Bovee-Geurts, P. H. M., DeGrip, W. J., and Rothschild, K. J. (1993). Fourier transform infrared difference spectroscopy of rhodopsin mutants: Light activation of rhodopsin

- causes hydrogen-bonding changes in residue aspartic acid-83 during meta II formation. *Biochemistry-USA*, 32, 10277 - 10282.
15. DeCaluwé, G. L. J., Bovee-Geurts, P. H. M., Rath, P., Rothschild, K. J., and DeGrip, W. J. (1995). Effect of carboxyl mutations on functional properties of bovine rhodopsin. *Biophys. Chem.*, 56, 79 - 87.
 16. Fahmy, K., Jäger, F., Beck, M., Zvyaga, T. A., Sakmar, T. P., and Siebert, F. (1993). Protonation states of membrane-embedded carboxylic acid groups in rhodopsin and metarhodopsin II: A Fourier-transform infrared spectroscopy study of site-directed mutants. *Proc. Nat. Acad. Sci. USA*, 90, 10206 - 10210.
 17. Nagata, T., Terakita, A., Kandori, H., Shichida, Y., and Maeda, A. (1998). The hydrogen-bonding network of water molecules and the peptide backbone in the region connecting Asp83, Gly120, and Glu113 in bovine rhodopsin. *Biochemistry-USA*, 37, 17216 - 17222.
 18. Weitz, C. J. and Nathans, J. (1993). Rhodopsin activation: Effects on the metarhodopsin I-metarhodopsin II equilibrium of neutralization or introduction of charged amino acids within putative transmembrane segments. *Biochemistry-USA*, 32, 14176 - 14182.
 19. Rath, P., Bovee-Geurts, P. H. M., DeGrip, W. J., and Rothschild, K. J. (1994). Photoactivation of rhodopsin involves alterations in cysteine side chains: Detection of an S-H band in the meta I → meta II FTIR difference spectrum. *Biophys. J.*, 66, 2085 - 2091.
 20. Kunkel, T. A. (1985). Rapid and efficient site-specific mutagenesis without phenotypic selection. *Proc. Nat. Acad. Sci. USA*, 82, 488 - 492.
 21. Janssen, J. J. M., Bovee-Geurts, P. H. M., Merkx, M., and DeGrip, W. J. (1995). Histidine tagging both allows convenient single-step purification of bovine rhodopsin and exerts ionic strength-dependent effects on its photochemistry. *J. Biol. Chem.*, 270, 11222 - 11229.
 22. Summers, M. D. and Smith, G. E. (1987). A manual of methods for baculovirus vectors and insect culture procedures. *Texas Exp. Station Bulletin*, no.1555.
 23. DeCaluwé, G. L. J., VanOostrum, J., Janssen, J. J. M., and DeGrip, W. J. (1993). *In vitro* synthesis of bovine rhodopsin using recombinant baculovirus. *Meth. Neurosci.*, 15, 307 - 321.
 24. Possee, R. D. and Howard, S. C. (1987). Analysis of the polyhedrin gene promoter of the *Autographa californica* nuclear polyhedrosis virus. *Nucl. Acid. Res.*, 15, 10233 - 10248.
 25. Janssen, J. W. H., Bovee-Geurts, P. H. M., Peeters, A. P. A., Bowmaker, J. K., Cooper, H. M., David-Gray, Z. K., Nevo, E., and DeGrip, W. J. (2000). A fully functional rod visual pigment in a blind mammal - A case for adaptive functional reorganization? *J. Biol. Chem.*, 275, 38674 - 38679.
 26. Klaassen, C. H. W. and DeGrip, W. J. (2000). Baculovirus expression system for expression and characterization of functional recombinant visual pigments. *Meth. Enzymology*, 315, 12 - 29.
 27. Klaassen, C. H. W., Bovee-Geurts, P. H. M., DeCaluwé, G. L. J., and DeGrip, W. J. (1999). Large-scale production and purification of functional recombinant bovine rhodopsin using the baculovirus expression system. *Biochem. J.*, 342, 293 - 300.
 28. DeGrip, W. J., VanOostrum, J., and Bovee-Geurts, P. H. M. (1998). Selective detergent-extraction from mixed detergent/lipid/protein micelles, using cyclodextrin inclusion compounds: A novel generic approach for the preparation of proteoliposomes. *Biochem. J.*, 330, 667 - 674.
 29. DeLange, F., Merkx, M., Bovee-Geurts, P. H. M., Pistorius, A. M. A., and DeGrip, W. J. (1997). Modulation of the metarhodopsin I/metarhodopsin II equilibrium of bovine rhodopsin by ionic strength - Evidence for a surface charge effect. *Eur. J. Biochem.*, 243, 174 - 180.
 30. DeLange, F., Klaassen, C. H. W., Wallace-Williams, S. E., Bovee-Geurts, P. H. M., Liu, X.-M., DeGrip, W. J., and Rothschild, K. J. (1998). Tyrosine structural changes detected during the photoactivation of rhodopsin. *J. Biol. Chem.*, 273, 23735 - 23739.
 31. Fahmy, K. and Sakmar, T. P. (1993). Light-dependent transducin activation by an ultraviolet-absorbing rhodopsin mutant. *Biochemistry-USA*, 32, 9165 - 9171.
 32. Koutalos, Y. (1992). High-pH form of bovine rhodopsin. *Biophys. J.*, 61, 272 - 275.
 33. Pittler, S. J., Fliesler, S. J., and Baehr, W. (1992). Primary structure of frog rhodopsin. *FEBS Lett.*, 313, 103 - 108.
 34. Gibson, S. K., Parkes, J. H., and Liebman, P. A. (1999). Phosphorylation alters the pH-dependent active state equilibrium of rhodopsin by modulating the membrane surface potential. *Biochemistry-USA*, 38, 11103 - 11114.
 35. Weitz, C. J. and Nathans, J. (1992). Histidine residues regulate the transition of photoexcited rhodopsin to its active conformation, metarhodopsin II. *Neuron*, 8, 465 - 472.
 36. Imai, H., Kojima, D., Oura, T., Tachibana, S., Terakita, A., and Shichida, Y. (1997). Single amino acid residue as a functional determinant of rod and cone visual pigments. *Proc. Nat. Acad. Sci. USA*, 94, 2322 - 2326.
 37. Phillips, W. J. and Cerione, R. A. (1988). The intrinsic fluorescence of the α subunit of transducin - Measurement of receptor-dependent guanine nucleotide exchange. *J. Biol. Chem.*, 263, 15498 - 15505.
 38. Higashijima, T. and Ferguson, K. M. (1991). Tryptophan fluorescence of G proteins: Analysis of guanine nucleotide binding and hydrolysis. *Meth. Enzymology*, 195, 321 - 328.

39. Hunt, D. M., Fitzgibbon, J., Slobodyanyuk, S. J., and Bowmaker, J. K. (1996). Spectral tuning and molecular evolution of rod visual pigments in the species flock of cottoid fish in lake Baikal. *Vision Res.*, 36, 1217 - 1224.
40. Fasick, J. I. and Robinson, P. R. (1998). Mechanism of spectral tuning in the dolphin visual pigments. *Biochemistry-USA*, 37, 433 - 438.
41. Hope, A. J., Partridge, J. C., Dulai, K. S., and Hunt, D. M. (1997). Mechanisms of wavelength tuning in the rod opsins of deep-sea fishes. *Proc. Roy. Soc. London Ser. B*, 264, 155 - 163.
42. Fasick, J. I. and Robinson, P. R. (2000). Spectral-tuning mechanisms of marine mammal rhodopsins and correlations with foraging depth. *Visual Neurosci.*, 17, 781 - 788.
43. Wang, J. P. and El-Sayed, M. A. (2001). Time-resolved Fourier transform infrared spectroscopy of the polarizable proton continua and the proton pump mechanism of bacteriorhodopsin. *Biophys. J.*, 80, 961 - 971.
44. Zundel, G. (2000). Hydrogen bonds with large proton polarizability and proton transfer processes in electrochemistry and biology. *Advan. Chem. Phys.*, 111, 1 - 217.
45. Rammelsberg, R., Huhn, G., Lübber, M., and Gerwert, K. (1998). Bacteriorhodopsin's intramolecular proton-release pathway consists of a hydrogen-bonded network. *Biochemistry-USA*, 37, 5001 - 5009.
46. Barth, A. (2000). The infrared absorption of amino acid side chains. *Prog. Biophys. Mol. Biol.*, 74, 141 - 173.
47. Isele, J., Sakmar, T. P., and Siebert, F. (2000). Rhodopsin activation affects the environment of specific neighboring phospholipids: An FTIR spectroscopic study. *Biophys. J.*, 79, 3063 - 3071.
48. Beck, M., Siebert, F., and Sakmar, T. P. (1998). Evidence for the specific interaction of a lipid molecule with rhodopsin which is altered in the transition to the active state metarhodopsin II. *FEBS Lett.*, 436, 304 - 308.



Chapter 3

Development of a base-mutant for
cysteine scanning mutagenesis in
rhodopsin

Abstract

The contribution of most individual protein residues of rhodopsin to the photoactivation process, especially of those located in the transmembrane domain, is not or only poorly understood. Our first target was to study the involvement of residues in the second transmembrane helix in the activation mechanism of rhodopsin using cysteine scanning mutagenesis in combination with Fourier transform infrared (FT-IR) difference spectroscopy. Hereto single protein residues need to be replaced by a unique cysteine the -SH group of which is used as a reporter group. To prevent a large background in the introduced signal by native cysteines and possible reciprocal interactions of the introduced cysteine with native cysteine residues, we aimed to create a base-mutant in which all potentially active cysteine residues are substituted without major functional side-effects. We constructed a recombinant baculovirus expressing a cysteine-free mutant (SOH Δ C) in which all cysteines were replaced by serine except for the cysteines involved in the disulfide bridge. However, this construct yielded significant less functional protein than the corresponding wild type rhodopsin. Attempts to increase the amount of functional recombinant base-mutant by alternative cysteine substitutions were not successful, so far, and the properties of the Cys-Ser base-mutant SOH Δ C were further explored. This species could be purified with reasonable recovery, showed no significant free cysteine residue activity, and retained wild type-like functional activity according to FT-IR analysis. These properties would make it a suitable base-mutant.

3.1 Introduction

Recently, the 3D-crystal structure of ground-state rhodopsin was determined with a resolution of 2.8 Å [2]. The crystal structure gives detailed information on the structure of rhodopsin and its three-dimensional arrangement. However, it does not show which elements of the protein are involved in the photoactivation of rhodopsin. The role of most individual protein residues, especially of those located in the transmembrane domain, during the photoactivation of rhodopsin is not yet known. Chapter 2 describes that the carboxyl group of Asp83 as well as the sulfhydryl group of a cysteine residue at the same position report local changes upon Meta II formation. Asp83 forms part of a H-bonded network [2,4]. Since during Meta II formation major rearrangements occur in the H-bonded networks of rhodopsin [5,6] it is most likely that the second transmembrane domain (TM II) of rhodopsin is involved in and hence undergoes structural changes during photoactivation. Our first target will therefore be to study the involvement of second transmembrane helix residues in the activation mechanism of rhodopsin.

To investigate the contribution of residues of the second transmembrane helix we aim to use cysteine scanning mutagenesis in combination with Fourier transform infrared (FT-IR) difference spectroscopy. In cysteine scanning mutagenesis single protein residues are replaced by a cysteine, that then is used as a reporter group to analyse the structural and functional properties of a protein, here rhodopsin. FT-IR spectroscopy is a non-invasive technique; it uses no labels and therefore protein residues located in the intracellular and extracellular loops as well as those that are located in the transmembrane domain can be studied with minimal disturbance of the structure of the protein. In FT-IR difference spectroscopy the spectrum after illumination is subtracted

from the spectrum before illumination and thus only shows changes that occur during this phototransition. The -SH stretch vibration of the cysteine sulfhydryl groups can be detected in the 2500-2600 cm^{-1} region of the FT-IR difference spectrum [5,7]. This is an isolated region that allows to detect small changes in -SH vibrational activity, which is quite sensitive to local structural changes, without interference from other membrane components. However, the cysteine peak will appear on a background of native cysteines. This will require double-difference spectroscopy introducing additional errors and possibly obviating subtle changes in the newly introduced -SH group. To prevent a large background in the introduced signal by native cysteines and possible reciprocal interactions of introduced cysteines with native cysteine residues, we aimed to create a base-mutant in which all potentially active cysteine residues are substituted. The disulfide bond forms an important determinant of the stability of rhodopsin as well as the Meta II conformation [8] and is therefore retained. Next, the protein residues to be studied can be mutated into a cysteine for cysteine scanning mutagenesis studies.

This chapter describes the development of a suitable base-mutant that can be used in cysteine scanning mutagenesis using FT-IR difference spectroscopy. We started with a mutant in which all potentially reactive cysteines were replaced by a serine except for the cysteines 110 and 187 that form the disulfide bridge. Base-mutants in which most of the cysteines are replaced by serines have been used before in studies of other membrane proteins without disturbing their structural and functional properties [9,10]. Database analysis shows that serine is the most frequently occurring natural substitution for cysteine [11]. Valine is the second natural preference, but because valine is larger than serine and cannot engage in H-bonding interactions we preferred to use serine in our base-mutant. Alanine is a good alternative [11]. Alanine conserves the hydrophobic character, is smaller than cysteine and is in general structurally and functionally very well tolerated [12]. Computational data also suggest serine and alanine as suitable substitutes for cysteine [13]. Cysteine to methionine changes are less likely to occur in natural substitution [11], probably since methionine is sterically more demanding than cysteine, but it preserves the sulfur atom of cysteine, and hence could be an alternative to serine or alanine. Since previous single mutation of Cys167 and Cys264 into a serine on a wild type background resulted in lower functional yields and a decrease in stability (M.J.M. Portier-Vandeluytgaarden, unpublished results), we therefore also considered substitution of cysteine 167 and 264 for alanine or methionine.

3.2 Materials and methods

3.2.1 Cloning and expression

Synthetic, cysteine-free cDNA of bovine opsin (Synthetic Opsin His-tagged; SOH Δ C) was kindly provided by D. Oprian (Brandeis University, Waltham, USA) in the PMT vector. In SOH Δ C all cysteines have been replaced by a serine except for the cysteines of the disulfide bridge (Cys110 and Cys187). Unique restriction sites were introduced as silent mutations to allow modification by cassette mutagenesis and analysis by means of restriction enzymes. All constructs were extended with a 6X his-tag to allow rapid purification by immobilized metal affinity chromatography (IMAC) [14]. Mutants SOH Δ C/C167A and SOH Δ C/C167M were constructed by means of QuikChange Site-Directed Mutagenesis according to the manufacturer's instructions (Stratagene). The primers used for site-directed mutagenesis are described in Table 1. The PCR was

Mutant	forward	reverse
SOH ΔC/C167A	5'-GTCATGGCGCT <u>AGCCGCT</u> GCG GCCCCGCCGCTC-3'	5'-GAGCGGGGGGCCGC <u>AGCGGCT</u> AGGCCATGAC-3'
SOH ΔC/C167M	5'-ATGGCGCT <u>AGCCAT</u> GGCGGCC CCGCCGCTCGTCGGC-3'	5'-CGGCGGGGCCGCC <u>ATGGCT</u> AGC GCCATGACCCAGGT-3'
SOH ΔC/C264A	5'-CGCGCATGGTTATCATCATGG TCATCGCTTTCCTAATCGCTTGGC TGCCA-3'	5'-TATGGCAGCCA <u>AGCG</u> GATTAGGA AAGCGATGACCATGATGATAACCA TG-3'
SOH ΔC/C264M	5'-CGCGTATGGTTATCATCATGG TCATCGCTTTCCTAAT <u>CAT</u> TGGC TGCCC-3'	5'-TAGGGCAGCCAC <u>ATG</u> GATTAGGA AAGCGATGACCATGATGATAACCA TA-3'

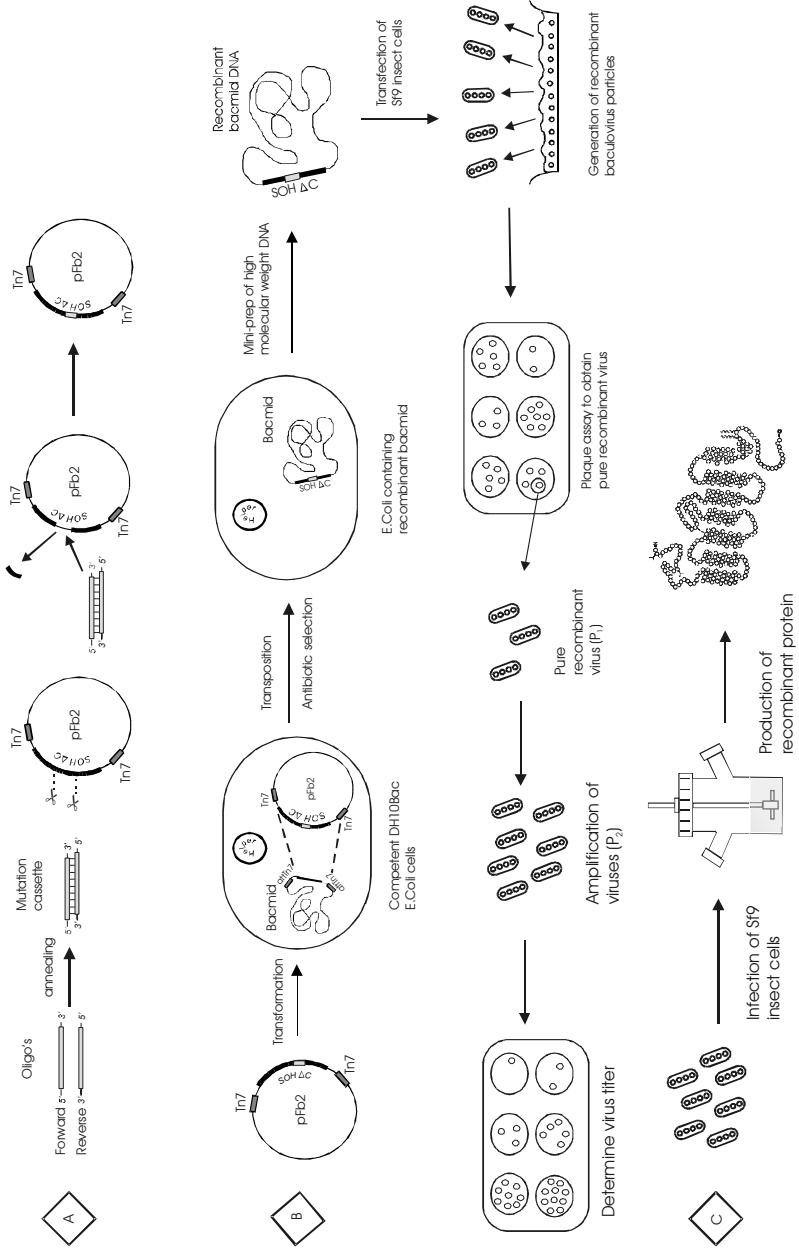
Table 1: Oligo nucleotides used for QuikChange Site-Directed Mutagenesis (C167 mutants) and cassette mutagenesis (C264 mutants). SOH ΔC/C167: the cysteine → alanine and the cysteine → methionine mutations respectively are underlined; substitution of C167 disrupts a Sfi I-site; the silent mutation introduced to create a Nhe I-site is indicated in italic. SOH ΔC/C264: the cysteine → alanine and the cysteine → methionine mutations respectively are underlined; the silent mutation introduced to remove the Mlu I-site (C264A) is indicated in bold; the silent mutation introduced to remove the Nde I-site (C264M) is indicated in italic.

performed on SOH ΔC in the pBluescript II SK⁻ vector as described in the manufacturer's manual with the following modifications: annealing temperature was 75°C and the reaction was run for 18 cycles with an extension time of 13 minutes at 72°C. Next, the SOH ΔC/C167 mutants were subcloned into the pFastbac DUAL vector under control of the polyhedrin promoter (Life Technologies Inc.) by means of restriction sites for BamH I and Not I. Mutants SOH ΔC/C264A and SOH ΔC/C264M were constructed by means of cassette mutagenesis (Fig. 1). For this purpose SOH ΔC was cloned into the pFastbac DUAL vector under control of the polyhedrin promoter by means of restriction sites for BamH I and Not I. The pFastbac DUAL vector was chosen since it can subsequently be used to generate recombinant baculovirus as will be discussed below. Part of the rhodopsin cDNA containing the mutation target was cut out of the SOH ΔC base-mutant using the restriction enzymes Mlu I and Nde I (Life Technologies Inc.). Next, a cassette containing the mutation and the corresponding restriction enzyme overhang was ligated into the base-mutant. The cassettes consist of a sense and an antisense oligo (Eurogentec), containing the desired mutation(s) (table 1). An Eppendorf cup containing the oligos (ratio forward: reverse = 1:1) was put in 100°C water and left to slowly cool down to room temperature (RT) to anneal the oligos and form the cassette. The cassettes contained a silent mutation to allow identification by means of restriction enzyme analysis. The mutants were checked by cycle-sequencing using primer 5'-cagttttgtaataaaaaaacctataaat-3' located in the polyhedrin region of the pFastbac DUAL vector or appropriate rhodopsin primers [15].

The Bac-to-bac Baculovirus recombination system (Life Technologies Inc.) was used to

Fig. 1: Mutation scheme from cDNA to recombinant protein. This figure shows the different stages in the generation of recombinant baculovirus from cDNA, suited to produce recombinant protein. **A:** two oligos, both containing the mutation of interest, are annealed to form a cassette which will be used in cassette mutagenesis. The cassette is exchanged with the target region in rhodopsin by means of restriction enzymes to obtain recombinant rhodopsin cDNA. **B:** The recombinant rhodopsin is transformed into DH10Bac E.Coli cells to obtain recombinant bacmid DNA. With this DNA Sf9 insect cells will be transfected. These cells will produce recombinant baculovirus containing the recombinant rhodopsin cDNA. After isolation of pure recombinant baculovirus, the virus titer is scaled up and determined by a plaque assay. **C:** Sf9 cells are infected with the recombinant baculovirus in order to produce recombinant protein.

Development of a rhodopsin base-mutant



generate recombinant baculovirus for expression of recombinant rhodopsin in the *Spodoptera frugiperda* Sf9 cell line. First, the transfer vector pFastbac DUAL containing our cDNA of interest was transformed into DH10Bac competent cells which contain a helper plasmid and bacmid DNA (containing the baculovirus genome) with an attachment site for the bacterial transposon Tn7 (mini-attTn7). The transfer vector contains a mini-Tn7 element flanking the promoter-insert region. After transformation, the mini-attTn7 site on the bacmid DNA that contains part of the *lacZα* gene is exchanged with aid of a transposase expressed by the helper plasmid for the mini-Tn7 element containing the rhodopsin cDNA. Colonies containing recombinant bacmid are identified by disruption of the *lacZα* gene. Next, high molecular weight mini-prep DNA was prepared from selected *E. Coli* clones containing the recombinant bacmid DNA. The selected colonies were inoculated into Luria-Bertani (LB) medium containing appropriate antibiotics and grown overnight at 37°C shaking at 250 to 300 r.p.m.. After centrifugation at 13,000 r.p.m. for 1 minute in an Eppendorff centrifuge the pellet containing the DH10Bac cells was resuspended in 0.3 ml solution I (15 mM Tris-HCl pH 8.0, 10 mM EDTA, 100 µg/ml RNase A) and lysed in 0.3 ml solution II (0.2 N NaOH, 1% SDS) for 5 minutes at room temperature. Subsequently, proteins and *E. Coli* genomic DNA were precipitated with 0.3 ml 3 M potassium acetate (pH 5.5) and the samples were put on ice for 5-10 minutes. After centrifugation at 13,000 r.p.m. for 10 minutes the supernatant was transferred to a tube containing 0.6 ml absolute isopropanol, gently mixed and put on ice for 5-10 minutes to precipitate the bacmid DNA. Next, the sample was centrifuged at 13,000 r.p.m. for 15 minutes and the pellet of bacmid DNA was rinsed with 70% ethanol, air dried and dissolved in TE pH 8.0 (10 mM Tris, 1 mM EDTA). This DNA was used to transfect Sf9 insect cells using CellFECTIN according to the manufacturer's instructions (Life technologies, Inc.) except for the culturing media used: instead of Sf-900 II SFM, InsectXpress medium (Cambrex) was used for incubation with the CellFECTIN-bacmid DNA mixture and subsequently the InsectXpress medium was replaced by TNM-FH medium (Grace's basal insect cell medium, plus 3.3 g/l yeastolate, 3.3 g/l lactalbumin hydrolysate and 5.5 g/l fraction V bovine serum albumin supplemented with 10% (v/v) fetal calf serum (PAA Laboratories GmbH), 50 units/ml penicilline and 50 µg/ml streptomycin (Life technologies, Inc.)). Generation and amplification of the isolated recombinant baculovirus was performed in a cell monolayer, cultured in TNM-FH, from which baculovirus was harvested at 4 days after transfection. To obtain pure recombinant baculovirus a plaque assay was performed. Sf9 insect cells were seeded in a 6 well plate, infected with a dilution series of the viral stock solution and covered with agarose (SeaPlaque, Biozym) to obtain single, monoclonal virus colonies. At 6-10 days post infection (d.p.i.) a single colony was picked and the virus was eluted from the agarose into TNM-FH medium. With this monoclonal virus Sf9 insect cells, seeded in a 6 well plate, were infected and the pure, recombinant virus was harvested at 6 d.p.i.. After harvesting, the recombinant virus (P₁) was tested for production of recombinant opsin by SDS-PAGE of total cellular protein followed by immunoblotting with an anti-rhodopsin antibody. Cells were harvested and lysed in milli-Q by freeze-thawing. After centrifugation at 13,000 r.p.m. for 10 minutes the pellet was resuspended in 200 µl milli-Q. 50 µl sample was solubilized for 10 min at RT in 2% SDS, 15 mM DTE, 15 mM Tris-HCl buffer pH 6.8, 10% glycerol, 0.006% bromophenol blue and milli-Q added to a final volume of 100 µl. SDS-polyacrylamide gel electrophoresis was performed in 12% (w/v) slab gels (0.7 mm thickness) using the (mini)ProteanII

equipment (Bio-Rad). 10 μ l of the solubilized sample was analyzed on gel. After separation by gel electrophoresis the proteins were electrophoretically transferred to nitrocellulose paper (Amersham) in blotting buffer (25 mM Tris, 200 mM glycine, 20% methanol) using the (mini)Trans-blot (Bio-Rad). Subsequently free protein binding sites on the nitrocellulose filter were blocked with 5% BSA in PBS. The blots were incubated with the first antibody (CERN922 1:10.00) diluted in PBS during the night at RT or for 2 hours at 37°C. After rinsing twice in excess PBS, primary antibody was localized via incubation with a second antibody (SAR, 1:300) (Dako) followed by incubation with a third antibody conjugated to peroxidase (RPAP, 1:500 in PBS) (Dako). After rinsing twice in excess PBS, the blots were incubated with the peroxidase substrate 4-chloro-1-naphthol (0.3% w/v in PBS containing 16.5% v/v methanol and 0.02% v/v H₂O₂). Incubation was stopped by rinsing with excess milli-Q when the desired staining intensity had been achieved.

The viral DNA was tested for the correct sequence of the rhodopsin insert by restriction enzyme analysis and sequencing of viral DNA. Isolation of viral DNA from the nucleus of Sf9 cells was performed as follows: infected Sf9 cells were lysed with lysis buffer (0.03 M Tris pH 7.5, 0.01 M MgAc, 1 % Nonidet P-40) and centrifuged briefly at 13,000 r.p.m.. The pellet, containing the nuclei, was resuspended in extraction buffer (100 mM Tris pH 7.5, 100 mM EDTA, 100 mM KCl) and incubated for 1 hour with 100 μ g/ml proteinase K and subsequently 1 hour with 1% SDS which dissolves the proteins and stimulates the activity of proteinase K. Next, the viral DNA was extracted from the solution by means of phenol/chloroform extraction, precipitated with 3 M NaAc and 100% ethanol and after centrifugation at 13,000 r.p.m. the pellet was dissolved in TE pH 8.0. The rhodopsin insert was amplified by means of polymerase chain reaction (PCR) with an annealing temperature of 60°C. The primers used were: 5'-cagtttgaataaaaaaacctataaat-3' (forward) and 5'-caaatgggatggctgattatg-3' (reverse). The PCR product was analyzed by means of restriction enzyme analysis or sequencing.

The recombinant virus was amplified by inoculating Sf9 insect cells seeded in a T₁₈₂ culture flask with 10 μ l P₁ virus and was harvested at 6 d.p.i. (P₂). To determine the virus titer a plaque assay was performed with 10⁵x-, 10⁶x- and 10⁷x-diluted virus. For expression of recombinant protein Sf9 cells were adapted to serum-free InsectXpress medium for suspension culture in 250-ml spinner flasks (Bellco) or in mono-layer culture in T₁₈₂ culture flasks. The cells were infected in mid log phase with a multiplicity of infection of 0.05-0.1, and finally harvested at 4 or 5 d.p.i. as described before [16,17].

3.2.2 Analysis of recombinant rhodopsins

The capacity of the recombinant opsins produced by Sf9 cells to bond with 11-*cis* retinal to form a photosensitive pigment was assayed by incubation of total cellular membrane preparations with a five-fold excess of 11-*cis* retinal in darkness or under dim red light (Schott 610 long pass filter), as described before [17]. Formation of photosensitive pigment was analyzed by recording UV-VIS spectra before (1) and after (2) illumination in the presence of 20 mM hydroxylamine [18] and is presented as difference spectra (1-2).

Total recombinant protein production was analyzed by SDS-PAGE (12% acrylamide) of total cellular protein as described earlier in this paragraph, except that after transfer of the proteins to nitrocellulose paper free protein binding sites on the nitrocellulose filter

were blocked in 5% BSA, 0.1% Tween-20 in PBS (w/v) for 15 min at RT. The blots were incubated with the first antibody (CERN922 1:20.000) diluted in PBS, 0.05% Tween-20 over night at RT or for 2 hours at 37°C. After rinsing twice in excess PBS, 0.05% Tween-20, detection was accomplished using a second antibody (GARPO 1:10.000). The blots were incubated with GARPO for 1-2 hours at RT. Next, the blots were rinsed in excess PBS, 0.05% Tween-20 and incubated for 5 min at RT with a 10 times diluted solution of Lumino/Enhancer solution - Stable Peroxide Solution (1:1) (Pierce). The signal was transferred to an autoradiographic film by incubation for 10-60 sec with the nitrocellulose blot in the dark. Finally, the film was developed in a Kodak x-Omat 2000 processor.

SOH Δ C and wild type (wt) rhodopsin were purified by means of IMAC as described before [14,16] except that SOH Δ C was extracted in CHAPS/nonylglycose (1% w/v) and purified in nonylglycose. After purification the pigment was reconstituted into retina lipids as described previously [19].

FT-IR analyses were performed on a Bruker IFS 66v/S spectrometer equipped with a liquid nitrogen-cooled MCT detector. Spectra were taken at 8 cm⁻¹ resolution. Sample temperature was computer-controlled using an ADP cryostat (Advanced Research Systems Inc.). Samples, prepared by isopotential spin-drying 2-3 nmol of pigment on an AgCl window (Fisher Scientific Co.), were rehydrated with 1 μ l of buffer and sealed using a second AgCl window and a rubber O-ring spacer as described [1,20,21]. Samples were illuminated in the spectrometer using a 150 W halogen lamp equipped with a fiber optical ring (Schott). Each spectrum consists of 2560 scans taking about 2 min to record in the dark, followed by similar blocks of spectra after illumination. Difference spectra were calculated by subtracting these blocks of spectra. Meta I was analyzed by cooling to 253 K and irradiation with yellow light (OG530, 2 min). Meta II was generated in the same way and analyzed at 283 K.

The -SH content of rhodopsin and mutants was determined by reaction with DTNB in 1% SDS as described in [22].

3.3 Results

The capacity of the recombinant opsins to bond with 11-*cis* retinal to form a photosensitive pigment was analysed by measuring the UV-VIS spectrum before and after illumination. Subtraction of the spectrum after illumination from the spectrum before illumination gives a difference spectrum, where interference with e.g. sloping

	% of wt
wt	100
SOH Δ C	26 \pm 12 (n = 5)
SOH Δ C/C264A	20 \pm 7 (n = 3)
SOH Δ C/C264M	n.d.

Table 2: Production of functional protein of various base-mutants. The amount of functional protein produced by wild type rhodopsin (wt) is set at 100%. n.d.: not detectable. Average of at least three independent assays are given with SD.

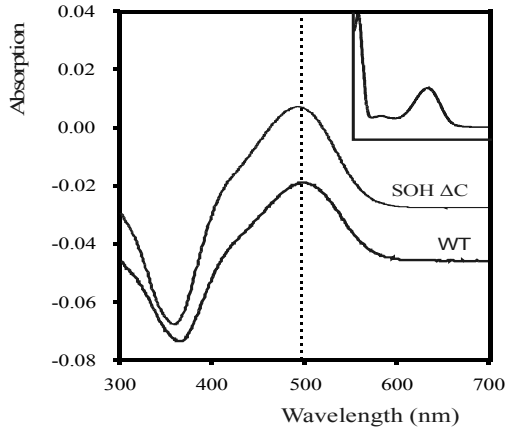


Fig. 2: Absorbance dark-minus light difference spectra of wild type rhodopsin and SOH Δ C after purification. Spectra were obtained by subtracting a spectrum after illumination in the presence of 20 mM hydroxylamine from the original spectrum before illumination. Illumination then produces the all-*trans*-retinoxime absorbing at 365 nm. Note that SOH Δ C shows a blue-shift (λ_{max} : 498 \rightarrow 492 nm). Insert: absorbance spectrum of purified SOH Δ C.

baselines is cancelled out. This allows a better estimation of the λ_{max} and the amount of recombinant protein that is produced. Figure 2 shows the spectra of wild type rhodopsin and SOH Δ C. The spectrum of SOH Δ C is similar in bandshape to that of wild type rhodopsin but shows a blue-shift (λ_{max} : 498 nm \rightarrow 492 nm). The recombinant proteins were analysed for production of functional rhodopsin at several d.p.i.. Relative to the amount of wild type rhodopsin produced (\equiv 100%) SOH Δ C only produced $26\% \pm 12$ functional pigment (Table 2).

Figure 3 shows total protein production analyzed by SDS-PAGE and immunoblotting. SOH Δ C yielded a protein product represented by a band near 38 kDa similar to wild type rhodopsin that as demonstrated before [23] corresponds to fully glycosylated opsin (Fig. 3, thick arrow). In contrast to wild type rhodopsin which yields large quantities of glycosylated protein, SOH Δ C produced significantly more non-glycosylated protein [23] (Fig. 3, thin arrow). It is also clear that non-glycosylated protein is only poorly extracted into detergent solution (+ lanes).

Because of the low amount of functional protein, production of SOH Δ C was not very satisfactory. We decided to test whether A/M mutation of C167 and C264 would improve functional levels. Unfortunately, the SOH Δ C/C264 mutants behaved even worse. SOH Δ C/C264A produced only $20\% \pm 7$ functional protein relative to wild type, whereas for SOH Δ C/C264M no functional protein could be detected. Both SOH Δ C/C264A and SOH Δ C/C264M produced even larger quantities of non-glycosylated protein than SOH Δ C. Again, non-glycosylated protein was poorly (C264A) or hardly (C264M) solubilized. At this stage, we were not able to test mutants SOH Δ C/C167A and SOH Δ C/C167M for either production of functional rhodopsin or total opsin production.

In view of these results we decided to select SOH Δ C as base-mutant for cysteine scanning. Since this would also require proper purification and retention of functional properties very similar to wild type, these aspects were addressed subsequently.

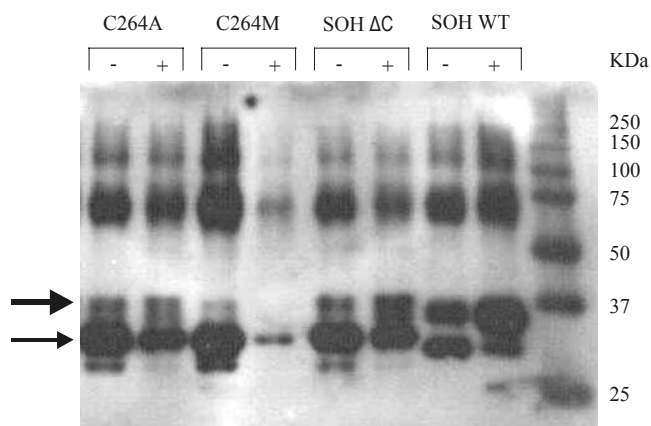


Fig. 3: Immunoblot analysis of total protein production of Sf9 cells infected with recombinant baculovirus expressing wild type rhodopsin, SOH Δ C, SOH Δ C/C264A and SOH Δ C/C264M. Blots were screened with primary antibody CERN922 (polyclonal). Each lane was loaded with 1000 cells. The lanes indicated with - show samples before solubilization (4 d.p.i.), lanes indicated with + show (rhodopsins after extraction in DoM (5 d.p.i)). The thick arrow indicates glycosylated opsin, the thin arrow non-glycosylated opsin. The bands at $M_w > 50$ kD represent oligomers, mainly of non-glycosylated species, artificially produced upon solubilization in SDS [22,33].

Purification was based on the approach developed for wild type rhodopsin [14,24]. In short: regenerated rhodopsin was purified by means of IMAC using a Ni^{2+} -nitrilotriacetic acid (NTA) column. The pigment was dissolved in Dodecylmaltose (DOM), applied to the column (10 μl matrix per nmol rhodopsin) and purified using the same buffer containing nonylglucoside and increasing concentrations histidine to eventually elute rhodopsin from the column. In contrast to wild type rhodopsin, extraction of SOH Δ C in DOM was poor and a CHAPS/nonylglucose (1:1) mixture was selected as detergent to extract the pigment. Elution was performed in nonylglucose since this detergent is easier removed for reconstitution. SOH Δ C was purified with $40\% \pm 14$ ($n = 2$) recovery, with a purity of 60 – 70% (ratio $280/492 = 2.8$) and gave a spectrum that is very similar to wild type (Fig. 2). Wild type rhodopsin was purified with 40 - 70% ($n = 10$) recovery and a purity of 70 – 90%. After purification, SOH Δ C was reconstituted into a native bovine retina lipid environment using a method based upon cyclodextrin extraction [14,24]. SOH Δ C was reconstituted with about 50% recovery where wild type was reconstituted with at least 80% recovery. Reconstitution further improved the purity to over 80%.

Next, SOH Δ C was tested on functional properties. We estimated the number of -SH groups per mole of pigment by their reactivity with DTNB. We found 5.6 ± 0.2 per mole of pigment for wild type rhodopsin ($n = 4$) and 0.08 for SOH Δ C, in agreement with the six cysteines in wild type rhodopsin and the lack of cysteines in SOH Δ C. This also demonstrates that at least 96% of the Cys110 and Cys187 residues have generated a disulfide bond. To analyse the photoinduced structural changes in SOH Δ C, FT-IR difference spectroscopy was performed. Figure 4 shows the 1800-1500 cm^{-1} region of the FT-IR difference spectrum of the rhodopsin \rightarrow Meta II transition. This region defines Meta II and is very similar between SOH Δ C and wild type rhodopsin. In particular the bilobal peak of the Asp83 carboxyl group at 1767 and 1748 cm^{-1} [1] and the band at 1712 cm^{-1} reflecting Glu113 protonation [3] are typical for a functional

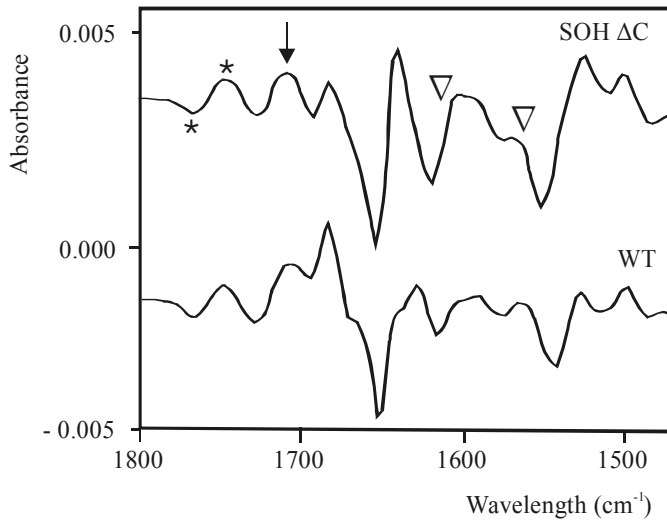


Fig. 4: The 1800-1500 cm^{-1} region of the FT-IR difference spectra of the rhodopsin \rightarrow Meta II transition of wild type rhodopsin and base-mutant SOH Δ C. This region e.g. shows the bilobal peak of the Asp83 carboxyl group (*) at 1767 and 1748 cm^{-1} [1] and E113 protonation (\downarrow) at 1712 cm^{-1} [3]. Note that the difference spectrum of SOH Δ C is very similar to that of wild type rhodopsin: Although intensities may differ somewhat, most peak frequencies are accurately reproduced. Slight changes in Amide I and II peaks (∇) indicate very small, hence subtle differences in secondary structure. Spectra were scaled on the chromophore peaks at 1230 and 970 cm^{-1} .

rhodopsin to Meta II transition. Figure 5 shows the 2600 - 2500 cm^{-1} region of the rhodopsin \rightarrow meta II transition which contains the sulfhydryl (-SH) vibration of cysteine. Wild type rhodopsin shows a -SH vibration pattern around 2548 cm^{-1} , while SOH Δ C only exhibits base-line noise in this region

3.4 Discussion

3.4.1 Novel application of cysteine scanning mutagenesis: combination with FT-IR difference spectroscopy

To investigate the involvement of protein residues of the second transmembrane segment in the photoactivation mechanism of rhodopsin we aim to use cysteine scanning mutagenesis in combination with FT-IR difference spectroscopy. Cysteine scanning mutagenesis is a technique which uses cysteines as a reporter group to study the structural and functional properties of a protein, here rhodopsin. Single amino acids are replaced by a cysteine residue and a variety of methods is available as described in Chapter 1, to probe the properties of this cysteine residue. FT-IR spectroscopy can directly probe the cysteine sulfhydryl group, hence does not need chemical modification, which only indirectly reports on the dynamics and microenvironment of the residue. Another important advantage of the no-modification requirement is that all protein residues are accessible, including buried or highly constrained ones. In FT-IR

difference spectroscopy the spectrum of a photointermediate is subtracted from the “dark” spectrum, which highlights the changes that occur during this transition. Vibrational changes in cysteine sulfhydryl (-SH) groups can be detected in the FT-IR difference spectrum around 2550 cm^{-1} [5,7]. The -SH group is very sensitive to changes in local structure and polarity and small structural changes can therefore easily be observed. The $2500\text{-}2600\text{ cm}^{-1}$ region is an isolated region in the FT-IR difference spectrum. This, in combination with the environmental sensitivity of the -SH group of cysteine, makes it possible to detect relatively small changes in -SH vibrational activity. Protein residues that are replaced by a cysteine and that are structurally active, i.e. undergo a change in their micro-environment during the rhodopsin photocascade, will give rise to a difference peak in the $2500\text{-}2600\text{ cm}^{-1}$ region of the FT-IR difference spectrum. However, this peak will appear on a background reflecting changes in native cysteines. To avoid this background as well as possible reciprocal interactions with native cysteine residues, we wanted to create a base-mutant in which all potentially active cysteine residues are substituted. Subsequently, protein residues to be probed can be mutated into a cysteine for cysteine scanning mutagenesis studies.

3.4.2 Base-mutant

In SOH Δ C all cysteine residues were replaced by serine except for the cysteines involved in the disulfide bridge. The disulfide bridge is formed by residues Cys110 and Cys187 and is conserved in all known visual pigments and many transmembrane receptors that are coupled to G proteins [25-28]. The disulfide bond forms an important determinant in the thermal stability of rhodopsin as well as its photointermediates and in coupling to G protein activation [8].

Cysteine and serine differ only in the hetero-atom in the side chain and replacement of

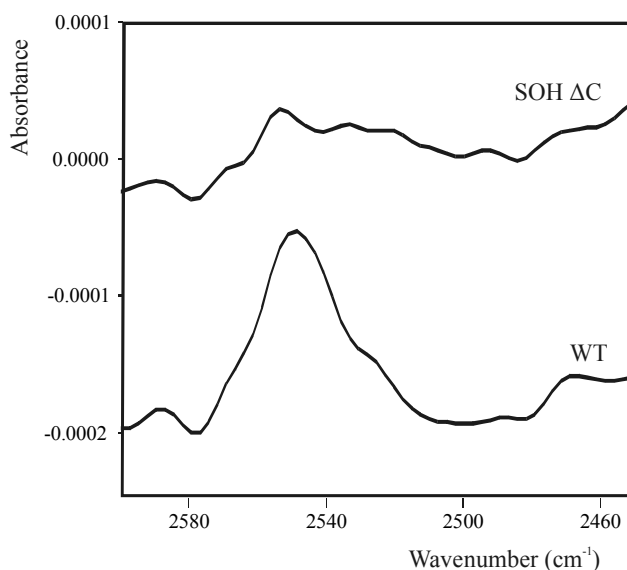


Fig. 5: The -SH stretch region in the FT-IR difference spectra of the rhodopsin \rightarrow Meta II transition of wild type rhodopsin and base-mutant SOH Δ C. In this region the stretch vibration of sulfhydryl groups appears around 2550 cm^{-1} . Spectra were scaled on the chromophore peaks at 1230 and 970 cm^{-1} .

cysteine by serine involves the exchange of two relatively small side chains. Unfortunately, we observed that baculovirus expression produced SOH Δ C in significant less functional yield than wild type rhodopsin. In fact, in a previous study using COS cells for expression of SOH Δ C-like mutants production of functional protein was also lower than that of wild type protein [29]. In addition, the absorbance band of SOH Δ C was blue-shifted relative to wild type (λ_{max} : 498 nm \rightarrow 492 nm). The shift in λ_{max} is probably due to the C176S mutation, since the single C167S mutant exhibits the same blue shift (M.J.M. Portier-VandeLuytgaarden, unpublished results). Rhodopsin requires posttranslational modifications like palmitoylation, disulfide bridge formation and glycosylation to fulfil its structural and functional activities. Analysis of total protein production on Western blot showed that SOH Δ C produced much less glycosylated and much more non-glycosylated protein than wild type rhodopsin. The relatively high amount of non-glycosylated protein in SOH Δ C probably reflects the presence of large amounts of incorrectly folded protein [30], which would explain the relative low yield of functional protein for SOH Δ C (26%) in comparison to wild type rhodopsin. Incorrect folding will enhance aggregation of the protein that also may explain the much lower solubility of the non-glycosylated protein in solutions of mild detergents (Fig. 3).

To obtain sufficient amounts of functional SOH Δ C protein for purification and further experiments, large culture volumes will be necessary. Apart from the costs, the relatively large amount of non-functional protein will also hamper protein purification, which will lead to lower recovery of functional protein (P. Bovee-Geurts, unpublished results). We therefore attempted to increase the amount of functional recombinant base-mutant by alternative cysteine substitutions. Some cysteine to serine mutants of the platelet activating factor were not delivered to the plasma membrane and failed to demonstrate ligand binding in contrast to the corresponding cysteine to alanine mutants [8,31]. Base-mutants in which cysteine residues were replaced by alanine have successfully been used before in studies of membrane proteins [32] in agreement with evolutionary studies showing that alanine is a relatively frequent occurring substitute for cysteine [11]. Methionine is not a natural substitute and is larger than cysteine but it also carries a hydrophobic side chain and retains the sulfur atom. Therefore, we tested whether selected replacement by alanine and methionine would improve base-mutant expression. Residues Cys167 and Cys264 form part of the retinal binding site and are shown to be structurally active during photoactivation (DeGrip et al., unpublished results). The single mutants C167S and C264S on a wild type background already showed lower levels of functional protein and reduced stability during purification (M.J.M. Portier-VandeLuytgaarden, unpublished results). Mutation of cysteine into a serine involves the replacement of a relatively hydrophobic side chain by a relatively hydrophylic side chain and might disturb subtle elements in chromophore binding or binding site organization and thus impair formation of functional protein. Hence, we aimed to examine whether substitution of cysteine 167 or 264 by an alanine or a methionine would increase the expression level of functional recombinant base-mutant. So far, we have not yet been able to test production of SOH Δ C/C167 mutants. The C264A/M mutants generated total levels of recombinant protein comparable to SOH Δ C and wild type. However, the production level of functional recombinant protein by mutant SOH Δ C/C264A was even less than that of SOH Δ C, whereas SOH Δ C/C264M mainly generated intact but non-glycosylated protein with very little production of functional protein. Non-glycosylated C264A again demonstrated much lower solubility

in mild detergent solution, while non-glycosylated C264M was hardly detected. SOH Δ C/C264M probably displays a serious folding defect leading to a very aggregation-prone protein. The relatively large side chain of methionine apparently severely disturbs proper folding.

We conclude that substitution of Cys264 by an alanine or a methionine does not improve the production of functional protein relative to SOH Δ C. Since the highest functional expression levels of cysteine-free rhodopsins were still obtained for SOH Δ C and this species could be purified with reasonable recoveries ($40\% \pm 14$), showed no significant free cysteine residue activity, and retained wild type-level functional activity according to FT-IR analysis, we decided to use SOH Δ C as a base-mutant for our subsequent cysteine scanning mutagenesis studies.

References

- Rath, P., DeCaluwé, G. L. J., Bovee-Geurts, P. H. M., DeGrip, W. J., and Rothschild, K. J. (1993). Fourier transform infrared difference spectroscopy of rhodopsin mutants: Light activation of rhodopsin causes hydrogen-bonding changes in residue aspartic acid-83 during meta II formation. *Biochemistry-USA*, 32, 10277 - 10282.
- Palczewski, K., Kumasaka, T., Hori, T., Behnke, C. A., Motoshima, H., Fox, B. A., LeTrong, I., Teller, D. C., Okada, T., Stenkamp, R. E., Yamamoto, M., and Miyano, M. (2000). Crystal structure of rhodopsin: A G protein-coupled receptor. *Science*, 289, 739 - 745.
- Fahmy, K., Jäger, F., Beck, M., Zvyaga, T. A., Sakmar, T. P., and Siebert, F. (1993). Protonation states of membrane-embedded carboxylic acid groups in rhodopsin and metarhodopsin II: A Fourier-transform infrared spectroscopy study of site-directed mutants. *Proc. Nat. Acad. Sci. USA*, 90, 10206 - 10210.
- Okada, T., Fujiyoshi, Y., Silow, M., Navarro, J., Landau, E. M., and Shichida, Y. (2002). Functional role of internal water molecules in rhodopsin revealed by x-ray crystallography. *Proc. Nat. Acad. Sci. USA*, 99, 5982 - 5987.
- Breikers, G., Bovee-Geurts, P. H. M., DeCaluwé, G. L. J., and DeGrip, W. J. (2001). A structural role for Asp83 in the photoactivation of rhodopsin. *Biol. Chem.*, 382, 1263 - 1270.
- Nagata, T., Terakita, A., Kandori, H., Shichida, Y., and Maeda, A. (1998). The hydrogen-bonding network of water molecules and the peptide backbone in the region connecting Asp83, Gly120, and Glu113 in bovine rhodopsin. *Biochemistry-USA*, 37, 17216 - 17222.
- Rath, P., Bovee-Geurts, P. H. M., DeGrip, W. J., and Rothschild, K. J. (1994). Photoactivation of rhodopsin involves alterations in cysteine side chains: Detection of an S-H band in the meta I \rightarrow meta II FTIR difference spectrum. *Biophys. J.*, 66, 2085 - 2091.
- Davidson, F. F., Loewen, P. C., and Khorana, H. G. (1994). Structure and function in rhodopsin: Replacement by alanine of cysteine residues 110 and 187, components of a conserved disulfide bond in rhodopsin, affects the light-activated metarhodopsin II state. *Proc. Nat. Acad. Sci. USA*, 91, 4029 - 4033.
- Frillingos, S., Sahin-Tóth, M., Persson, B., and Kaback, H. R. (1994). Cysteine-scanning mutagenesis of putative helix VII in the lactose permease of *Escherichia coli*. *Biochemistry-USA*, 33, 8074 - 8081.
- Casey, J. R., Ding, Y., and Kopito, R. R. (1995). The role of cysteine residues in the erythrocyte plasma membrane anion exchange protein, AE1. *J Biol. Chem.*, 270, 8521 - 8527.
- Jones, D. T., Taylor, W. R., and Thornton, J. M. (1994). A mutation data matrix for transmembrane proteins. *FEBS Lett.*, 339, 269 - 275.
- Ward, W. H., Timms, D., and Fersht, A. R. (1990). Protein engineering and the study of structure-function relationships in receptors. *Trends Pharmacol. Sci.*, 11, 280 - 284.
- Donnelly, D., Overington, J. P., Ruffe, S. V., Nugent, J. H. A., and Blundell, T. L. (1993). Modeling a-helical transmembrane domains: The calculation and use of substitution tables for lipid-facing residues. *Protein Sci.*, 2, 55 - 70.
- Janssen, J. J. M., Bovee-Geurts, P. H. M., Merckx, M., and DeGrip, W. J. (1995). Histidine tagging both allows convenient single-step purification of bovine rhodopsin and exerts ionic strength-dependent effects on its photochemistry. *J. Biol. Chem.*, 270, 11222 - 11229.
- DeCaluwé, G. L. J., VanOostrum, J., Janssen, J. J. M., and DeGrip, W. J. (1993). In vitro synthesis of bovine rhodopsin using recombinant baculovirus. *Meth. Neurosci.*, 15, 307 - 321.

16. Klaassen, C. H. W., Bovee-Geurts, P. H. M., DeCaluwé, G. L. J., and DeGrip, W. J. (1999). Large-scale production and purification of functional recombinant bovine rhodopsin using the baculovirus expression system. *Biochem. J.*, 342, 293 - 300.
17. Klaassen, C. H. W. and DeGrip, W. J. (2000). Baculovirus expression system for expression and characterization of functional recombinant visual pigments. *Meth. Enzymology*, 315, 12 - 29.
18. Janssen, J. W. H., Bovee-Geurts, P. H. M., Peeters, A. P. A., Bowmaker, J. K., Cooper, H. M., David-Gray, Z. K., Nevo, E., and DeGrip, W. J. (2000). A fully functional rod visual pigment in a blind mammal - A case for adaptive functional reorganization? *J. Biol. Chem.*, 275, 38674 - 38679.
19. DeGrip, W. J., VanOostrum, J., and Bovee-Geurts, P. H. M. (1998). Selective detergent-extraction from mixed detergent/lipid/protein micelles, using cyclodextrin inclusion compounds: A novel generic approach for the preparation of proteoliposomes. *Biochem. J.*, 330, 667 - 674.
20. DeLange, F., Merckx, M., Bovee-Geurts, P. H. M., Pistorius, A. M. A., and DeGrip, W. J. (1997). Modulation of the metarhodopsin I/metarhodopsin II equilibrium of bovine rhodopsin by ionic strength - Evidence for a surface charge effect. *Eur. J. Biochem.*, 243, 174 - 180.
21. Clark, N. A., Rothschild, K. J., Simon, B. A., and Luippold, D. A. (1980). Surface induced orientation of multilayer membrane arrays: Theoretical analysis and a new method with application to purple membrane fragments. *Biophys. J.*, 31, 65 - 96.
22. DeGrip, W. J., VanDeLaar, G. L. M., Daemen, F. J. M., and Bonting, S. L. (1973). Sulfhydryl groups and rhodopsin photolysis. *Biochim. Biophys. Acta*, 325, 315 - 322.
23. Janssen, J. J. M., Mulder, W. R., DeCaluwé, G. L. J., Vlak, J. M., and DeGrip, W. J. (1991). In vitro expression of bovine opsin using recombinant baculovirus: The role of glutamic acid (134) in opsin biosynthesis and glycosylation. *Biochim. Biophys. Acta*, 1089, 68 - 76.
24. Bosman, G. J. C. G. M., VanOostrum, J., Breikers, G., Bovee-Geurts, P. H. M., Klaassen, C. H. W., and DeGrip, W. J. (2003). Functional expression of his-tagged rhodopsin in Sf9 insect cells. *Meth. Mol. Biol.*, 228, 73 - 86.
25. Applebury, M. L. and Hargrave, P. A. (1986). Molecular biology of the visual pigments. *Vision Res.*, 26, 1881 - 1895.
26. Dixon, R. A., Kobilka, B. K., Strader, D. J., Benovic, J. L., Dohlman, H. G., Frielle, T., Bolanowski, M. A., Bennett, C. D., Rands, E., Diehl, R. E., Mumford, R. A., Slater, E. E., Sigal, E. S., Caron, M. G., Lefkowitz, R. J., and Strader, C. D. (1986). Cloning of the gene and cDNA for mammalian β -adrenergic receptor and homology with rhodopsin. *Nature*, 321, 75 - 79.
27. Julius, D., MacDermott, A. B., Jessel, T. M., Huang, K., Molineaux, S., Schieren, I., and Axel, R. (1988). Functional expression of the 5-HT_{1c} receptor in neuronal and nonneuronal cells. *Cold Spring Harb. Symp. Quant. Biol.*, 53, 385 - 393.
28. Krause, J. E., Hershey, A. D., Dykema, P. E., and Takeda, Y. (1990). Molecular biological studies on the diversity of chemical signalling in tachykinin peptidergic neurons. *Ann. N. Y. Acad. Sci.*, 579, 254 - 272.
29. Karmik, S. S., Sakmar, T. P., Chen, H.-B., and Khorana, H. G. (1988). Cysteine residues 110 and 187 are essential for the formation of correct structure in bovine rhodopsin. *Proc. Nat. Acad. Sci. USA*, 85, 8459 - 8463.
30. Webel, R., Menon, I., O'Tousa, J. E., and Colley, N. J. (2000). Role of asparagine-linked oligosaccharides in rhodopsin maturation and association with its molecular chaperone, NinaA. *J. Biol. Chem.*, 275, 24752 - 24759.
31. LeGouill, C., Parent, J.-L., Rola-Pleszczynski, M., and Staňková, J. (1997). Role of the Cys90, Cys95 and Cys173 residues in the structure and function of the human platelet-activating factor receptor. *FEBS Lett.*, 402, 203 - 208.
32. Lane, L. K. (1993). Functional expression of rat α 1 Na,K-ATPase containing substitutions for cysteines 454, 458, 459, 513 and 551. *Biochem. Mol. Biol. Int.*, 31, 817 - 822.



Chapter 4

Cysteine scanning mutagenesis in
rhodopsin on a cysteine-free
background

Abstract

A Cys → Ser-mutant of rhodopsin (SOH ΔC) was selected as base-mutant for cysteine scanning mutagenesis. Previously we showed that this base-mutant shows wild-type functional behaviour according to FT-IR analysis. Here, this is complemented with G-protein activation studies, demonstrating that it retains full activity in this respect, as well.

Earlier experiments indicate that residue Asp83, located in the second transmembrane domain of rhodopsin, contributes to spectral tuning and photoactivation, the two major functional elements of visual pigments. Our first target was therefore to study the involvement of residues of the second transmembrane segment in these processes. In this chapter we describe the construction, production and analysis of single cysteine mutants of residues 74-90 of this transmembrane segment of rhodopsin. Unexpectedly, most mutants produce little or no functional protein, show poor glycosylation and are largely retained intracellularly, suggesting major folding defects. The reason for this remains largely unclear. A relationship may appear between the extent of conservation of a protein residue and the amount of glycosylated, functional rhodopsin mutant produced. However, this needs further investigation. Remarkably some single-cys mutations resulted in relatively high levels of functional protein. One of these, mutant L77C, could already be purified and partially analyzed. It exhibits similar properties as the base-mutant and no evidence for contribution of residue 77 to the photoactivation process. This is plausible, since according to the crystal structure, L77 is located in the lipid face of TM II and hence probably inserted in the lipid matrix.

4.1 Introduction

Rhodopsin is a membrane-spanning protein containing seven transmembrane segments (TM), which requires posttranslational modification (thiopalmitylation, disulfide bridge formation, glycosylation) and subsequently targeting to the rod outer segment membrane to fulfil its structural and functional tasks. Rhodopsin belongs to the family of G protein-coupled receptors and is a unique member of this family because its ligand, 11-*cis* retinal, is covalently bound to the protein, opsin. The visual process begins with the absorption of light by rhodopsin inducing ultrafast *cis/trans* isomerization of the ligand after which photoexcited rhodopsin relaxes via a series of transient photointermediates (Rhodopsin → Bathorhodopsin (Batho) ↔ Blue-shifted-intermediate (BSI) → Lumirhodopsin (Lumi) → Metarhodopsin I (Meta I) ↔ Metarhodopsin II (Meta II) → Metarhodopsin III (Meta III)) that within milliseconds leads to the generation of the active state (Meta II), which binds and activates the G protein transducin (G_T) [1].

The 3D-crystal structure of ground-state rhodopsin (2.8 Å resolution) [2] gives detailed information on the three-dimensional structure of rhodopsin but does not show which elements of the protein are involved in the photoactivation of rhodopsin. Earlier experiments suggest that residue Asp83, located in the second transmembrane domain of rhodopsin, is involved in this process. This residue reports local changes upon Meta II formation and participates in a H-bonded network [2,3] that shows major rearrangements during Meta II [4,5]. Our first target will therefore be to study the involvement of residues of the second transmembrane domain in rhodopsin activation.

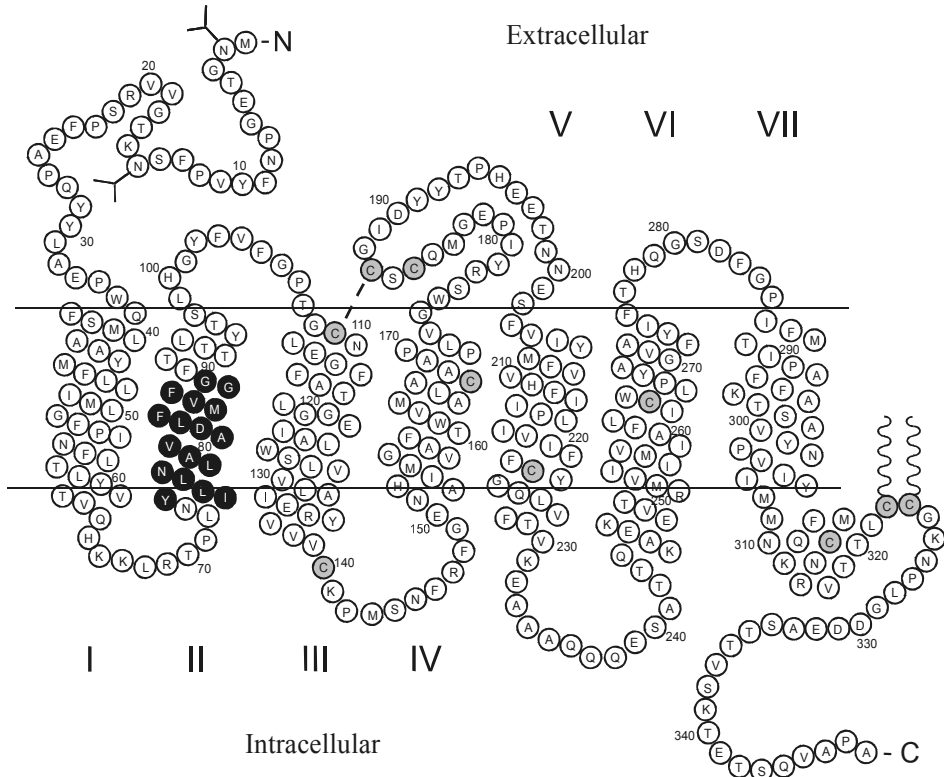


Fig. 1: Schematic representation of the two-dimensional structure of rhodopsin. The transmembrane segments are numbered. Modified from Hargrave and McDowell [34] and Palczewski et al. [2]. Black circles indicate the mutated residues discussed in this chapter, grey circles indicate the Cys \rightarrow Ser mutations of base-mutant SOH Δ C.

For this purpose we aim to use cysteine scanning mutagenesis in combination with FT-IR difference spectroscopy as described in Chapter 3. To prevent a large background in the introduced signal by native cysteines and possible reciprocal interactions of introduced cysteines with native cysteine residues we use SOH Δ C, in which all potentially active cysteine residues were removed (see Chapter 3), as base-mutant to substitute single residues by a cysteine. In this chapter we will describe the production and analysis of single cysteine mutants of residue 74-90 of the second transmembrane segment of rhodopsin (Fig. 1).

4.2 Materials and methods

4.2.1 Cloning and expression

Synthetic, cysteine-free cDNA of bovine rhodopsin (SOH Δ C) was kindly provided by D. Oprian (Brandeis University, Waltham) in the PMT vector. In SOH Δ C all cysteines have been replaced by a serine except for the cysteines of the disulfide bridge (Cys110

and Cys187). Unique restriction sites were introduced as silent mutations to allow modification and analysis by means of restriction enzymes. All constructs were extended with a 6x his-tag to allow rapid purification by immobilized metal affinity chromatography (IMAC) [6]. The mutant rhodopsins were constructed by means of cassette mutagenesis. For this purpose SOH Δ C was cloned either into a modified pBluescript II SK⁻ vector (mutants Y74C-F85C and G90C) or into the pFastbac DUAL vector (Life Technologies Inc.) under control of the polyhedrin promoter (mutants M86C-G89C). The pBluescript II SK⁻ vector was manipulated and lacks part of the multiple cloning site between restriction enzyme sites Dra II and BamH I. Part of the rhodopsin cDNA containing the mutation target was cut out of the SOH Δ C base-mutant using the restriction enzymes (Life Technologies Inc.) Hind III and Bgl II for mutants SOH Δ C/Y74C-A82C, Hind III and Nco I for SOH Δ C/D83C, Bgl II and Nco I for SOH Δ C/L84C-G90C. Next, a cassette containing the mutation and the corresponding restriction enzyme overhang was ligated into the base-mutant. The cassettes consist of two oligos (Eurogentec), a sense and an antisense oligo (Table 1), containing the desired mutation(s). An Eppendorf cup containing the oligos (ratio forward: reverse = 1:1) was put in 100°C water and let slowly cool down to room temperature to anneal the oligos and form the cassette. The cassettes were provided with a restriction site created by a silent mutation to allow identification by means of restriction enzyme analysis. After cloning of the cassette into the base-mutant, the recombinant opsins generated in the pBluescript II SK⁻ vector were subcloned into the pFastbac DUAL vector under control of the polyhedrin promoter using restriction enzymes BamH I and Not I. The construct was checked by cycle-sequencing using primer 5'-cagttttgtaataaaaaaacctataaat-3' located in the polyhedrin promoter site of pFastbac DUAL or appropriate rhodopsin primers [7].

The Bac-to-bac Baculovirus Recombination system (Life Technologies Inc.) was used to generate recombinant baculovirus for expression of recombinant rhodopsin in Sf9 *Spodoptera frugiperda* cells as described in Chapter 3. In short, the pFastbac DUAL transfer vector containing the recombinant opsin cDNA was transformed into DH10Bac competent cells to obtain recombinant bacmid DNA through transposition of the promoter-cDNA insert in the transfer vector. This DNA was used to transfect Sf9 insect cells in order to produce recombinant baculovirus. The recombinant virus (P₁) was tested for production of (recombinant) opsin by means of immunoblotting and viral DNA was tested for the correct rhodopsin insert by restriction enzyme analysis or sequencing of viral DNA as described in Chapter 3.

The recombinant virus was amplified (P₂) and the virus titer was determined by means of a plaque assay (see Chapter 3). For expression of recombinant protein Sf9 cells were

Table 1: List of sense and antisense oligos used to construct the SOH Δ C-mutants. The cysteine substitutions are indicated in bold. The silent mutations introduced to identify a mutant by means of restriction enzyme analysis are underlined.

¹ Mutation V81C creates a Fsp I-site.

² Mutation A82C removes the Bgl II- site.

³ Mutation D83C removes the Bgl II-site and creates a Sph I-site.

⁴ Mutation L84C-mutatie removes the Bgl II-site.

⁵ Mutation V87C creates a Hinf I-site.

⁶ Mutation F88C creates a Hinf I-site and removes the Nco I-site.

⁷ Mutation G89C creates a Hinf I-site.

Table 1

Mutant	forward oligo	reverse oligo
SOH ΔC/Y74C	5'-AGCT <u>G</u> CGCACACCGCTCAACT GCATCCTGCTCAACCTGGCCGTGG CA-3'	5'-GATCTGCCACGGCCAGGTTGAGCA GGATGCAGTTGAGCGGTGTGCGC-3'
SOH ΔC/I75C	5'-AGCT <u>G</u> CGCACACCGCTCAACT ACT <u>G</u> CCTGCTCAACCTGGCCGTG GCT-3'	5'-GATC <u>A</u> GCCACGGCCAGGTTGAGCA GGCAGTAGTTGAGCGGTGTGCGC-3'
SOH ΔC/L76C	5'-AGCTTCGCACACCGCTCAACTA CATCTGCCTCAACCTGGCCGTGGC T-3'	5'-GATC <u>A</u> GCCACGGCCAGGTTGAGGC AGATGTAGTTGAGCGGTGTGCGA-3'
SOH ΔC/L77C	5'-AGCT <u>A</u> CGCACACCGCTCAACT ACATCCTGTGCAACCTGGCCGTG GCA-3'	5'-GATCTGCCACGGCCAGGTTGCACA GGATGTAGTTGAGCGGTGTGCGT-3'
SOH ΔC/N78C	5'-AGCT <u>A</u> CGCACACCGCTCAACT ACATCCTGCTCTGCCTGGCCGTGG CT-3'	5'-GATC <u>A</u> GCCACGGCCAGGCAGAGC AGGATGTAGTTGAGCGGTGTGCGT-3'
SOH ΔC/L79C	5'-AGCTTCGCACACCGCTCAACTA CATCCTGCTCAACTGCGCCGTGGC A-3'	5'-GATCTGCCACGGCCAGTTGAGCA GGATGTAGTTGAGCGGTGTGCGA-3'
SOH ΔC/A80C	5'-AGCTGCGCACACCGCTCAACT ACATCCTGCTCAACCTGTGCGTGG CA-3'	5'-GATCTGCCACGCACAGGTTGAGCA GGATGTAGTTGAGCGGTGTGCGC-3'
SOH ΔC/V81C ¹	5'-AGCTTCGCACACCGCTCAACTA CATCCTGCTCAACCTGGCCTGCGC A-3'	5'-GATCTGCGCAGGCCAGGTTGAGCA GGATGTAGTTGAGCGGTGTGCGA-3'
SOH ΔC/A82C ²	5'-AGCTTCGCACACCGCTCAACTA CATCCTGCTCAACCTGGCCGTGTG C-3'	5'-GATCGCACACGGCCAGGTTGAGCA GGATGTAGTTGAGCGGTGTGCGC-3'
SOH ΔC/D83C ³	5'-AGCTTCGCACACCGCTCAACTA CATCCTGCTCAACCTGGCCGTGGC ATGCCTCTTCATGGTCTTCGGTGG CTTACCACCACCCTCTACACCTC TCTC-3'	5'-CATGGAGAGAGGTGTAGAGGGTGG TGGTGAAGCCACCGAAGACCATGAAG AGGCATGCCACGGCCAGGTTGAGCAG GATGTAGTTGAGCGGTGTGCGA-3'
SOH ΔC/L84C ⁴	5'-GATTGCTTTCATGGTCTTCGGTG GCTTACCACCACCCTCTACACCT CTCTC-3'	5'-CATGGAGAGAGGTGTAGAGGGTGG TGGTGAAGCCACCGAAGACCATGAAG CAATC-3'
SOH ΔC/F85C	5'-GATCTCTGCATGGTCTTCGGTG GCTTACCACCACCCTCTACACCT CTCTG-3'	5'-CATGCAGAGAGGTGTAGAGGGTGG TGGTGAAGCCACCGAAGACCATGCAG A-3'
SOH ΔC/M86C	5'-GATCTGTTCTGCGTCTTCGGTG GCTTACCACCACCCTCTACACCT CTCTG-3'	5'-CATGCAGAGAGGTGTAGAGGGTGG TGGTGAAGCCACCGAAGACGCAGAA CA-3'
SOH ΔC/V87C ⁵	5'-GATCTCTTCATGTGCTTCGGTG GATCACCACCACCCTCTACACCT CTCTC-3'	5'-CATGGAGAGAGGTGTAGAGGGTGG TGGTGAATCCACCGAAGCACATGAAG A-3'
SOH ΔC/F88C ⁶	5'-GATCTCTTCATGGTCTGCGGTG GATCACCACCACCCTCTACACCT CTCTG-3'	5'-CATGCAGAGAGGTGTAGAGGGTGG TGGTGAATCCACCGCAGACCATGAAG A-3'
SOH ΔC/G89C ⁷	5'-GATCTGTTTCATGGTCTTCTGCG GATCACCACCACCCTCTACACCT CTCTC-3'	5'-CATGGAGAGAGGTGTAGAGGGTGG TGGTGAATCCGCAGAAGACCATGAAC A-3'
SOH ΔC/G90C	5'-GATCTCTTCATGGTCTTCGGTT GCTTACCACCACCCTCTACACCT CTCTG-3'	5'-CATGCAGAGAGGTGTAGAGGGTGG TGGTGAAGCAACCGAAGACCATGAA GA-3'

adapted to serum-free InsectXpress medium (Cambrex) in suspension culture in 250-ml spinner bottles (Bellco) or in monolayer culture in T₁₈₂ culture flasks. For large-scale production in bioreactors (1 - 10 litre), InsectXpress medium-adapted cells were scaled up in spinner flasks to obtain a minimum cell density of $5 \cdot 10^5$ cells/ml in the bioreactor. The cells were infected in mid log phase with a multiplicity of infection of 0.05 - 0.1 and harvested at 4 d.p.i. as described before [7-9].

4.2.2 Analysis of recombinant rhodopsins

Total recombinant protein production was estimated by SDS-PAGE (12% acrylamide) of total membrane protein followed by immunoblotting with an anti-rhodopsin antibody as described in Chapter 3.

The capacity of the recombinant opsins produced by Sf9 cells to bond with 11-*cis* retinal to form a photosensitive pigment was assayed as described before [7,10].

SOH Δ C, SOH Δ C/L77C and wild type (wt) rhodopsin were purified by means of immobilized metal chromatography (IMAC) over Ni²⁺ agarose as described before in [9] except that SOH Δ C and SOH Δ C/L77C were extracted in CHAPS/nonylglycose and purified in nonylglycose as described in Chapter 3. After purification the pigments were reconstituted into retina lipids as described previously [11].

The pH dependence of the Meta I \rightarrow Meta II transition was measured according to DeLange *et al.*, 1997 [12]. In short, rhodopsin proteoliposomes were resuspended in buffer with appropriate pH. A spectrum was recorded between 750 and 250 nm of the initial, unbleached sample (spectrum 1). After illumination, a second spectrum was recorded (spectrum 2). The relative amount of Meta I formed after illumination was derived from the linear relationship between the λ_{\max} of the difference spectrum (spectrum 1 – spectrum 2) and the percentage photoproduct formed [12].

Activation of the bovine G protein transducin (G_T) by recombinant rhodopsin was measured by the intrinsic fluorescence enhancement of the G protein α -subunit upon binding of GTP γ S (Roche) as earlier described [10,13]. In short, bovine transducin (final concentration 100 nM) was added to reconstituted recombinant rhodopsin (5 nM) in buffer containing 100 mM NaCl, 3 mM MgCl₂, 1 mM dithioerythritol, 0.01% (w/v) DoM, 20 mM HEPES pH 7.4 in the dark. After illumination of the sample the fluorescence was measured using a Shimadzu RF-5301-PC spectrofluorometer with excitation at 295 nm and emission at 337 nm. Then GTP γ S (final concentration 2.5 μ M) was added and the subsequent increase in relative fluorescence intensity represents pigment-triggered activation of G_T α . The same assay performed with opsin was used as a negative control.

FT-IR analyses were performed on a Bruker IFS 66v/S spectrometer using set-up and settings as described in Chapter 3. The -SH content of rhodopsin and mutants was determined by reaction with DTNB in 1% SDS as described in [14].

Intracellular localization of the mutant rhodopsins was studied using confocal laser scanning microscopy. Cells were seeded on cover slips in 6 wells plates and grown to 50% confluency. The cells were infected with (recombinant) baculovirus with a M.O.I. of 0.1 - 1.0 depending on cell density. At 4 d.p.i., the cells were washed in phosphate-buffered saline (PBS), fixed with methanol at -20°C and permeabilized with 0.2% Triton X-100. After rinsing with PBS, the cover slips were incubated with PBS, 0.05% Tween-20, 1% gelatin, 2% Fetal calf serum (FCS) at RT to block non-specific binding sites. Next, the cells were incubated with anti-rhodopsin CERN886 antiserum (1:2000 diluted in PBS, 0.05% Tween-20, 1% gelatine and 2% FCS) for 1 hour at RT. After

	% Conservation [32]		Localization: L(lipid face) P(protein face)	λ_{\max} (nm) (purified)	Functional protein (% ± SD) (wt ≡ 100%)	Total protein production	
	R	C				Glycosylated	Non-glycosylated
SOH WT				498 ± 1	100	++++	++++
SOH ΔC				492 ± 2	26 ± 12 (n= 12)	++	++++
Y74	18	68	L		2 ± 5 (n = 3)	+	++++
I75	3	88	P		18 ± 1 (n = 2)	++	+
L76	37	85	P		14 ± 4 (n = 2)	+	++++
L77	31	48	L	492	66 ± 2 (n = 2)	++++	+
N78	51	92	P		9	+	+
L79	91	98	P		< 1	++	+
A80	74	80	P		< 1	-	-
V81	30	40	L		< 1	+	+
A82	58	63	P		< 1	+	++++
D83	94	95	P		7 ± 12 (n = 3)	+++	+++
L84	60	85	P		n.d.	n.d.	n.d.
F85	7	77	L		44 (n = 1)	+	++++
M86	7	55	P		19 ± 27 (n = 2)	+	++++
V87	11	45	P		10 ± 9 (n = 3)	+	++++
F88	7	58	L		38 ± 14 (n = 3)	+++	++++
G89	5	18	P		53 ± 4 (n = 2)	+++	++++
G90	3	22	P		11 ± 15 (n = 2)	++	+

Table 2: Protein production analysis: this table compiles localization and conservation of the mutated residues, production of functional protein, λ_{\max} and conclusions from immunoblot analysis of wild type rhodopsin, SOH ΔC and subsequent mutations SOH ΔC/Y74C to SOH ΔC/G90C. Y74 indicates mutant SOH ΔC/Y74C, I75 indicates SOH ΔC/I75C etc; % conservation: the percentage conservation within the GPCR family; R (Residue) = percentage absolute conservation of a residue within the GPCR family, C (Class) = % percentage conservation within the same residue subclass within the GPCR family. Classification of subclasses of residues: apolar, large: Y/L/I/F/M, apolar, small: A/G/V/P, polar, non-charged: S/T/N/P/H, polar, charged: D/E/K/R. Localization: localization of the amino acid residue in either the lipid face (L) or protein face (P) of helix II, based upon the crystal structure [1-3]. Immunoblot analysis was performed on total cellular protein of Sf9 cells infected with baculovirus expressing recombinant opsins. Blots were screened with primary, polyclonal antibody CERN886 or CERN922. The plusses indicate the relative amount of respectively glycosylated or non-glycosylated opsin relatively to wild type assessed by visual inspection. Protein production by wild type was set at 100%. + = ≤ 25%, ++ = 25 – 50%, +++ = 50 – 75%, ++++ ≥ 75% compared to wild type (some mutants appear to produce larger amounts of protein than wild type). About 40% of wild type protein production consists of glycosylated and about 60% consists of non-glycosylated opsin. Functional protein was measured by UV-VIS spectra before (1) and after (2) illumination in the presence of 20 mM hydroxylamine [10]. n.d.= not determined, n = number of independent experiments.

rinsing twice in PBS, 0.05% Tween-20, the cells were incubated with the secondary antibody SAR-TRITC (1:200) in PBS containing 0.05% Tween-20, 1% gelatine and 2% FCS. Again the cells were washed rinsing twice in PBS, 0.05% Tween-20. Finally the coverslips were brought to slides with a drop of PBS/glycerol and the edges were sealed with colourless nail-polish to avoid dehydration. To identify the localization of the endoplasmic reticulum (ER) in Sf9 insect cells, cover slips were incubated for 30 minutes to 2 hours with ER-tracker Blue-White DPX (Molecular Probes) under normal growth conditions. These coverslips were treated in a similar way as the coverslips containing infected Sf9 cells.

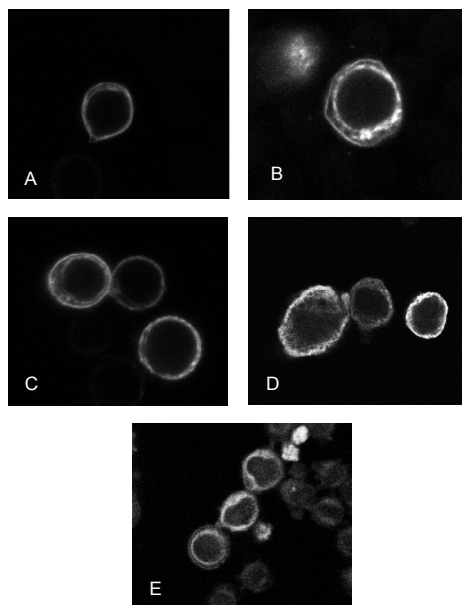


Fig. 2: Typical patterns observed for intracellular localization of wild type and mutant rhodopsins in Sf9 insect cells analysed by confocal immunofluorescence microscopy. A: wild type rhodopsin; B: SOH Δ C; C: SOH Δ C/L77C; D: SOH Δ C/I75C; E: localization of the E.R.. D is typical for pigments producing low amounts of functional protein. Cells were seeded on coverslips, grown to 50% coverage of the coverslip and infected with recombinant baculovirus. Opsins were localized with the anti-rhodopsin antiserum CERN886 (1:2000). The E.R. was localized using ER-tracker Blue-White DPX (Molecular Probes). The immunopositive shell evident in (A) (B) and (C) represents staining of the plasma membrane. Similar staining was never observed in condition (D).

4.3 Results

4.3.1 Protein production

The total amount of recombinant opsin produced was estimated by means of immunoblot analysis (Table 2). All mutants except SOH Δ C/A80C gave a protein product. Both glycosylated as well as non-glycosylated opsin were generated [15] (see Fig. 3, Chapter 3 for general glycosylation patterns). Most mutants produced amounts of non-glycosylated protein similar to or even higher than glycosylated protein, with the exception of SOH Δ C/L77C (Table 2).

The capacity of the recombinant opsins to bond with 11-*cis* retinal to form a photosensitive pigment was analysed at 4 d.p.i. by measuring the resulting UV-VIS spectrum before and after illumination. Subtraction of the spectrum after illumination from the spectrum before illumination gives a difference spectrum, where interference with e.g. sloping baselines is cancelled out. This allows a better estimation of the λ_{\max} and the amount of recombinant protein that is produced. Base-mutant SOH Δ C produced $26\% \pm 12$ ($n = 12$) functional protein compared to wild type rhodopsin (wt) ($\equiv 100\%$). Functional protein production of SOH Δ C/L84C has not yet been determined. Mutants Y74C, I75C, L76C, N78C, D83C, M86C, V87C and G90C produced less

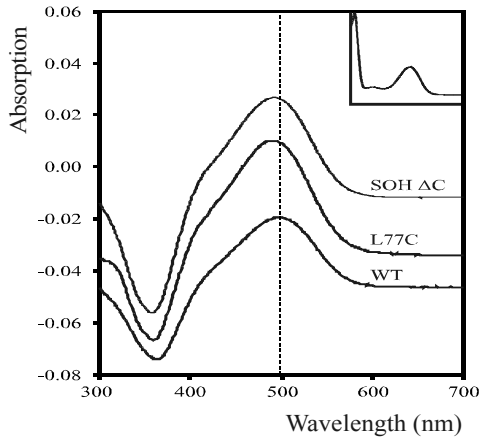


Fig. 3: Difference absorbance spectra of wild type rhodopsin, base-mutant SOH Δ C and mutant SOH Δ C/L77C. Spectra were obtained by subtracting a spectrum after illumination in the presence of 20 mM hydroxylamine from the original spectrum before illumination. Note the blue shift of the λ_{max} of both SOH Δ C and SOH Δ C/L77C compared to wild type rhodopsin. The insert shows the spectrum of SOH Δ C after purification by IMAC.

functional protein than SOH Δ C, while the mutants L79C, A80C, V81C and A82C even produced no detectable amount of functional protein (Table 2). On the other hand, the mutants L77C, F85C, F88C and G89C yielded more functional protein than the base-mutant (30 – 66% of wild type, Table 2). Due to temporal and logistic restrictions only mutant SOH Δ C/L77C and base-mutant SOH Δ C could be analysed for their structural and functional properties.

Confocal laser scanning microscopy was used to analyse the intracellular distribution of

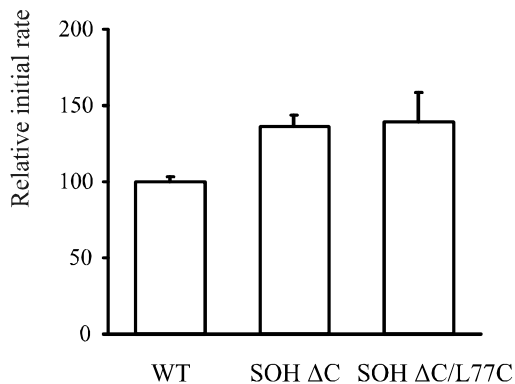


Fig. 4: G protein activation capability of purified pigments. Intrinsic fluorescence enhancement (excitation: 295 nm; emission: 337 nm) of the G protein α -subunit upon GTP γ S binding was used to monitor activation by wild type rhodopsin, SOH Δ C and SOH Δ C/L77C. The measuring sample contained 100 nM of transducin and 5 nM of pigment. The sample was illuminated and after an equilibration period the reaction was initiated by the addition of guanosine 5'-O-(3-thiotriphosphate) (GTP γ S) to a concentration of 2.5 μ M (arrow). The G protein activation capability of SOH Δ C and SOH Δ C/L77C was higher but not significantly different from wild type rhodopsin. n = 3.

wild type and mutant rhodopsins upon baculovirus expression in Sf9 insect cells (Fig. 2). To distinguish between localization in the endoplasmic reticulum (ER) and other intracellular membranes we used a specific marker for the ER, ER-tracker Blue-White DPX (Molecular Probes) as shown in Figure 2.E. Base-mutant SOH Δ C was retained mainly in the E.R. and targeted to a smaller extent to the plasma membrane (Fig. 2.B) whereas wild type was preferentially targeted to the plasma membrane (Fig. 2.A) [16]. SOH Δ C/L77C was also present both in the plasma membrane and the ER, but showed stronger plasma membrane labeling than SOH Δ C (Fig. 2.C). The localization pattern of SOH Δ C/I75C is representative for the mutants that produced less than 20% of functional protein relative to wild type (Fig. 2.D). These mutants showed no detectable targeting to the plasma membrane but largely accumulated intracellularly in the E.R..

4.3.2 Purification and reconstitution

Mutant SOH Δ C/L77C and base-mutant SOH Δ C were the only mutants that timely produced sufficient amounts of functional protein for purification by IMAC and further analysis. Purification was performed based on the approach developed for wild type rhodopsin as described before [6,9]. This method uses DoM for extraction. However,

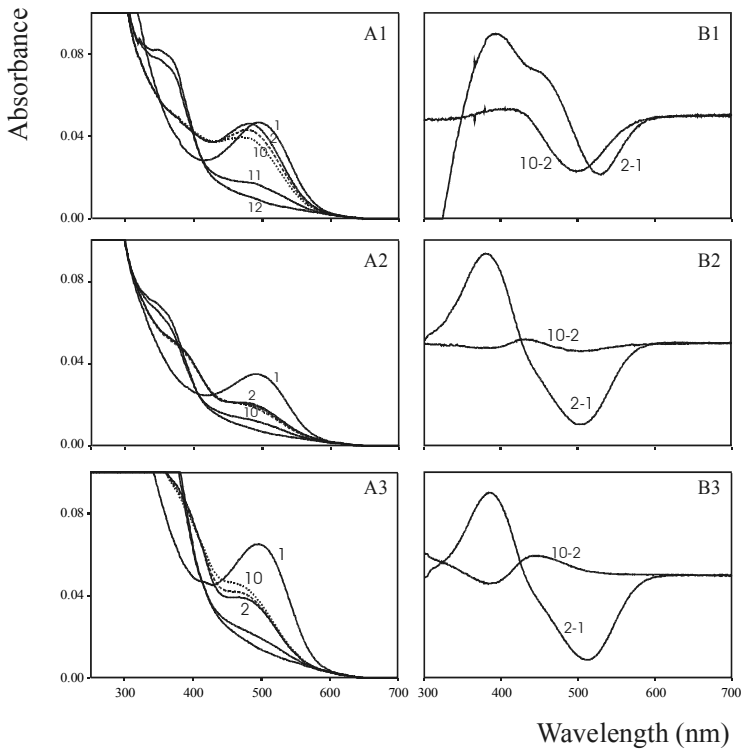


Fig. 5: Photocascade of wild type rhodopsin, SOH Δ C and SOH Δ C/L77C measured at pH 6.5, 10°C. A1-A3: overview photocascade; A1: SOH Δ C/L77C, A2: SOH Δ C, A3: wild type rhodopsin; B1-B3: spectrum 2-1 shows the formation of Meta I and Meta II, spectrum 10-2 reflects the Meta II to Meta III transition of respectively SOH Δ C/L77C (B1), SOH Δ C (B2) and wild type rhodopsin (B3).

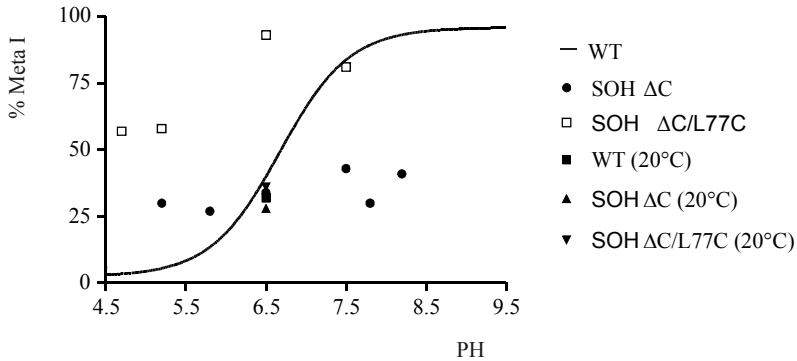


Fig. 6: pH dependence of the Meta I \leftrightarrow Meta II equilibrium of wild type rhodopsin, SOH Δ C and SOH Δ C/L77C. Measurements were performed at 10°C or 20°C. The solid line represents best fits with a Michaelis-Menten equation. The pKa of SOH Δ C and SOH Δ C/L77C could not be determined at 10°C. At 20°C and pH 6.5 the three species seem to coincide.

extraction of SOH Δ C and SOH Δ C/L77C in DOM was poor and CHAPS/nonylglucoside was eventually selected as optimal detergent mixture allowing extraction of the pigment as well as binding to the Ni²⁺-matrix. Washing and elution was performed with nonylglucose as detergent. In parallel experiments base-mutant SOH Δ C was purified with a recovery of $40\% \pm 14$ ($n = 2$) (ratio 280/492 = 2.8 ± 0.2), wild type rhodopsin with 40% recovery ($n = 1$) (ratio 280/498 = 2.4) and SOH Δ C/L77C with 75% recovery ($n = 1$, ratio 280/492 = 2.4). A ratio of 1.7 – 1.8 indicates highly purified rhodopsin. We also determined the amount of reactive -SH groups for SOH Δ C, SOH Δ C/L77C and wild type rhodopsin using the DTNB assay. We found 5.6 ± 0.2 ($n = 4$) for wild type rhodopsin, 0.08 for SOH Δ C and 0.8 for SOH Δ C/L77C, in agreement with the theoretical value of six free -SH groups in SOH WT, none in SOH Δ C and one free -SH group in SOH Δ C/L77C. The spectra of SOH Δ C and SOH Δ C/L77C were very similar in bandshape to wild type rhodopsin but show a blue-shift that is comparable for both mutants (λ_{\max} : 498 nm \rightarrow 492 nm) (Fig. 3). The inset in Figure 3 shows the spectrum of purified SOH Δ C. After purification, SOH Δ C and SOH Δ C/L77C were reconstituted into a native bovine retina lipid environment using detergent extraction with cyclodextrin as described in [6,9]. SOH Δ C was reconstituted with 50% recovery, SOH Δ C/L77C with 65% recovery and wild type was reconstituted with 77% recovery.

4.3.3 Functional analysis

The G protein activation capability was determined by measuring the intrinsic fluorescence enhancement of the G protein α -subunit upon GTP binding. Base-mutant SOH Δ C and mutant SOH Δ C/L77C showed a similar activation capacity that was higher than that of wild type rhodopsin but considering the limited number of experiments was not yet significantly different (Fig. 4).

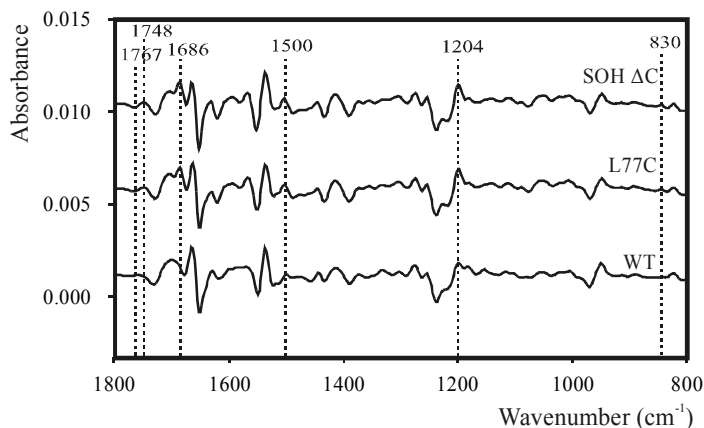


Fig. 7: FT-IR difference spectra of the rhodopsin \rightarrow Meta I transition of wild type rhodopsin, SOH Δ C and SOH Δ C/L77C. The 1800-800 cm^{-1} region, where the major changes occur, is shown. Spectra were taken at -20°C , where wild type Meta I intermediate is stable. Note that SOH Δ C and SOH Δ C/L77C display several peaks typical for Meta II at respectively 1767, 1748, 1586, 1500 and 830 cm^{-1} .

Figure 5.A shows the photocascade of SOH Δ C/L77C (A1), SOH Δ C (A2) and wild type rhodopsin (A3). Rapid and slow changes are given as difference spectra in the B panel, highlighting the formation of Meta I and Meta II (spectrum 2 - 1) and the decay of Meta II and the formation of Meta III (spectrum 10 - 2). The photocascade of SOH Δ C (Fig 5, A2) seems to be very similar to wild type rhodopsin (Fig. 5, A3) but more detailed analysis showed that SOH Δ C formed less Meta I and a reduced decay of Meta II to Meta III compared to wild type rhodopsin (Fig. 5, B2). SOH Δ C/L77C behaved even more aberrant than SOH Δ C. It again showed little Meta III formation but compared to SOH Δ C it produced more Meta I that however seems to decay fairly rapidly (Fig. 5, B1). In wild type rhodopsin the late photointermediates Meta I and Meta II are in a pH-dependent equilibrium [17-21] that determines the level of activated receptor (Meta II). The Meta I \leftrightarrow Meta II equilibrium was analysed for SOH Δ C, SOH Δ C/L77C and wild type rhodopsin in the pH range 4.5 - 8.8 (Fig. 6). At pH values higher than 8.8 Meta I becomes very unstable and can not be reliably determined. The assay was performed at 10°C , where Meta II is sufficiently stable ($t_{1/2} > 20$ min.). Wild type rhodopsin has a pK_a of 6.5 ± 0.2 ($n = 5$) for this equilibrium but in SOH Δ C it was not very pH-dependent indicating that the pK_a was outside this range or the pH-dependence was lost. The pK_a of SOH Δ C/L77C could not be accurately determined but seems to have shifted to lower pH. A single measurement at 20°C , pH 6.5 suggests that at this pH and this temperature SOH Δ C and SOH Δ C/L77C behave more similarly to wild type (Fig. 6).

Figure 7 shows the FT-IR difference spectrum of the rhodopsin \rightarrow Meta I transition of SOH Δ C, SOH Δ C/L77C and wild type rhodopsin. The spectra of both mutants showed marked similarity to that of wild type rhodopsin but exhibits more pronounced peaks at 1767, 1748, 1686, 1500, 1204 and 830 cm^{-1} . The FT-IR difference spectra of the rhodopsin \rightarrow Meta II transition of both mutants were highly similar to that of wild type in the 1800-800 cm^{-1} range, accurately copying all positive and negative peaks except

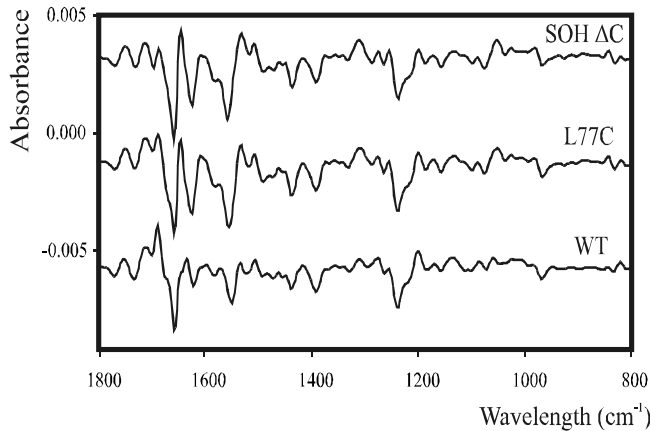


Fig. 8: The 1800-800 cm^{-1} region of the FT-IR difference spectra of the rhodopsin \rightarrow Meta II transition of wild type rhodopsin, SOH Δ C and SOH Δ C/L77C. Spectra were taken at 10°C and pH 6.0 within 5 minutes after illumination, in order to minimize interference by the slow decay of Meta II (half life of > 20 minutes under these conditions). The spectra of SOH Δ C and SOH Δ C/L77C are nearly identical in this region and highly similar to that of wild type rhodopsin.

for some minor changes around 1650 cm^{-1} (Fig. 8). However, the 2600-2500 cm^{-1} region in the difference spectrum of the mutant rhodopsins is obviously different from that of wild type rhodopsin. Both SOH Δ C and SOH Δ C/L77C lack the band near 2550 cm^{-1} that can be assigned to -SH stretch vibrations (Fig. 9) [22].

4.4 Discussion

4.4.1 Expression of single TM II cysteine mutants

Total levels of recombinant protein production were estimated from SDS-PAGE. About half of the mutants produced quantities of recombinant protein at least 50% of that observed for base-mutant SOH Δ C. Correctly folded and functional opsin will be transported to the plasma membrane. The intracellular distribution of the recombinant proteins was studied in Sf9 insect cells by means of confocal laser scanning immunofluorescence microscopy. Most mutants were retained intracellularly in the ER except for base-mutant SOH Δ C and mutant SOH Δ C/L77C which showed partial localization in the plasma membrane. Wild type rhodopsin on the other hand is preferentially targeted to the plasma membrane. These results suggest that the majority of the mutants displays folding and/or transport defects.

In addition to targeting to the rod outer segment membrane, rhodopsin requires posttranslational modifications like palmitoylation, disulfide bridge formation and glycosylation to reach structural and functional maturity. Correct folding is thought to be necessary for proper glycosylation [23,24]. Most mutants showed poor glycosylation except for SOH Δ C/L77C which produced a relative amount of glycosylated protein that is comparable to wild type rhodopsin. This is in agreement with their intracellular localization pattern: mutant SOH Δ C/L77C showed targeting to the plasma membrane whereas most mutants were retained intracellularly. This supports the suggestion that

most mutants suffer from folding defects. SOH Δ C/A80C showed no protein product at all in initial experiments. This has not been investigated further.

4.4.2 Functional properties of single TM II cysteine mutants

The mutant rhodopsins were tested for production of functional protein in Sf9 insect cells. Base-mutant SOH Δ C produced about 75% less functional protein than wild type rhodopsin. While most of the cysteine mutants produced even less functional protein than SOH Δ C or no detectable amounts of functional protein at all, some (L77C, F85C, V87C, F88C and G89C) produced similar or even much higher amounts of functional protein. For technical reasons only SOH Δ C/L77C could be further analysed so far. Analysis of the relative amount of glycosylated species showed that base-mutant SOH Δ C displayed poor levels of glycosylation compared to wild type rhodopsin, whereas SOH Δ C/L77C showed wild type-like levels of glycosylation. This supports the concept that glycosylation is an indication for the presence of functional protein.

To obtain sufficient amounts of functional mutant rhodopsins for purification and further analysis, large culture volumes would be necessary. In addition, the relatively large amount of non-functional protein produced by most mutant rhodopsins will hamper protein purification and will significantly affect recovery of functional protein (P. Bovee-Geurts, unpublished results). Until now, only base-mutant SOH Δ C and SOH Δ C/L77C could be purified sufficiently to allow analysis of structural and functional properties. Both mutants were purified with a recovery similar to or even higher than that of wild type rhodopsin, although their reconstitution into retina lipids was less efficient. These preparations allowed more detailed analysis of their spectral and photochemical properties. The UV/VIS difference spectra of the mutants showed a very similar bandshape to that of wild type except for a blue-shift in their λ_{max} that was

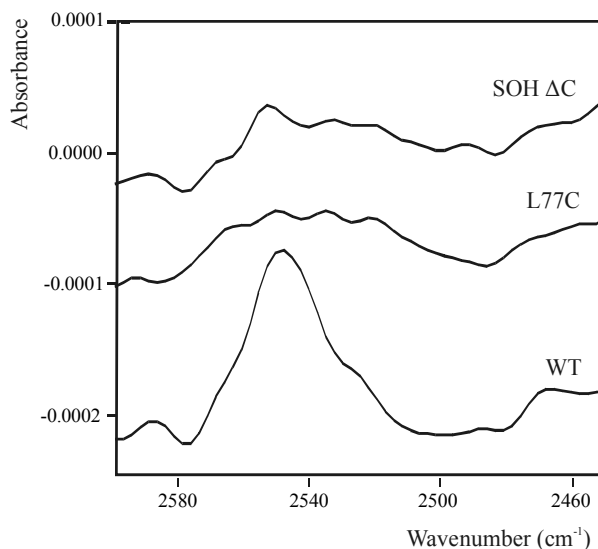


Fig. 9: FT-IR difference spectra of the rhodopsin \rightarrow Meta II transition of wild type rhodopsin, SOH Δ C and SOH Δ C/L77C. The 2600-2500 cm^{-1} region is shown where the stretch vibration of the sulfhydryl group absorbs. Spectra were scaled on the 1750 cm^{-1} band, typical for the Meta II state. Note that -SH band activity is virtually absent in SOH Δ C and SOH Δ C/L77C.

comparable for both SOH Δ C and SOH Δ C/L77C (498 nm \rightarrow 492 nm, Fig. 3). The shift in λ_{max} is probably due to the C167S mutation, since the single C167S mutant on a wild type background exhibits a similar blue shift (M.J.M. Portier-VandeLuytgaarden, unpublished results). Residue C167 participates in the lining of the retinal binding site and in the formation of the active state of Meta II (DeGrip *et al.*, unpublished results), hence may be close enough to influence the electronic properties of the chromophore. The blue shift indicates that light of higher energy is required for the mutant to reach the activated state, indicating that the C167S substitution stabilizes the ground state and/or destabilizes the excited state.

Estimation of the number of -SH groups per mole of rhodopsin by their reactivity with DTNB confirmed the phenotypes: 5.6 ± 0.2 per mole of pigment for wild type rhodopsin ($n = 4$) in agreement with the native six cysteines, 0.08 for SOH Δ C reflecting the lack of cysteines in SOH Δ C and 0.8 for SOH Δ C/L77C representing the -SH group derived from the Leu \rightarrow Cys mutation at position 77. The number of -SH groups of SOH Δ C also demonstrates that at least 96% of the Cys110 and Cys187 residues in the purified pigment have generated a disulfide bond.

The purified pigments SOH Δ C and SOH Δ C/L77C were tested for their functional properties. The photocascade of SOH Δ C, SOH Δ C/L77C and wild type rhodopsin was analysed at 10°C, pH 6.5 (Fig. 5). SOH Δ C formed similar amounts of Meta I as wild type rhodopsin where SOH Δ C/L77C formed more Meta I than wild type. Both showed only little decay of Meta II into Meta III. Analysis of the MI \leftrightarrow MII equilibrium at 10°C showed that the mutants displayed either no pH dependence in the range analysed (SOH Δ C) or that the pKa seemed to be shifted to the left but this could not be exactly determined (SOH Δ C/L77C). The pKa of the Meta I \leftrightarrow Meta II equilibrium is largely determined by residues E134 and H211 that form part of an H-bonded network in rhodopsin [1,25,26]. There is strong evidence that residue Asp83 also forms part of an H-bonded network [1,4,27,28]. Mutation of Asp83 into a cysteine did retain wild type-like properties and we concluded that cysteine -SH residues can also participate in this H-bonded network (Chapter 2) [4]. Cysteine 167 and 264 are structurally active during the photoactivation of rhodopsin (DeGrip *et al.*, unpublished results) as indicated by changes in their -SH group vibration. This is strongly suggestive of a change in H-bonding properties, and of participation in (a) H-bonded network(s). If these communicate with the pH-sensor of the Meta I \leftrightarrow Meta II equilibrium, it might explain why mutation of these cysteine residues could disturb the Meta I \leftrightarrow Meta II equilibrium and the lack of pH dependence of base-mutant SOH Δ C. This suggests that -SH residues might be involved in pH-sensing. Residue L77 is located close to a water molecule located in a cavity between helix II, VI and VII. Mutation of this residue into a cysteine introduces a -SH group at this position which may H-bond to and/or perturb the position of this water molecule. Whether such subtle conformational changes are sufficient to explain the different pH dependency of SOH Δ C/L77C relative to SOH Δ C presents a fascinating topic for further research.

FT-IR difference spectroscopy is very sensitive to changes in protein structure. We used this technique first of all to probe whether substitution of the residues of the second transmembrane helix by a cysteine caused long-range structural perturbations and secondly to identify participation of the newly introduced -SH groups in rhodopsin activation. The difference spectra of the rhodopsin \rightarrow Meta I transition of SOH Δ C and SOH Δ C/L77C were quite similar to that of wild type rhodopsin except for peaks around 1767, 1748, 1686, 1500 and 830 cm^{-1} . These peaks reflect typical Meta II

vibrations indicating that the mutants show conformational changes that are typical for Meta II at a temperature where wild type Meta I is still fully stable. This suggests that the temperature dependence of the Meta I \rightarrow Meta II transition has changed in the base-mutant. The FT-IR difference spectrum of the rhodopsin \rightarrow Meta II transition of SOH Δ C was very similar to wild type rhodopsin accurately copying all positive and negative peaks in the 1700-800 cm^{-1} range except for some minor changes around 1650 cm^{-1} . These data indicate that the cysteine mutants do not cause long-range perturbations in protein structure. As expected the 2600-2500 cm^{-1} region of SOH Δ C and SOH Δ C/L77C clearly differs from that of wild type. This region can be assigned to -SH stretch vibrations which peak at 2548 cm^{-1} in wild type rhodopsin [22]. This peak is absent in the rhodopsin \rightarrow Meta II FT-IR difference spectrum of SOH Δ C because in this base-mutant all (potentially) reactive cysteines have been replaced by a serine. The Rho \rightarrow Meta II difference spectrum of mutant SOH Δ C/L77C was very similar to SOH Δ C and also shows no -SH stretch vibration. This indicates that residue 77 is not structurally involved in the photoactivation of rhodopsin.

The MI \leftrightarrow MII equilibrium measured at 10°C showed no pH dependency for SOH Δ C whereas the pKa for SOH Δ C/L77C could not be determined. At pH 7.4 and at 10°C, base-mutant SOH Δ C produced a higher percentage of Meta II than wild type. The FT-IR difference spectra of SOH Δ C at -20°C, at which wild type Meta I is stable, show a mixture of Meta I and Meta II, also suggesting changes in the MI \leftrightarrow MII equilibrium in support of the higher level of Meta II evident in the UV/VIS spectral analysis. If this difference persists at 20°C it might explain the somewhat higher G protein activation capability of the mutant since higher levels of Meta II, the active state, are present. On the other hand, the FT-IR difference spectrum of Meta II of both mutants shows no indication for the presence of significant amounts of Meta I. This is in contradiction with the UV/VIS data showing an increased amount of Meta I in the L77C mutant at 10°C. We have not yet been able to resolve this discrepancy. At 20°C and pH 6.5 the equilibrium constants of the MI \leftrightarrow MII equilibrium of the three species coincide again. Clearly, further experiments, both at various temperatures and pH values will be necessary to properly evaluate the photochemical changes induced by these mutations.

The question remains why the majority of the mutants produced little or no functional protein. We chose to study the second transmembrane domain of rhodopsin because from earlier experiments we know that Asp83 forms part of a H-bonded network [2,3] that shows major rearrangements during photoactivation and hence most likely is involved in the photoactivation of rhodopsin. In order to prevent a large background in the introduced signal by native cysteines and possible reciprocal interactions of introduced cysteines with native cysteine residues, we used SOH Δ C as base-mutant to substitute single residues by a cysteine (Chapter 3). In this base-mutant all (potentially) active cysteines were replaced by a serine. Cysteine and serine differ only in the heteroatom in the side chain and replacement of cysteine by serine involves the exchange of two relatively small side chains. Although substitution of cysteine by serine involves the replacement of a non-polar by a polar residue, serine has been reported as a suitable substitute for cysteine in base-mutants of other membrane proteins without disturbing their structural and functional properties [29,30]. However, although total amounts of recombinant protein do not differ strongly, base-mutant SOH Δ C produces much lower quantities of functional recombinant protein than wild type rhodopsin. Cysteine 167 and 264 form part of the retinal binding site and are structurally active during the photoactivation of rhodopsin. Single substitution of these residues by a serine on a wild

type background significantly reduced their stability during purification (M.J.M. Portier-VandeLuytgaarden, unpublished results). Since conformational stability is considered to be a positive factor in the protein folding process [31], reduced stability might be a cause for the less successful folding of the base-mutant under overexpression conditions. The observation that this is aggravated by certain cys-substitutions and partially rescued by others is a very intriguing phenomenon that deserves further studies.

The residues of the second transmembrane helix analysed in this study show a varying extent of relative conservation of their position in this helix within the family of G protein-coupled receptors (Table 2) [32]. Mutation of residues with 30% or higher degree of residue conservation gave very low amounts of functional protein and showed little glycosylation except for SOH Δ C/L77C which gave 65% functional protein compared to wild type and showed wild type-like glycosylation (Table 2). Mutation of residues with less than 30% residue conservation within the family of G protein coupled receptors in general produced reasonable amounts of functional protein, sometimes even higher than SOH Δ C, except for mutant Y74C. Tyr74 contains an aromatic side chain and is located in the lipid face of TM II. Substitution by a cysteine introduces a smaller residue which might cause a local structural rearrangement, explaining the lower amounts of functional protein production. However, this is only speculative and further experiments are needed to resolve this question. Residues that play an important role in protein structure and/or function are in general well conserved. Thus, mutation of such residues might display a more pronounced effect on functional protein production than mutation of less conserved residues. This suggests that the degree of conservation can be an indication for the production of functional protein in cysteine scanning mutagenesis. Considering this, it is interesting to note that no relationship was evident between class-based conservation and production of functional and/or glycosylated protein (Table 2). The residues of TM II are either located in the lipid face or in the protein face of the transmembrane helix (Table 2). Residues that are located in the protein face are located in closer contact with residues from neighbouring helices and mutations of these residues might therefore more easily disturb rhodopsin structure and functionality. However, no clear relationship could be found between localization and the extent of functional protein production and/or glycosylation of the recombinant opsins. It should be noted that reduced production of functional protein can be caused either by reduced ability to fold, producing non-glycosylated protein, or by disturbance of ligand binding in spite of proper folding and glycosylation. In our experiments, ligand binding was primarily used as a marker for functionality. For instance, SOH Δ C/G90C produced no detectable amount of functional protein. Residue G90 is located in the vicinity of E113, the counterion for the protonated Schiff base formed between retinal and K296. Mutation of this residue might therefore disturb the formation of the Schiff base. On the other hand, mutation G90D on a wild type background is known to produce functional protein in similar amounts as wild type rhodopsin [33]. Nevertheless, we cannot exclude that sterical hindrance interfering with ligand binding may account for several mutants yielding low protein functionality.

In summary, there might be a relationship between the extent of conservation and the amount of glycosylated, functional rhodopsin protein production that should be further investigated. Nevertheless, it remains largely unclear why most mutants produce little or no functional protein. So far, the only conclusion we can draw from these cysteine scanning efforts is that residue L77 is not involved in structural or enzymatical changes underlying rhodopsin activation. Indeed, residue L77 is located in the lipid face of TM

II and hence probably inserted in the lipid matrix (Table 2) which makes it plausible that this residue does not participate in photoactivation.

References

- Okada, T., Ernst, O. P., Palczewski, K., and Hofmann, K. P. (2001). Activation of rhodopsin: New insights from structural and biochemical studies. *Trends Biochem. Sci.*, 26, 318 - 324.
- Palczewski, K., Kumasaka, T., Hori, T., Behnke, C. A., Motoshima, H., Fox, B. A., LeTrong, I., Teller, D. C., Okada, T., Stenkamp, R. E., Yamamoto, M., and Miyano, M. (2000). Crystal structure of rhodopsin: A G protein-coupled receptor. *Science*, 289, 739 - 745.
- Okada, T., Fujiyoshi, Y., Silow, M., Navarro, J., Landau, E. M., and Shichida, Y. (2002). Functional role of internal water molecules in rhodopsin revealed by x-ray crystallography. *Proc. Nat. Acad. Sci. USA*, 99, 5982 - 5987.
- Breikers, G., Bovee-Geurts, P. H. M., DeCaluwé, G. L. J., and DeGrip, W. J. (2001). A structural role for Asp83 in the photoactivation of rhodopsin. *Biol. Chem.*, 382, 1263 - 1270.
- Nagata, T., Terakita, A., Kandori, H., Shichida, Y., and Maeda, A. (1998). The hydrogen-bonding network of water molecules and the peptide backbone in the region connecting Asp83, Gly120, and Glu113 in bovine rhodopsin. *Biochemistry-USA*, 37, 17216 - 17222.
- Janssen, J. J. M., Bovee-Geurts, P. H. M., Merckx, M., and DeGrip, W. J. (1995). Histidine tagging both allows convenient single-step purification of bovine rhodopsin and exerts ionic strength-dependent effects on its photochemistry. *J. Biol. Chem.*, 270, 11222 - 11229.
- Klaassen, C. H. W. and DeGrip, W. J. (2000). Baculovirus expression system for expression and characterization of functional recombinant visual pigments. *Meth. Enzymology*, 315, 12 - 29.
- Klaassen, C. H. W., Bovee-Geurts, P. H. M., DeCaluwé, G. L. J., and DeGrip, W. J. (1999). Large-scale production and purification of functional recombinant bovine rhodopsin using the baculovirus expression system. *Biochem. J.*, 342, 293 - 300.
- Bosman, G. J. C. G. M., VanOostrum, J., Breikers, G., Bovee-Geurts, P. H. M., Klaassen, C. H. W., and DeGrip, W. J. (2003). Functional expression of his-tagged rhodopsin in Sf9 insect cells. *Meth. Mol. Biol.*, 228, 73 - 86.
- Janssen, J. W. H., Bovee-Geurts, P. H. M., Peeters, A. P. A., Bowmaker, J. K., Cooper, H. M., David-Gray, Z. K., Nevo, E., and DeGrip, W. J. (2000). A fully functional rod visual pigment in a blind mammal - A case for adaptive functional reorganization? *J. Biol. Chem.*, 275, 38674 - 38679.
- DeGrip, W. J., VanOostrum, J., and Bovee-Geurts, P. H. M. (1998). Selective detergent-extraction from mixed detergent/lipid/protein micelles, using cyclodextrin inclusion compounds: A novel generic approach for the preparation of proteoliposomes. *Biochem. J.*, 330, 667 - 674.
- DeLange, F., Merckx, M., Bovee-Geurts, P. H. M., Pistorius, A. M. A., and DeGrip, W. J. (1997). Modulation of the metarhodopsin I/metarhodopsin II equilibrium of bovine rhodopsin by ionic strength - Evidence for a surface charge effect. *Eur. J. Biochem.*, 243, 174 - 180.
- Fahmy, K. and Sakmar, T. P. (1993). Regulation of the rhodopsin-transducin interaction by a highly conserved carboxylic acid group. *Biochemistry-USA*, 32, 7229 - 7236.
- DeGrip, W. J., VanDeLaar, G. L. M., Daemen, F. J. M., and Bonting, S. L. (1973). Sulfhydryl groups and rhodopsin photolysis. *Biochim. Biophys. Acta*, 325, 315 - 322.
- Janssen, J. J. M., Mulder, W. R., DeCaluwé, G. L. J., Vlak, J. M., and DeGrip, W. J. (1991). In vitro expression of bovine opsin using recombinant baculovirus: The role of glutamic acid (134) in opsin biosynthesis and glycosylation. *Biochim. Biophys. Acta*, 1089, 68 - 76.
- DeCaluwé, G. L. J., VanOostrum, J., Janssen, J. J. M., and DeGrip, W. J. (1993). In vitro synthesis of bovine rhodopsin using recombinant baculovirus. *Meth. Neurosci.*, 15, 307 - 321.
- Matthews, R. G., Hubbard, R., Brown, P. K., and Wald, G. (1963). Tautomeric forms of metarhodopsin. *J. Gen. Physiol.*, 47, 215 - 240.
- Ostroy, S. E., Erhardt, F., and Abrahamson, E. W. (1966). Protein configuration changes in the photolysis of rhodopsin. II. The sequence of intermediates in thermal decay of cattle metarhodopsin in vitro. *Biochim. Biophys. Acta*, 112, 265 - 277.
- Emeis, D., Kühn, H., Reichert, J., and Hofmann, K. P. (1982). Complex formation between metarhodopsin II and GTP-binding protein in bovine photoreceptor membranes leads to a shift of the photoproduct equilibrium. *FEBS Lett.*, 143, 29 - 34.
- Parkes, J. H. and Liebman, P. A. (1984). Temperature and pH dependence of the metarhodopsin I-Metarhodopsin II kinetics and equilibria in de bovine rod disk membrane suspensions. *Biochemistry-USA*, 23, 5054 - 5061.

21. Parkes, J. H., Gibson, S. K., and Liebman, P. A. (1999). Temperature and pH dependence of the metarhodopsin I - metarhodopsin II equilibrium and the binding of metarhodopsin II to G protein in rod disk membranes. *Biochemistry-USA*, 38, 6862 - 6878.
22. Rath, P., Bovee-Geurts, P. H. M., DeGrip, W. J., and Rothschild, K. J. (1994). Photoactivation of rhodopsin involves alterations in cysteine side chains: Detection of an S-H band in the meta I \rightarrow meta II FTIR difference spectrum. *Biophys. J.*, 66, 2085 - 2091.
23. Marquardt, T. and Helenius, A. (1992). Misfolding and aggregation of newly synthesized proteins in the endoplasmic reticulum. *J. Cell Biol.*, 117, 505 - 513.
24. Helenius, A. (1994). How N-linked oligosaccharides affect glycoprotein folding in the endoplasmic reticulum. *Mol. Biol. Cell*, 5, 253 - 265.
25. Weitz, C. J. and Nathans, J. (1992). Histidine residues regulate the transition of photoexcited rhodopsin to its active conformation, metarhodopsin II. *Neuron*, 8, 465 - 472.
26. Weitz, C. J. and Nathans, J. (1993). Rhodopsin activation: Effects on the metarhodopsin I-metarhodopsin II equilibrium of neutralization or introduction of charged amino acids within putative transmembrane segments. *Biochemistry-USA*, 32, 14176 - 14182.
27. Fahmy, K., Jäger, F., Beck, M., Zvyaga, T. A., Sakmar, T. P., and Siebert, F. (1993). Protonation states of membrane-embedded carboxylic acid groups in rhodopsin and metarhodopsin II: A Fourier-transform infrared spectroscopy study of site-directed mutants. *Proc. Nat. Acad. Sci. USA*, 90, 10206 - 10210.
28. Rath, P., DeCaluwé, G. L. J., Bovee-Geurts, P. H. M., DeGrip, W. J., and Rothschild, K. J. (1993). Fourier transform infrared difference spectroscopy of rhodopsin mutants: Light activation of rhodopsin causes hydrogen-bonding changes in residue aspartic acid-83 during meta II formation. *Biochemistry-USA*, 32, 10277 - 10282.
29. Frillingos, S., Sahin-Tóth, M., Persson, B., and Kaback, H. R. (1994). Cysteine-scanning mutagenesis of putative helix VII in the lactose permease of *Escherichia coli*. *Biochemistry-USA*, 33, 8074 - 8081.
30. Casey, J. R., Ding, Y., and Kopito, R. R. (1995). The role of cysteine residues in the erythrocyte plasma membrane anion exchange protein, AE1. *J Biol. Chem.*, 270, 8521 - 8527.
31. Conn, P. M., Leños, M. A., and Janovick, J. A. (2002). Protein origami: Therapeutic rescue of misfolding gene products. *Mol. Interv.*, 2, 308 - 316.
32. Mirzadegan, T., Benko, G., Filipek, S., and Palczewski, K. (2003). Sequence analyses of G-protein-coupled receptors: Similarities to rhodopsin. *Biochemistry-USA*, 42, 2759 - 2767.
33. Rao, V. R., Cohen, G. B., and Oprian, D. D. (1994). Rhodopsin mutation G90D and a molecular mechanism for congenital night blindness. *Nature*, 367, 639 - 642.
34. Hargrave, P.A. and McDowell, J.H. (1992). Rhodopsin and phototransduction - A model system for G-protein-linked receptors. *FASEB J.*, 6, 2323 - 2331.



Chapter 5

Cysteine scanning mutagenesis in
rhodopsin on a wild type
background

Abstract

Mutation of the residues of the second transmembrane domain of rhodopsin on a cysteine-free background appeared to cause major problems in functional expression. Hence, we modified our initial approach and decided to evaluate cysteine scanning mutagenesis of the second transmembrane segment on a wild type background. In contrast to the cysteine-free background most wild type-based single cysteine mutants produced total levels of recombinant protein equal to wild type rhodopsin, and similar amounts of glycosylated protein, as well. All mutants produced quantities of functional protein that would be sufficient for purification by IMAC and for further analysis. Until now, the mutants L76C, L79C, V81C, D83C, F85C, F88C, G89C and G90C have been partially analyzed. It was shown before that residue Asp83 does not play an essential role in signal transduction by rhodopsin, but that it contributes to structure and photochemistry by interaction with H-bonded networks. Our data so far indicate that residues Leu76, Val81 and Phe85 do not seem to be essential for signaling, but residues Phe88, Gly89 and Gly90 most likely participate in Meta II formation and receptor activation. Due to the prominent wild-type background in the -SH peak region of the FT-IR difference spectrum, the activity of the substituted cysteine residues is difficult to interpret. We therefore conclude that for an effective combination with FI-IR difference spectroscopy cysteine scanning mutagenesis is better performed on a background free of endogenous cysteine activity.

5.1 Introduction

Rhodopsin is a membrane spanning protein containing seven transmembrane segments (TM) that belongs to the family of G protein-coupled receptors. Rhodopsin is a unique member of this family because its ligand, 11-*cis* retinal, is covalently bound to the protein, opsin. Upon photoactivation, the retinal ligand isomerizes to the all-*trans* form and drives the protein through a series of transient photointermediates (Rhodopsin → Bathorhodopsin (Batho) ↔ Blue-shifted intermediate (BSI) → Lumirhodopsin (Lumi) → Metarhodopsin I (Meta I) ↔ Metarhodopsin II (Meta II) → Metarhodopsin III (Meta III)) that within milliseconds leads to the generation of the active state (Meta II), which binds and activates the G protein transducin (G_T) [1].

The 3D-crystal structure of ground-state rhodopsin (2.8 Å resolution) [2] does not show what elements of the protein are involved in the photoactivation of rhodopsin. Results from earlier experiments indicate that the second transmembrane domain (TM II) of rhodopsin undergoes structural changes during photoactivation [2-6]. Our aim is to study the contribution of the protein residues of the second transmembrane domain to the photoactivation of rhodopsin by means of cysteine scanning mutagenesis in combination with FT-IR difference spectroscopy. However, the cysteine sulfhydryl peak will appear on the background of native cysteines and might interfere with native cysteine residues. Our initial goal therefore was to study the residues of TM II on a cysteine-free background (SOH ΔC) (see Chapter 3) but mutation of these residues on this background appeared to cause major production problems (see Chapter 4). In Chapter 2 of this thesis we showed that a change in the vibrational properties of a single cysteine sulfhydryl group can be measured on the background of native cysteines. With this knowledge in mind we modified our initial plan and decided to perform cysteine

scanning mutagenesis of TM II on a wild type (wt) background since this was likely to generate less severe functional expression problems.

5.2. Materials and methods

5.2.1 Cloning and expression

Synthetic cDNA of bovine rhodopsin (SOH WT) was kindly provided by Oprian (Brandeis University, Waltham) in the PMT vector. Restriction sites were introduced by means of silent mutations to allow modification and analysis by means of restriction enzymes. All constructs were extended with a 6X his-tag to allow rapid purification by immobilized metal affinity chromatography (IMAC) [7]. Mutants SOH WT/Y74C – N78C and SOH WT/L84C – G90C were constructed by means of cassette mutagenesis as described in Chapter 4 using the same cassettes as used in the cysteine-free mutants. After cloning of the cassette into SOH WT, the recombinant SOH WT was cloned into the transfer vector pFastbac DUAL under control of the polyhedrin promoter. This transfer vector was used to generate recombinant baculovirus as described in Chapter 3. The cassettes were checked for the correct mutation by cycle-sequencing using primer 5'-cagttttgtaataaaaaacctaataat-3' located in the polyhedrin promoter site of pFastbac DUAL or appropriate rhodopsin primers [8]. Mutants SOH WT/L79C – A82C were constructed by exchange of the corresponding mutation from the SOH Δ C-mutant (pBlueScript II SK⁻ vector) to SOH WT (pFastbac DUAL vector) using restriction enzymes BamH I and Nco I (Life Technologies Inc.). To prevent digestion of the Nco I-site located in the p10 promoter site of the pFastbac DUAL vector, this restriction site was first removed by digesting the vector with Nco I, after which the sticky ends of the restriction site were filled to create blunt ends using T4 DNA polymerase. Next, the vector was closed by ligation and SOH WT was subcloned from the pBlueScript II SK⁻ vector into this modified pFastbac DUAL vector. The mutation of interest could now be excised of the SOH Δ C-mutant and cloned into SOH WT in the pFastbac DUAL vector using the BamH I and Nco I restriction sites. The cassettes were checked for the correct mutation by cycle-sequencing as described above. SOH WT/D83C was directly subcloned from the pAcRP23 vector [9] into the pFastbac DUAL vector.

The Bac-to-bac Baculovirus Recombination system (Life Technologies Inc.) was used as described in Chapter 3 to generate recombinant baculovirus for expression of recombinant rhodopsin in Sf9 *Spodoptera frugiperda* cells. The recombinant virus (P₁) was tested for production of (recombinant) opsin by means of Western blotting and viral DNA was tested for the correct rhodopsin insert by restriction enzyme analysis or sequencing of viral nuclear DNA as described in Chapter 3.

The recombinant virus was amplified (P₂) and the virus titer was determined by means of a plaque assay (see Chapter 3). For expression of recombinant protein Sf9 cells were adapted in monolayer culture in T₁₈₂ culture flasks to serum-free InsectXpress medium (Cambrex). For large scale productions in the bioreactor (1 - 10 litre), InsectXpress medium-adapted cells were scaled up in spinner flasks to obtain a minimum concentration of $5 \cdot 10^5$ cells/ml in the bioreactor. The cells were infected in mid log phase with a multiplicity of infection of 0.05-0.1 and finally harvested at 4 d.p.i. as described before [8,10,11].

5.2.2 Analysis of recombinant rhodopsins

Total recombinant protein production was analyzed by SDS-PAGE (12% acrylamide) of total cellular protein followed by immunoblotting with an anti-rhodopsin antibody as described in Chapter 3.

The capacity of the recombinant opsins produced by Sf9 cells to bond with 11-*cis* retinal to form a photosensitive pigment was assayed by incubation of total cellular membrane preparations with a five-fold excess of 11-*cis* retinal under dim red light (Schott 610 long pass filter) or in darkness, as described before [8]. Formation of photosensitive pigment was analyzed by recording UV-VIS spectra before (1) and after (2) illumination in the presence of 20 mM hydroxylamine [12] and is presented as difference spectra (1-2).

The mutants and wild type rhodopsin were purified by means of immobilized metal chromatography (IMAC) over Ni²⁺ agarose as described before in [11] except that after regeneration with 11-*cis* retinal the samples were treated with 2 M dimethyl thiourea in 20 mM Pipes, 130 mM NaCl, 10 mM KCl, 3 mM MgCl₂, 2 mM CaCl₂, 0.1 mM EDTA, pH 6.5 for 30 min at 4°C to remove non-intrinsic membrane proteins. After centrifugation (30 min, 92,000xg, 4°C) the supernatant could be used for IMAC. Not every mutant pigment was efficiently extracted in DOM and therefore alternative detergents were used. For SOH WT/L76C, SOH WT/G89C extraction was performed in DOM (10 mM)/CHAPS (10 mM) and SOH WT/F88C, SOH WT/G90C and wild type rhodopsin were extracted in nonylglycose (20 mM). After centrifugation (30 min, 92,000xg, 4°C), the supernatant was treated on ice with ammonium sulphate to a final concentration of 1.79 M to remove part of contaminating protein. After incubation for 120 min and another centrifugation step (30 min, 92,000xg, 4°C) the supernatant could directly be applied to a Ni²⁺ NTA agarose column. After washing, the bound pigments were eluted with 20 mM bis-trispropane, 150 mM NaCl, 15% glycerol, 5 mM β-mercaptoethanol, 20 mM nonylglycose, 50 mM histidine, pH 6.5. After purification the pigments were reconstituted into retina lipids as described previously [13].

pH dependence of the Meta I → Meta II transition was measured according to DeLange *et al.*, 1997 [14]. In short, rhodopsin proteoliposomes were resuspended in buffer with appropriate pH. A spectrum was recorded between 750 and 250 nm of the initial, unbleached sample. (spectrum 1). After illumination a second spectrum was recorded (spectrum 2). The relative amount of Meta I formed after illumination was derived from the linear relationship between the λ_{\max} of the difference spectrum (spectrum 1 – spectrum 2) and the percentage photoproduct formed.

Activation of the bovine G protein transducin (G_T) by recombinant rhodopsin was measured by the intrinsic fluorescence enhancement of the G protein α-subunit upon binding of GTPγS (Roche) as earlier described [12,15] (Chapter 3).

FT-IR analyses were performed on a Bruker IFS 66v/S spectrometer using set up and settings as described in Chapter 3.

5.3 Results

5.3.1 Protein production

The total amount of recombinant opsin produced was estimated by means of immunoblot analysis. Most mutants produced total amounts of recombinant protein of at least 75% compared to wild type but the ratio of glycosylated opsin [16] to non-

SOH WT Mutant	Total protein production		Functional protein
	Glycosylated	Non- glycosylated	% \pm SD (wt \equiv 100%)
wild type	++++	++++	100
Y74C	++	+	33 (n = 1)
I75C	+++	++++	67 (n = 1)
L76C	++	+	167 (n = 1)
L77C	++++	++++	92 \pm 82 (n = 2)
N78C	++++	++	25 (n = 1)
L79C	++++	++++	44 (n = 1)
A80C	n.d.	n.d.	n.d.
V81C	++++	++	88 (n = 1)
A82C	+	++++	33 (n = 1)
D83C	+++	+	80 \pm 2 (n = 2)
L84C	n.d.	n.d.	n.d.
F85C	++	++++	100 (n = 1)
M86C	++	+++	40 \pm 3 (n = 3)
V87C	+++	++++	13 (n = 1)
F88C	++++	++++	63 \pm 18 (n = 2)
G89C	++++	++++	92 \pm 12 (n = 2)
G90C	+++	++++	72 \pm 24 (n = 2)

Table 1: Protein production analysis of mutants and wild rhodopsin produced in T₁₈₂ culture flasks. Immunoblot analysis was performed on total cellular protein of Sf9 cells infected with recombinant baculovirus expressing (recombinant) opsins. Blots were screened with primary, polyclonal antibody CERN922 (1:10.000). The plusses indicate the amount of respectively glycosylated or non-glycosylated opsin relative to wild type estimated by visual inspection of blots with cellular protein. Protein production by wild type was set at 100%. + = \leq 25%, ++ = 25 – 50%, +++ = 50 – 75%, ++++ \geq 75% compared to wild type (some mutants appear to produce larger amounts of protein than wild type). About 40% of wild type protein production consists of glycosylated and about 60% consists of non-glycosylated opsin. Functional protein was measured by recording UV-VIS spectra before (1) and after (2) illumination in the presence of 20 mM hydroxylamine [12]. n.d. = not determined, n = number of independent experiments.

glycosylated opsin varied (Table 1). Most mutants produced amounts of glycosylated protein in the same range as wild type. In addition, both wild type and mutants produced considerable quantities of non-glycosylated protein.

The mutant rhodopsins were tested for production of functional protein in Sf9 insect cells on a small scale (T₁₈₂ flasks). The capacity of the recombinant opsins to bond with 11-*cis* retinal to form a photosensitive pigment was analysed by UV-VIS spectroscopy. Subtraction of the spectrum after illumination from the spectrum before illumination gives a difference spectrum, in which interference with e.g. sloping baselines is cancelled out. This allows a better estimation of the λ_{max} and of the amount of recombinant protein that is produced. The quantity of functional protein (pmol/10⁶ cells) produced by the mutant rhodopsins compared to wild type varied strongly per mutant (13 – 167%; Table 1) but was high enough to obtain sufficient amounts of purified functional protein for further analysis through large scale production and purification by IMAC.

Mutant (SOH WT-based)	Production of functional protein (pmol/10 ⁶ cells)	Total protein production		λ_{\max} (nm) (purified pigment)	Recovery after purification (%)	Purity index [†] ($A_{280}/A_{\lambda_{\max}}$)
		glycosylated	non-glycosylated			
wild type	9	++++	++++	498 ± 1	40	2.4
L76C	9	++	+	495	27	3.5
L79C	6	+++	++++	497*	-	-
V81C	5	+++	++++	497	21	7.8
D83C	14	n.d.	n.d.	495 ± 2	75	2.3
F85C	6	+++	++++	499	25	5.1
F88C	5	+++	++++	497	67	2.8
G89C	6	++	++++	499	33	4.5
G90C	11	n.d.	n.d.	489	14	2.2

Table 2: Large scale expression and purification of SOH WT-mutants. For purification single-step Ni²⁺-affinity chromatography (IMAC) was used. Total protein production was estimated relative to wild type as explained in the legend of Table 1.

* Determined from non-purified spectrum.

n.d.: not determined.

[†] For highly purified rhodopsin this index = 1.8 ± 0.1

5.3.2 Purification and reconstitution

The mutants SOH WT/L76C, L79C, V81C, D83C, F85C, F88C, G89C and G90C were timely produced on a large scale (1 – 10 litre) to allow further analysis. Although significant amounts of functional protein could be generated, substantial losses were encountered during purification and reconstitution (Table 2), and some mutants could only be partly analyzed. The relative quantities of functional protein production at a bioreactor scale were roughly similar to those obtained in culture flasks. To allow detailed functional analysis the mutant rhodopsins were purified by IMAC as described for wild type rhodopsin [7,11]. This method uses DOM for extraction in which, however, mutants SOH WT/L76C, F88C, G89C and G90C were poorly dissolved and gave turbid solutions. Extraction was best for L76C and G89C in a combination of DOM/CHAPS (1:1) and for F88C and G90C in nonylglycose. Direct application of the resulting supernatant to the IMAC matrix, however, resulted in poor purification due to low binding efficiency to the matrix and substantial contamination with other proteins. Several approaches for reducing protein contamination before IMAC were tested, and

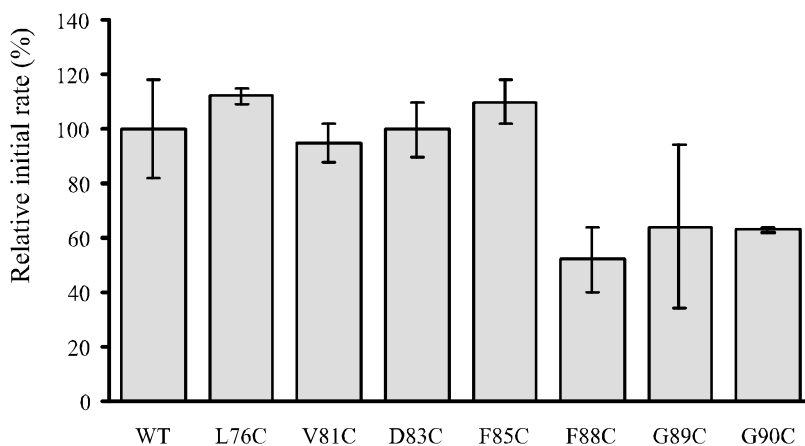


Fig. 1: G protein activation kinetics of rhodopsin mutants. Initial rate of intrinsic fluorescence enhancement (excitation: 295 nm; emission: 337 nm) of the G protein α -subunit upon GTP γ S binding was used to monitor activation by wild type and mutant rhodopsins. Wild type rate was set at 100%. Mutants SOH WT/L76C, V81C, F85C and G89C do not differ significantly from wild type rhodopsin, whereas the mutants SOH WT/F88C and SOH WT/G90C exhibit significant lower activity than wild type rhodopsin. Error bars reflect standard deviation of a concentration range ($n = 5$) in a single experiment.

incubation with 40-45% saturated ammoniumsulphate on ice for 30 min to precipitate part of the contamination usually gave satisfactory results. The resulting supernatant could be directly applied to the IMAC matrix. The mutants were purified in parallel experiments and recoveries varied from 14 – 67% ($n = 1$) with a recovery of 40% ($n = 1$) for wild type rhodopsin (Table 2). The ratio $A_{280}/A_{\lambda_{max}}$ represents a purity index and varied from 2.2 to 7.8. A ratio of 1.8 indicates highly pure rhodopsin. The spectra of the mutants were very similar in bandshape to that of wild type rhodopsin, but those of L76C, D83C, and G90C showed blue-shifts between 3 and 9 nm (Table 2). The purified pigments were reconstituted into a native bovine retina lipid environment using detergent extraction as described in [13] with recoveries of at least 90%.

5.3.3 Functional analysis

The G protein activation capability was determined by measuring the initial rate of the intrinsic fluorescence enhancement of the G protein α -subunit upon GTP binding under standardized conditions. Mutants SOH WT/L76C, V81C, D83C and F85C displayed a G protein activation capability similar to that of wild type rhodopsin, whereas the activity of mutants F88C, G89C and G90C was reduced (Fig. 1).

Figure 2 shows representative difference spectra of the photocascade of mutants SOH WT/L76C, D83C, F85C, F88C, G89C and G90C measured at 10°C, pH 6.5. Rapid and slow changes are given as difference spectra highlighting the formation of Meta I and Meta II (spectrum 1) and the decay of Meta II and formation of Meta III (spectrum 2), respectively. In general terms, the photocascade of all mutants was very similar to that of wild type rhodopsin under these conditions. The late photointermediates Meta I and Meta II are in a pH-dependent equilibrium [17-21]. Hence, the pKa of this equilibrium will determine the level of activated receptor (Meta II) at a fixed pH. The Meta I \leftrightarrow Meta II equilibrium was analyzed for mutants SOH WT/D83C and F88C and wild type rhodopsin in the pH range 5.8 – 7.5 (Fig. 3). The assay was performed at 10°C, where

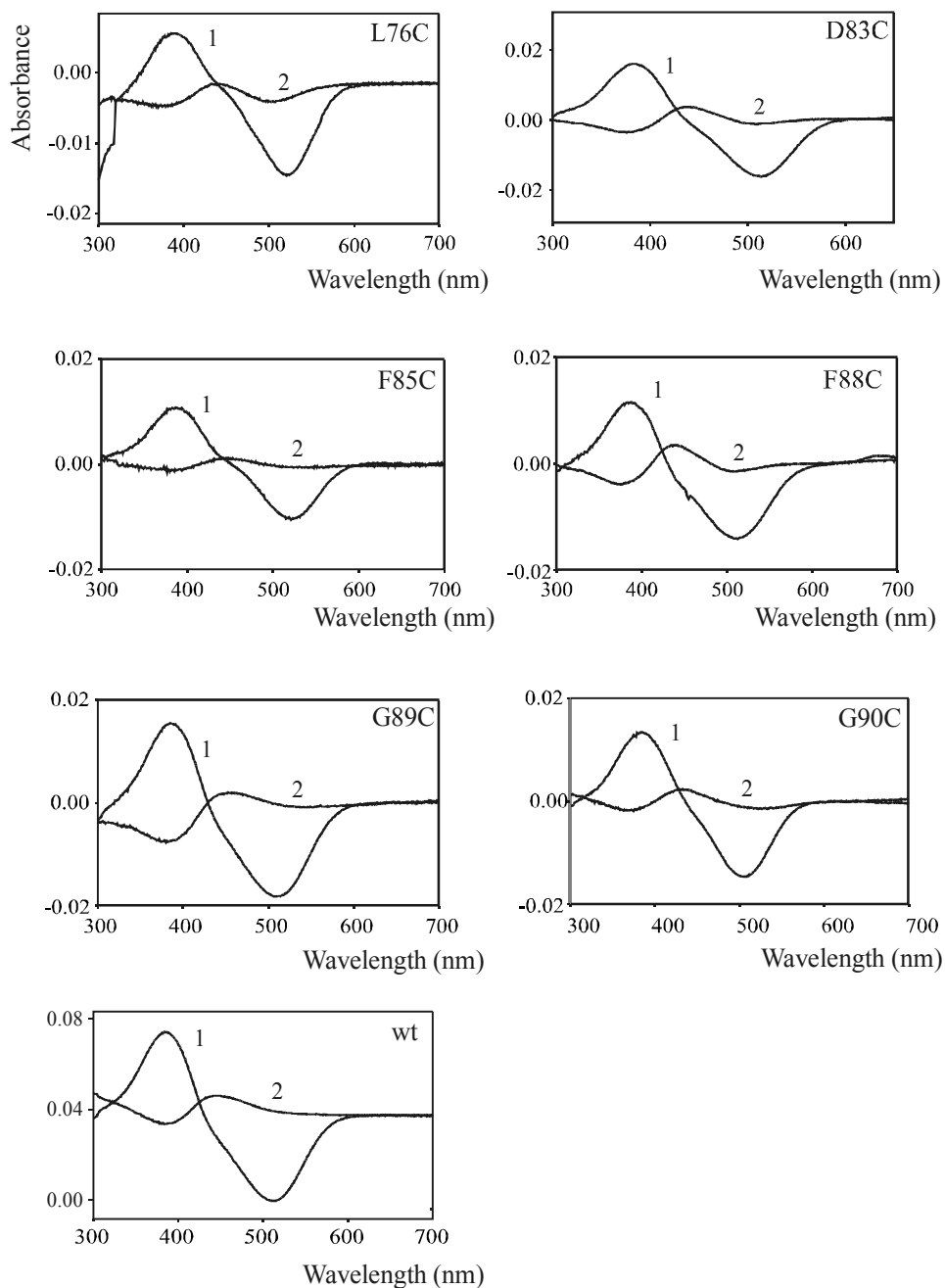


Fig. 2: Difference spectra representing major transitions in the photocascade of wild type rhodopsin and mutants SOH WT/L76C, D83C, F85C, F88C, G89C and G90C measured at 10°C, pH 6.5. Spectrum 1 shows the loss of rhodopsin concomitant formation of Meta I (480 nm) and Meta II (380 nm). Spectrum 2 reflects the decay of Meta II to several products, including Meta III (450 nm).

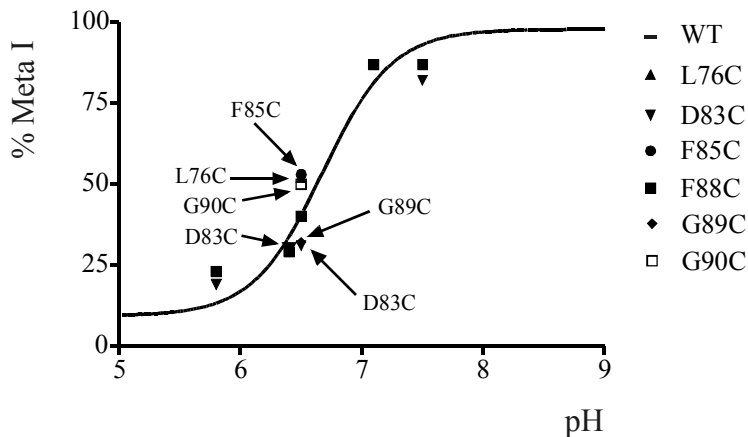


Fig. 3: pH dependence of the Meta I ↔ Meta II equilibrium of wild type rhodopsin and mutants SOH WT/D83C and F88C (full analysis) and L76C, F85C, G89C and G90C (single data point at pH 6.5). Measurements were performed at 10°C. The solid line represents best fit for wild type with a Michaelis-Menten equation. Arrows indicate coinciding data points. We conclude that there is no evidence for significant changes in the pKa of the Meta I ↔ Meta II equilibrium of these mutants.

Meta II is sufficiently stable ($t_{1/2} > 20$ min.). The pKa of D83C and F88C was not significantly different from wild type rhodopsin ($pK_a = 6.6 \pm 0.2$). For the mutants L76C, F85C, G89C and G90C only one data point, measured at pH 6.5, could be obtained. These data points again do not significantly deviate from wild type rhodopsin. The structural changes in the rhodopsin → Meta II transition were analyzed by FT-IR difference spectroscopy. Figure 4 shows this transition for the mutants L76C, D83C, F85C, F88C, G89C and wild type rhodopsin. The difference spectrum of SOH WT/D83C has been thoroughly analyzed in Chapter 2 and is very similar to that of wild type, except for the absence of the Asp83 carboxyl vibrations. The overall pattern of the other mutants is quite similar to wild type as well, indicating that the mutation has not induced long-range structural perturbations. Nevertheless, these mutants all clearly differ in intensity or bandshape from wild type in the Amide I ($1620\text{-}1680\text{ cm}^{-1}$) and Amide II ($1520\text{-}1560\text{ cm}^{-1}$) region, indicating subtle differences in secondary structure changes accompanying Meta II formation. In addition, small individual differences are observed for F85C (1356 and 1170 cm^{-1}), F88C (1160 , 1150 , 1134 and 1082 cm^{-1}) and G89C (1780 , 1060 and 1004 cm^{-1}). SOH WT/D83C displayed a significant increase in the band near 2550 cm^{-1} that can be assigned to $-\text{SH}$ stretch vibrations (Fig. 5) [22]. The FT-IR difference spectra of the other mutants show a large background noise in this region. Mutant L76C and F85C may have a $-\text{SH}$ peak area comparable to wild type but seem to show a peak shift. In order to quantify this phenomenon, additional data are required in order to reduce the noise level. In F88C and G89C the $-\text{SH}$ peak seems to be strongly decreased.

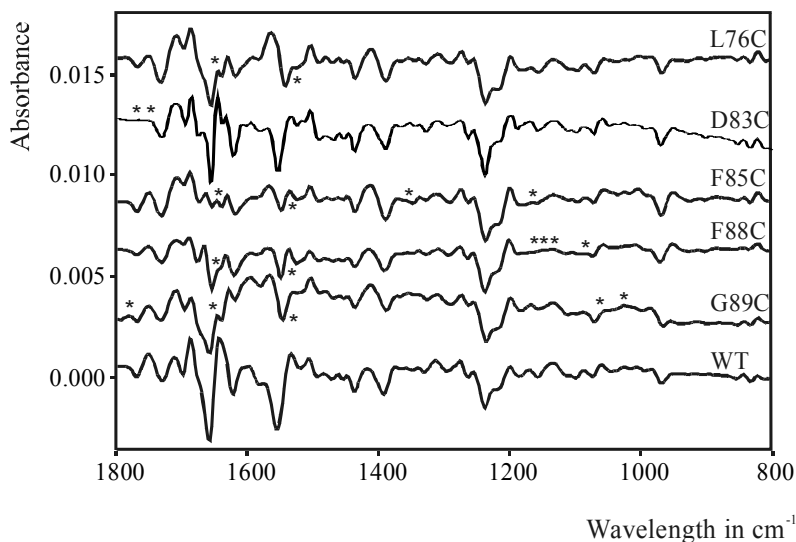


Fig. 4: The 1800-800 cm^{-1} region of the FT-IR difference spectra of the rhodopsin \rightarrow Meta II transition of wild type rhodopsin and mutants SOH WT/L76C, D83C, F85C, F88C and G89C. Spectra were taken at 10°C and pH 6.0 within 5 minutes after illumination, so as to minimize interference by the slow decay of Meta II (half life of > 20 minutes under these conditions). Overall, the spectra are very similar to that of wild type rhodopsin. The small individual differences, indicated by asterisks, could not yet be assigned.

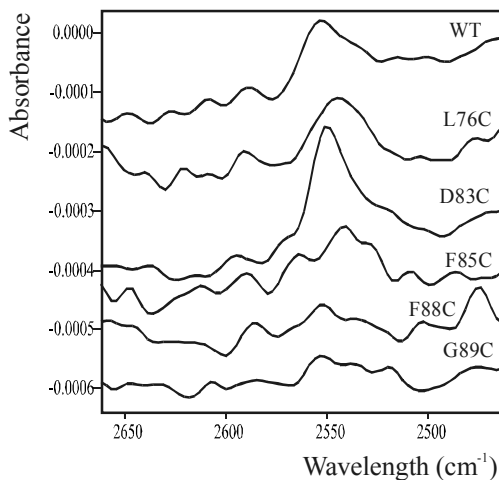


Fig. 5: FT-IR difference spectra of the rhodopsin \rightarrow Meta II transition of wild type rhodopsin and mutants SOH WT/L76C, D83C, F85C, F88C and G89C. The 2600-2500 cm^{-1} region is shown where the stretch vibration of the sulfhydryl group absorbs. Spectra were scaled on the chromophore peaks at 1230 and 970 cm^{-1} . The -SH peak of SOH WT/D83C shows a significant increase compared to wild type rhodopsin. These first data indicate that the -SH peak areas of mutants L76C and F85C are about similar to that of wild type, whereas that of F88C and G89C show a significant decrease. More detailed analysis will require averaging with additional spectra to improve signal to noise ratio.

5.4 Discussion

In the previous chapter we aimed to study the residues of the second transmembrane domain of rhodopsin by substituting single residues by a cysteine on the background of a cysteine-free base-mutant (SOH Δ C). Most mutants failed to produce sufficient amounts of functional protein to study their structural or functional properties. Earlier experiments demonstrated that it is possible to measure strong sulfhydryl group changes by FT-IR difference spectroscopy on a background of native cysteines (Chapter 2). Therefore, we decided to take the risk of native $-SH$ interference and study the residues of the second transmembrane domain using wild type rhodopsin as background.

5.4.1 Expression and purification of single TM II cysteine mutants

Small scale protein production (monolayer culture in T₁₈₂ flasks) was initially used to estimate the level of total and functional protein of the rhodopsin mutants and the extent of glycosylation. In strong contrast to the cysteine-free based mutants, most wild type-based mutants produced total levels of recombinant protein of at least 75% compared to wild type with similar amounts of glycosylated protein. Both wild type and mutants in general generated large quantities of non-glycosylated opsin. All mutants produced functional protein in amounts varying from 13% to 167% of that of wild type rhodopsin. No relationship was apparent between the quantity of glycosylated protein and the production of functional protein but the low number of experiments may obscure such a correlation. To obtain sufficient amounts of functional protein for structural and functional analysis, the recombinant rhodopsins were produced at a larger scale in bioreactors (1 – 10 litre). The total amount of protein produced was comparable to that in culturing flasks. Again a relatively high level of non-glycosylated protein product was generated (except for SOH WT/L76C). The relative amounts of functional protein produced in the bioreactor by the recombinant baculoviruses were roughly similar to those in culturing flasks. Several mutants could already be purified to a reasonable extent, although the recovery varied strongly (14 - 75%). The final purity also showed great variation (down to only 30% of wild type), but no correlation was observed with the recovery.

The amounts of functional protein produced by the wild type-based mutants were significantly increased compared to those produced by the SOH Δ C-based mutants. As argued in Chapter 3 the SOH Δ C base mutant will be less stable than wild type, as cysteine 167 and 264 form part of the retinal binding site and play a structural role during the photoactivation of rhodopsin. The wild type-based mutants differ only in the mutated residue from wild type rhodopsin and this should have less effect on the stability of the protein and hence probably on its folding ability. In addition these data demonstrate that the single cys-mutations by itself do not seriously interfere with ligand binding.

5.4.2 Functional properties of single TM II cysteine mutants

To date, only mutants SOH WT/L76C, L79C, V81C, D83C, F85C, F88C, G89C and G90C could be obtained in sufficient purity to begin to study their structural and functional properties. Due to technical problems the other mutants could not yet be produced in sufficient quantities to allow even preliminary functional analysis. D83C has already been extensively analyzed in Chapter 2 and this mutant will only briefly be discussed here. The UV/VIS difference spectra of the mutants were very similar in

bandshape compared to wild type. L76C and D83C exhibit a small blueshift in λ_{\max} suggesting subtle electronic perturbation of the chromophore. This has already been discussed for D83C in Chapter 2 considering that the carboxyl proton of Asp83 is thought to participate in an extended H-bonded network that is involved in wavelength regulation [6]. Residue 76 is also located in the neighbourhood of a water molecule. This water molecule mediates interaction between helices I (Thr62) and II (Asn73) [5]. If this water participates in a more extended H-bonded network, substitution of the apolar leucine residue with a cysteine might induce small changes in charge distribution affecting the electronic properties of the chromophore to cause the blueshift. SOH WT/G90C showed a significant 9 nm blue-shift in its λ_{\max} compared to wild type rhodopsin. The electronic properties of the chromophore, that govern the absorbance maximum, partly depend on interactions between the chromophore and the protein. In avian UV/violet pigments the residue corresponding to Gly90 in bovine rhodopsin is reported to be a very strong spectral tuning site and the S \rightarrow C substitution induces a 35 nm blue-shift [23]. In bovine rhodopsin residue 90 is located close to Lys296 and Glu113, since in the mutant G90D D90 can substitute for Glu113 as a counterion [24]. This mutant shows a blueshift in its λ_{\max} to 483 nm, is affected in its photochemical properties and is constitutively active [24]. Interestingly, the G90C mutation in bovine rhodopsin also induces a blue shift and slows down G protein activation, but does not have substantial effects on the photocascade. Cysteine is only very weakly acidic and Cys90 can therefore probably not substitute for Glu113 as a counterion. However, the G90C mutation does affect the electronic properties of the chromophore (λ_{\max} 498 nm \rightarrow 489 nm), probably via a H-bonded network.

The photocascades of mutants SOH WT/L76C, D83C, F85C, F88C, G89C and G90C were found to be very similar to wild type rhodopsin at 10°C and pH 6.5. Analysis of the MI \leftrightarrow MII equilibrium showed that D83C and F88C display a similar pH dependency at 10°C as wild type rhodopsin. For mutants L76C, F85C, F88C, G89C and G90C only one data point was yet available. These data points coincide with wild type and indicate that at 10°C these mutations also do not significantly affect the pKa of the Meta I \rightarrow Meta II transition. The signalling activity of the mutants was compared with wild type rhodopsin by measuring the capacity of the mutants to activate the G protein transducin. Mutants L76C, V81C, D83C and F85C displayed a similar G protein activation capacity as wild type rhodopsin. Apparently the residues at position 76, 81, 83 and 85 are not critical for signalling. Residue Leu76 points into the protein face in the neighbourhood of a water molecule that is positioned in a cavity between helix II, VI and VII. Mutation of this residue into a cysteine introduces minor conformational changes (see below) possibly since the -SH group may H-bond to and/or perturb the position of this water molecule. Apparently these changes do not affect the G protein activation capacity of this mutant. Residues Val81 and Phe85 point into the lipid bilayer and substitution of these residues by a cysteine is therefore not expected to cause significant functional perturbations. Asp83 is thought to participate structurally in an extended H-bonded network [6]. Because of the H-bonding potential of the cysteine sulfhydryl group, Cys83 might participate in this H-bonded network and largely maintain the wild type properties of Asp83 (Chapter 2). On the other hand, mutants F88C and G90C exhibit a respectively 50% and 40% reduced G protein activation rate compared to wild type, whereas results so far also indicate a reduced G protein activation rate for G89C. The 88-90 segment hence may have a role in receptor activation. In fact, Phe88 points into the lipid face but is located close to a water

molecule that is also situated close to residue Gly90. Potentially, Cys88 H-bonds with this water molecule and disturbs the local structure affecting the G protein activation kinetics of mutant F88C. Residue Gly89 and Gly90 are located close to Lys296 and Glu113 in close proximity to two water molecules. Cysteine may perturb local backbone mobility in the Gly-Gly region as well interact with the(se) water molecule(s) to induce local structural perturbations. Apart from this, mutation of a residue directly participating in Meta II formation may affect the activation kinetics by itself. In such conditions, structural perturbations in the rhodopsin to Meta II transition are expected and structural involvement of the cysteine side chain is anticipated.

We used FT-IR difference spectroscopy first of all to analyse whether substitution of the residues of the second transmembrane domain of rhodopsin by a cysteine caused long-range structural perturbations and secondly to identify participation of the newly introduced (-SH) groups in rhodopsin activation. Mutant D83C has been extensively discussed in Chapter 2. This mutation is quite exemplary since it abolishes the change in carboxyl group vibration of Asp83 upon Meta II formation (bilobal bands at 1767 and 1748 cm^{-1}) and shows participation of Cys83 in this transition by an increase of the -SH peak at 2550 cm^{-1} , that must arise in the additional sulfhydryl group of Cys83. Clearly, like the Asp83 carboxyl group, this sulfhydryl group can report on local changes occurring upon formation of Meta II. Further, the rhodopsin \rightarrow Meta II difference spectrum of D83C is very similar to wild type, confirming that this mutation has very few structural side-effects. This is reflected in its G protein activation capacity, which is very similar to that of wild type rhodopsin. The other mutants analyzed so far (L76C, F85C, F88C and G89C) indicate a slight structural perturbation. These mutants show small changes in the Amide I and II region upon Meta II formation, reflecting subtle changes in secondary structure during photoactivation. These changes might represent local structural perturbation as a consequence of the single amino acid substitutions and suggest that in these mutants a small loss in α -helical structure is less explicit. However, in spite of these structural changes, the signalling capacity of the mutants L76C and F85C was not affected, indicating that these structural effects here do not impair signal transduction and that Leu76 and Phe85 are not actively involved in this process. Mutants F88C and probably G89C on the other hand showed slower G protein activation kinetics. Since the small changes in the amide region observed in the F88C mutant are intermediate between those of F85C and G89C, it is not clear whether this is the cause of the decrease in signalling activity. More likely, if Phe88 participates in receptor activation, substitution for Cys cannot fully sustain this activity. In this case it is to be expected that the mutation also will induce small individual changes in the rhodopsin \rightarrow Meta II infrared difference spectrum, that will either reflect the loss of the original residue or the gain of a cysteine residue. Additional analyses to verify their reproducibility and to assign these changes will be necessary for a detailed structural and functional interpretation of the corresponding mutation. The 2600-2500 cm^{-1} region of the FT-IR difference spectra of the mutant rhodopsins is expected to show additional -SH activity, if any, since this region can be assigned to -SH stretch vibrations which peak at 2548 cm^{-1} in wild type rhodopsin [22]. Unfortunately, the noise level is quite substantial in the single spectrum of the mutants obtained so far, and averaging of a population of spectra will be required for a more accurate estimation of peak absorbance and area. At this stage we can conclude that the -SH peak areas of L76C and F85C are roughly similar to wild type, which suggests that these positions do not structurally participate in Meta II formation and agrees with their native-like G protein activation capacity. On the other hand, we cannot exclude that in F85C a bilobal peak is

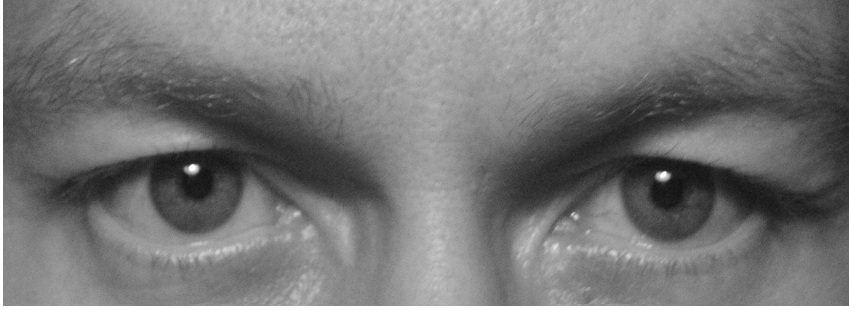
superpositioned on the wild type peak, but this also may reflect background noise. The –SH peaks in F88C and G89C are strongly reduced. This could be interpreted as a suppression of wild type –SH activity by these mutations, reflecting decreased structural participation in Meta II formation which might explain the reduced G protein activation capability. On the other hand, participation of the cysteine residue of these mutants in the photoactivation is expected, as discussed above, and might be reflected by a negative peak in the FT-IR difference spectrum. On a background of wild type cysteines this would then be observed as a decrease in the –SH peak height. This confirms our concern that on a background of native cysteines any activity of the substituted cysteine residues is difficult to interpret, unless there is a considerable increase in peak area as was observed for the D83C mutant.

In conclusion, all mutants on a wild type background produce sufficient amounts of functional protein to allow purification by IMAC and further analysis. As was already extensively discussed in chapter 2, Asp83 does not play an essential role in signal transduction by rhodopsin but does participate in a more structural role. Positions 76, 81, 83 and 85 analyzed so far do not seem to be essential for signalling. On the other hand, mutants F88C, G90C and probably G89C showed reduced G protein activation kinetics. These mutants display a wild type-like photocascade and the pKa of F88C is very similar to that of wild type rhodopsin while the single datapoints for G89C and G90C suggest that this is also true for these mutations. The lower activation kinetics and apparent –SH activity upon Meta II formation of these mutants indicate that residues Phe88, Gly89 and Gly90 participate in Meta II formation and receptor activation. It is conceivable that substitution of a large aromatic side chain or a mobile Gly-Gly segment with a cysteine side chain by itself affects the activation kinetics. On the other hand, small adaptations in secondary structure also may play a role. Because the small changes in secondary structure observed upon Meta II formation in F88C are intermediate between those of F85C and G89C this need not to be a major cause of the decrease in signalling activity. Residue Phe88 and Gly90 are both located close to structural water molecules and Gly90 is also located close to the Schiff base and the counterion site (Lys296 and Glu113). Cysteine residues of mutants F88C, G89C and G90C for instance might be able to participate in H-bonded networks near the chromophore linkage site, causing slight structural changes that affect the signalling kinetics of these mutant rhodopsins [5]. The –SH peak area in the Meta II FT-IR difference spectrum of F88C and G89C is strongly reduced suggesting either an indirect negative effect of these mutations on the wild type –SH activity or a direct participation of the cysteines that reflects itself in a negative peak in the difference spectrum and is thus observed as a decrease in the wild type –SH peak area. Both interpretations are in agreement with our observation that the signalling activity of these mutants is affected. Nevertheless, it is evident that due to the large background noise observed in the –SH peak region of the FT-IR difference spectrum the activity of the substituted cysteine residues is difficult to interpret, except for the D83C mutant which shows a considerable increase in peak area. We conclude that effective cysteine scanning mutagenesis studies will first require adequate production of functional cysteine-free rhodopsin to perform cysteine scanning mutagenesis on a background free of endogenous cysteine activity.

References

- Okada, T., Ernst, O. P., Palczewski, K., and Hofmann, K. P. (2001). Activation of rhodopsin: New insights from structural and biochemical studies. *Trends Biochem. Sci.*, 26, 318 - 324.
- Palczewski, K., Kumasaka, T., Hori, T., Behnke, C. A., Motoshima, H., Fox, B. A., LeTrong, I., Teller, D. C., Okada, T., Stenkamp, R. E., Yamamoto, M., and Miyano, M. (2000). Crystal structure of rhodopsin: A G protein-coupled receptor. *Science*, 289, 739 - 745.
- Fahmy, K., Jäger, F., Beck, M., Zvyaga, T. A., Sakmar, T. P., and Siebert, F. (1993). Protonation states of membrane-embedded carboxylic acid groups in rhodopsin and metarhodopsin II: A Fourier-transform infrared spectroscopy study of site-directed mutants. *Proc. Natl. Acad. Sci. USA*, 90, 10206 - 10210.
- Rath, P., DeCaluwé, G. L. J., Bovee-Geurts, P. H. M., DeGrip, W. J., and Rothschild, K. J. (1993). Fourier transform infrared difference spectroscopy of rhodopsin mutants: Light activation of rhodopsin causes hydrogen-bonding changes in residue aspartic acid-83 during meta II formation. *Biochemistry-USA*, 32, 10277 - 10282.
- Okada, T., Fujiyoshi, Y., Silow, M., Navarro, J., Landau, E. M., and Shichida, Y. (2002). Functional role of internal water molecules in rhodopsin revealed by x-ray crystallography. *Proc. Natl. Acad. Sci. USA*, 99, 5982 - 5987.
- Breikers, G., Bovee-Geurts, P. H. M., DeCaluwé, G. L. J., and DeGrip, W. J. (2001). A structural role for Asp83 in the photoactivation of rhodopsin. *Biol. Chem.*, 382, 1263 - 1270.
- Janssen, J. J. M., Bovee-Geurts, P. H. M., Merks, M., and DeGrip, W. J. (1995). Histidine tagging both allows convenient single-step purification of bovine rhodopsin and exerts ionic strength-dependent effects on its photochemistry. *J. Biol. Chem.*, 270, 11222 - 11229.
- Klaassen, C. H. W. and DeGrip, W. J. (2000). Baculovirus expression system for expression and characterization of functional recombinant visual pigments. *Meth. Enzymology*, 315, 12 - 29.
- Possee, R. D. and Howard, S. C. (1987). Analysis of the polyhedrin gene promoter of the *Autographa californica* nuclear polyhedrosis virus. *Nucl. Acid. Res.*, 15, 10233 - 10248.
- Klaassen, C. H. W., Bovee-Geurts, P. H. M., DeCaluwé, G. L. J., and DeGrip, W. J. (1999). Large-scale production and purification of functional recombinant bovine rhodopsin using the baculovirus expression system. *Biochem. J.*, 342, 293 - 300.
- Bosman, G. J. C. G. M., VanOostrum, J., Breikers, G., Bovee-Geurts, P. H. M., Klaassen, C. H. W., and DeGrip, W. J. (2003). Functional expression of his-tagged rhodopsin in Sf9 insect cells. *Meth. Mol. Biol.*, 228, 73 - 86.
- Janssen, J. W. H., Bovee-Geurts, P. H. M., Peeters, A. P. A., Bowmaker, J. K., Cooper, H. M., David-Gray, Z. K., Nevo, E., and DeGrip, W. J. (2000). A fully functional rod visual pigment in a blind mammal - A case for adaptive functional reorganization? *J. Biol. Chem.*, 275, 38674 - 38679.
- DeGrip, W. J., VanOostrum, J., and Bovee-Geurts, P. H. M. (1998). Selective detergent-extraction from mixed detergent/lipid/protein micelles, using cyclodextrin inclusion compounds: A novel generic approach for the preparation of proteoliposomes. *Biochem. J.*, 330, 667 - 674.
- DeLange, F., Merks, M., Bovee-Geurts, P. H. M., Pistorius, A. M. A., and DeGrip, W. J. (1997). Modulation of the metarhodopsin I/metarhodopsin II equilibrium of bovine rhodopsin by ionic strength - Evidence for a surface charge effect. *Eur. J. Biochem.*, 243, 174 - 180.
- Fahmy, K. and Sakmar, T. P. (1993). Regulation of the rhodopsin-transducin interaction by a highly conserved carboxylic acid group. *Biochemistry-USA*, 32, 7229 - 7236.
- Janssen, J. J. M., Mulder, W. R., DeCaluwé, G. L. J., Vlask, J. M., and DeGrip, W. J. (1991). *In vitro* expression of bovine opsin using recombinant baculovirus: The role of glutamic acid (134) in opsin biosynthesis and glycosylation. *Biochim. Biophys. Acta*, 1089, 68 - 76.
- Matthews, R. G., Hubbard, R., Brown, P. K., and Wald, G. (1963). Tautomeric forms of metarhodopsin. *J. Gen. Physiol.*, 47, 215 - 240.
- Ostroy, S. E., Erhardt, F., and Abrahamson, E. W. (1966). Protein configuration changes in the photolysis of rhodopsin. II. The sequence of intermediates in thermal decay of cattle metarhodopsin *in vitro*. *Biochim. Biophys. Acta*, 112, 265 - 277.
- Emeis, D., Kühn, H., Reichert, J., and Hofmann, K. P. (1982). Complex formation between metarhodopsin II and GTP-binding protein in bovine photoreceptor membranes leads to a shift of the photoproduct equilibrium. *FEBS Lett.*, 143, 29 - 34.
- Parkes, J. H. and Liebman, P. A. (1984). Temperature and pH dependence of the metarhodopsin I-Metarhodopsin II kinetics and equilibria in de bovine rod disk membrane suspensions. *Biochemistry-USA*, 23, 5054 - 5061.
- Parkes, J. H., Gibson, S. K., and Liebman, P. A. (1999). Temperature and pH dependence of the metarhodopsin I - metarhodopsin II equilibrium and the binding of metarhodopsin II to G protein in rod disk membranes. *Biochemistry-USA*, 38, 6862 - 6878.

22. Rath, P., Bovee-Geurts, P. H. M., DeGrip, W. J., and Rothschild, K. J. (1994). Photoactivation of rhodopsin involves alterations in cysteine side chains: Detection of an S-H band in the meta I → meta II FTIR difference spectrum. *Biophys. J.*, 66, 2085 - 2091.
23. Wilkie, S. E., Robinson, P. R., Cronin, T. W., Poopalasundaram, S., Bowmaker, J. K., and Hunt, D. M. (2000). Spectral tuning of avian violet- and ultraviolet-sensitive visual pigments. *Biochemistry-USA*, 39, 7895 - 7901.
24. Rao, V. R., Cohen, G. B., and Oprian, D. D. (1994). Rhodopsin mutation G90D and a molecular mechanism for congenital night blindness. *Nature*, 367, 639 - 642.



Chapter 6

Retinitis pigmentosa associated
rhodopsin mutations in three
membrane-located cysteine residues
present three different biochemical
phenotypes

Abstract

A large number of mutations in rhodopsin are associated with autosomal dominant retinitis pigmentosa (ADRP). We analyzed the biochemical phenotypes of the ADRP-associated cysteine mutants C167R, C222R and C264del. C222R behaved as wild type in every aspect testable and is classified as a class I mutant. C167R produced intact protein but did not regenerate with 11-*cis* retinal and was not transported to the plasma membrane. We confirm its classification as a class IIa mutant. C264del represents a novel phenotype, which we propose to call class III. It produced a truncated protein of 27 kDa that failed to regenerate with 11-*cis* retinal and was not targeted to the plasma membrane.

6.1 Introduction

Rhodopsin is the visual pigment of the rod photoreceptor cell in the vertebrate eye. Like all members of the family of G protein coupled receptors it contains seven transmembrane spanning segments (Fig. 1). Rhodopsin consists of a protein, opsin and an internal ligand or chromophore, 11-*cis* retinal bound to lysine 296 of opsin. Upon

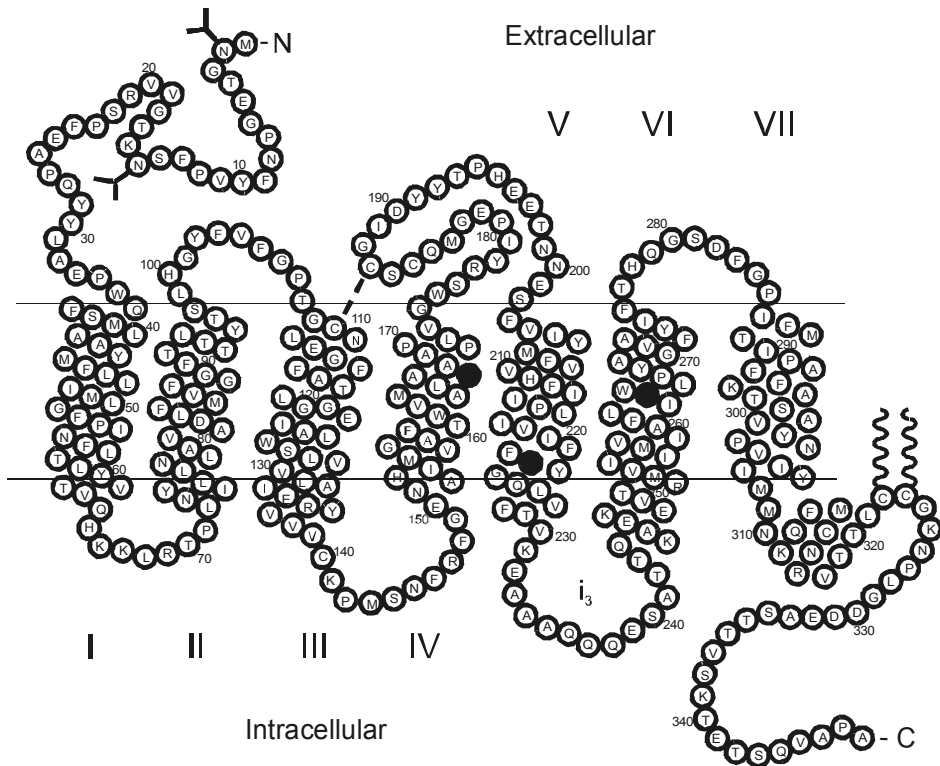


Fig. 1: Schematic representation of the two-dimensional structure of rhodopsin. The transmembrane segments are numbered. Modified from Hargrave and McDowell [1] and Palczewski et al. [3]. Black circles indicate the three cysteine residues addressed in this report. C167 is located in TM IV, C222 in TM V, and C264 in TM VI. i_3 indicates the third intracellular loop.

illumination, the retinal group isomerizes to the all-*trans* form and drives the protein through a series of transient photointermediates which within milliseconds leads to the generation of the active state (Meta II), that binds and activates the G protein transducin [2]. Rhodopsin is a complex integral membrane protein that requires posttranslational modification (thiopalmitoylation, disulfide bridge formation, glycosylation) and subsequently is targeted to the rod outer segment (ROS) membrane to fulfil its structural and functional properties.

While rhodopsin is essential for dim-light (scotopic) vision in all mammals, including human [4] it also has an important pathological component [5]. In the human population, over hundred mutations have been identified in rhodopsin that inflict a dominant form of the retinal disease, retinitis pigmentosa [6]. Retinitis pigmentosa (RP) manifests itself by a black-spotted fundus appearance [7,8] that reflects a degenerative process affecting the rod photoreceptors in the retina. It usually results in night blindness and tunnel vision, but can also lead to overall loss of vision already at a young age [8]. RP is a hereditary disease (incidence 1:4000) [9], which can be transmitted in an autosomal dominant (ADRP), autosomal recessive (arRP) or X-linked (x1RP) form [5]. ADRP accounts for at least 25% of the RP cases in the Western world [10-14]. ADRP can be divided in two distinct types: type 1 and type 2 [5]. Type 1 represents a more severe phenotype and is characterized by earlier onset, diffuse localization and/or rapid progression. Type 2 is characterized by more regional occurrence and/or slow progression. The mutations currently identified in rhodopsin are not randomly distributed. Most mutations ($\pm 60\%$) are found in the transmembrane domain. The extracellular loops account for 35% of the mutations and only a few mutations in the intracellular loops are RP-genic [8]. A large number of mutations in the transmembrane domain give rise to a charged residue that might destabilize the membrane domain and interfere with correct folding [15]. On the basis of expression in heterologous systems, mutations have been classified into three classes: class I mutants resemble wt rhodopsin in that they fold correctly, are targeted to the cell membrane, and bind 11-*cis* retinal to form a typical photosensitive pigment. Class IIa mutants do not fold correctly, do not leave the endoplasmic reticulum (ER) and fail to bind 11-*cis*-retinal. Class IIb mutants also show folding defects, but less severe than IIa and produce varying extents of folded protein capable of binding 11-*cis*-retinal [16,17]. It has therefore been proposed that class IIa and IIb mutants are RP-genic, since they encode an opsin, that exhibits folding defects, accumulates in the ER, and thereby may eventually produce protein overload that perturbs cellular homeostasis. Class I mutations do not perturb the basic properties of folding and binding of 11-*cis*-retinal, but may interfere with correct targeting or functional properties that cannot be assayed in heterologous systems [7,17].

In the course of our studies on the contribution of the transmembrane domain-located cysteine residues C167, C222, and C264 to structure and function of rhodopsin, a single mutation has been reported for every residue, that results in a RP phenotype: C167R [12], C222R [10], and C264del [15]. We have analyzed the biochemical phenotype of these mutants by heterologous expression using the insect cell/recombinant baculovirus system. Unexpectedly, mutant C222R exhibits a class I phenotype, while C167R belongs to class IIa. The 'in-frame' deletion C264del represents a novel phenotype, which we propose to define as class III. It does not seem to generate intact, completely translated protein. A major fragment of 27 kD was produced that was truncated downstream of the third intracellular loop and showed a complex intracellular distribution.

6.2 Materials and methods

6.2.1 Cloning and expression of rhodopsin mutants

The rhodopsin mutants C167S, C222S, C264S, C167R, C222R, and C264del were constructed by means of site-directed mutagenesis using the approach developed by Kunkel [18] incorporated in the Bio-Rad Mutagene kit. Cloning, isolation, and propagation of recombinant baculovirus producing the various mutants under control of the polyhedrin promoter were performed, as described before [19,20]. Recombinant virus was checked for the presence of the correct mutation by cycle sequencing using appropriate rhodopsin primers [20]. Sf9 cell culture and recombinant protein expression were performed as described before [20-22].

6.2.2 Analysis of recombinant rhodopsins

The capacity of the recombinant opsins to bond with 11-*cis* retinal into a photosensitive pigment was assayed by incubation of total cellular membrane preparations with a five-fold excess of 11-*cis* retinal under dim red light (Schott 610 long pass filter) or in darkness, as described before [21]. Formation of photosensitive pigment was analyzed by recording UV-VIS spectra before (1) and after (2) illumination in the presence of 20 mM hydroxylamine [23] and is presented as difference spectra (1-2). Recombinant protein production was analyzed by SDS-PAGE (12% acrylamide) of total cellular protein followed by immunoblotting with several anti-rhodopsin antibodies, as previously described [24]. The blots were probed with the polyclonal antibody CERN858 [25] and the monoclonal antibodies K57-142C, directed against the C-terminus [26], and K42-41L, directed against the i_3 loop [27]. N-glycosylation was analyzed through incubation with N-glycosidase F as described before [24]. Intracellular localization of the mutant proteins was studied using confocal laser scanning microscopy (with CERN858 (1:1000) as primary antibody) according to [24], except that 1×10^5 cells were seeded on a coverslip and subsequently infected with recombinant baculovirus (MOI = 1).

6.3 Results and discussion

Correct protein folding is essential for proper function. Incorrect folding will lead to non-functional proteins that can disturb cellular homeostasis and may have severe pathological consequences [28]. In the course of our studies on the contribution of membrane domain-located cysteine side chains (C167, C222, and C264) to structure and function of rhodopsin [29,30], we were intrigued by clinical genetic studies linking a single mutation in each of these cysteine residues to ADRP [10,12,15]. We therefore constructed the corresponding mutants (C167R, C222R, and C264del) and expressed them in Sf9 cells using the recombinant baculovirus expression system [22,31]. As a control we used the corresponding C→S mutations. In agreement with an earlier report [32], the mutants C167S, C222S, and C264S produced mature, glycosylated opsin that was targeted to the plasma membrane and generated a photosensitive pigment upon incubation with 11-*cis* retinal. The λ_{max} and bandshape of the absorbance bands of the C→S mutants are very close to that of wt rhodopsin, as is obvious from difference spectra (dark minus illuminated, Fig. 2). These rhodopsin mutants present a fully

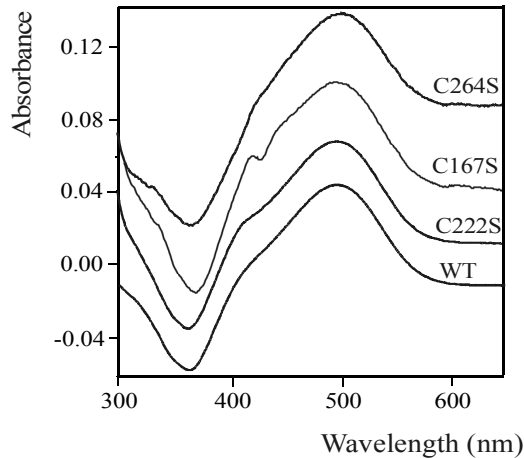


Fig. 2: Absorbance dark-minus-light difference spectra of wt rhodopsin and the mutants C167S, C222S, and C264S. Spectra were obtained by subtracting a spectrum obtained after illumination in the presence of 20 mM hydroxylamine from the original spectrum before illumination. Illumination then produces the all-*trans*-retinoxime absorbing at 365 nm.

functional, wild-type phenotype in every aspect testable [32] (P.H.M. Bovee-Geurts and W.J. DeGrip, unpublished). This demonstrates that mutation of these residues per se does not lead to an ADRP phenotype.

6.3.1 C222R

The clinical phenotype of the C222R ADRP mutation has not been reported in detail [10]. Without presenting any experimental evidence, this mutation was biochemically classified as a class IIa mutant by Kaushal and Khorana [17]. However, in full contrast our results indicate that C222R behaves like wild type and should be classified as a class I mutant. This was already indicated by immunoblot analysis. The major protein product for mutant C222R was represented by a band near 38 kDa (Fig. 3.a) that corresponds to fully glycosylated opsin (thick arrow) [33]. This band actually runs as a doublet, probably due to slight differences in carbohydrate composition, as is also observed in recombinant wild-type rhodopsin (Fig. 3.a). Variable but smaller amounts of non-glycosylated opsin at 31 kDa were also observed (thin arrow), similar again to wild-type expression [33]. Upon treatment with N-glycosidase F only the non-glycosylated species remains (Fig. 3, lanes designated with +). A positive immunoreaction with antibodies against the C-terminus and the i_3 -loop (Fig. 3b and 3c) demonstrates that an intact protein was produced. This was also reflected in its interaction with 11-*cis* retinal that resulted in a photosensitive pigment: the profile of the absorbance band of C222R was very similar to that of wt rhodopsin, with only a slight blue shift in λ_{\max} (Fig. 4; wt λ_{\max} : 498 ± 1 nm, C222R λ_{\max} : 496 ± 2 nm). Finally, the C222R mutant showed a similar intracellular distribution upon baculovirus expression as wild type [20] with clear evidence of targeting to the plasma membrane (Fig. 5.a). Hence the C222R mutation produces a protein with wild-type-like biochemical properties, but it nevertheless is RP-genic [10].

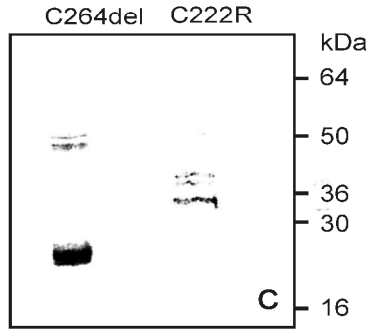
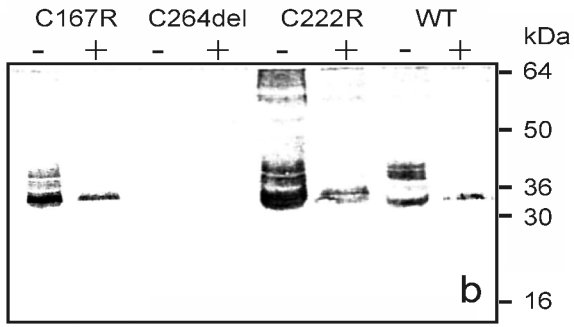
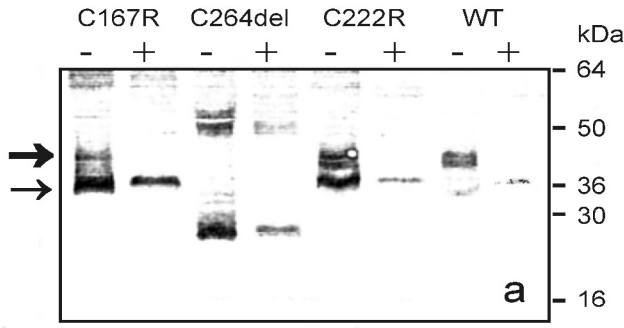


Fig. 3: Immunoblot analysis of Sf9 cells infected with recombinant baculovirus expressing wt or mutant opsins. Blots were screened with primary antibodies; (A) polyclonal antibody CERN858; (B) monoclonal antibody K57-142C (directed against the C-terminus) and (C) monoclonal antibody K42-41L (directed against the i_3 -loop). + Indicates pre-incubation with N-glycosidase F. The - lanes were loaded with extracts of 50,000 cells. The thick arrow indicates the position of intact glycosylated opsin, the thin arrow that of intact non-glycosylated opsin. The bands at $M_w > 50$ kDa represent oligomers, mainly of non-glycosylated species, artificially produced upon solubilization in SDS [24,33].

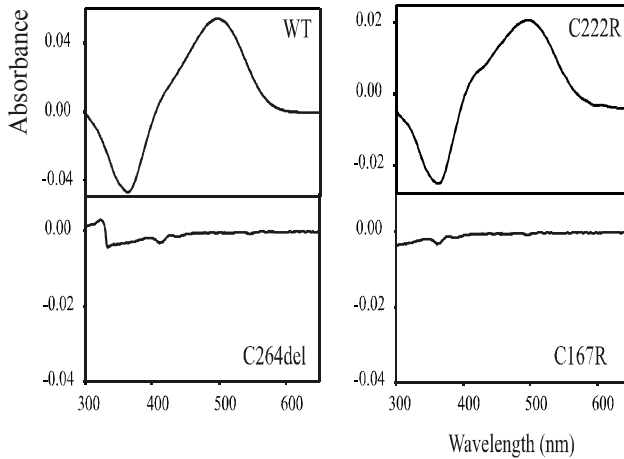


Fig. 4: Absorbance dark-minus-light difference spectra of C167R, C222R, C264del, and wt rhodopsin. Spectra were obtained by subtracting a spectrum obtained after illumination in the presence of 20 mM hydroxylamine from the original spectrum before illumination.

The wild type biochemical properties of C222R were surprising, as replacement of a neutral residue in a membrane-domain by a charged one usually results in folding defects [17]. However, according to the recently refined rhodopsin structure [34] C222 is located in the lipid face of TM V close to the intracellular surface. The side chain of R222 would be able to reach the polar lipid interface and/or could be stabilized by interaction with Y136 and/or Q225. The RP-genic nature of C222R is difficult to explain on basis of these data. Interference of this mutation with the specific targeting of rhodopsin to the rod outer segment is unlikely, since the major targeting signals reside in the C-terminal tail [35]. Several other RP-genic mutations outside the C-terminal region have been reported, that behave as class I (F45L, R135G and D190N) [13,17]. Probably, such mutations perturb subtle properties of rhodopsin involved in structural maintenance of the highly organized rod outer segment or in photoreceptor adaptation [28]. For instance R135 mutants are light-sensitive but do not activate transducin [36]. To resolve such issues, transgenic studies must be undertaken.

6.3.2 C167R

The disease induced by the mutation C167R has been clinically classified as type 1 RP [37]. It shows early onset and the first symptoms comprise night blindness and visual field shrinkage. The fundus of the eye shows typical RP pigmentation and rod function is altered at an early stage, while cones are not affected until the age of about 18 years [37]. Biochemically, the C167R mutation has been classified as class IIa upon expression in COS cells [17]. Our results in Sf9 cells fully agree with this classification. This mutant did not generate detectable amounts of photopigment upon incubation with 11-*cis* retinal (Fig 4). Nevertheless, intact recombinant protein was produced (immunoreaction with C-terminal antibody; Fig. 3.b) part of which was fully glycosylated (Fig. 3.a). The relative amount of non-glycosylated species was significantly larger however than in wild type and the C222R mutant. In addition, this mutant was not targeted to the plasma membrane but accumulated intracellularly in

organelles that with respect to distribution [38] (Chapter 4, Fig. 3) correspond to ER (Fig. 5B).

Residue Cys167 is highly conserved in rod and green cone pigments, and is located in the protein face of TM IV [34]. This suggests that this residue is of structural or functional importance. Cys167 participates in the lining of the retinal binding site and in formation of the active state Metarhodopsin II (W.J. DeGrip, F. DeLange, C.H.W. Klaassen, P.H.M. Bovee and K.J. Rothschild, unpublished). Hence, replacement of the neutral cysteine at this position by the larger and charged side chain of arginine might by itself already perturb binding of the ligand, but will certainly lead to folding defects [15]. Prolonged residence in ER or Golgi will presumably lead to overload of synthetic and degradative pathways in the photoreceptor cell, which could explain the RP-genic nature of this mutation.

6.3.3 C264del

So far, no clinical or biochemical classification has been reported for the mutant C264del. Here, we provide evidence that C264del represents a novel biochemical phenotype that we propose to name class III. Although the in frame deletion of Cys264 should theoretically result in a protein, one residue shorter than wt rhodopsin, this mutation seems to have much broader consequences. The product failed to regenerate with 11-*cis* retinal (fig. 4) and was not targeted to the plasma membrane (Fig. 5.c). In this respect it resembles class IIa mutations. However, immunoblot analysis revealed that the fully translated protein was not detectable (Fig. 3.b). Rather, the major product

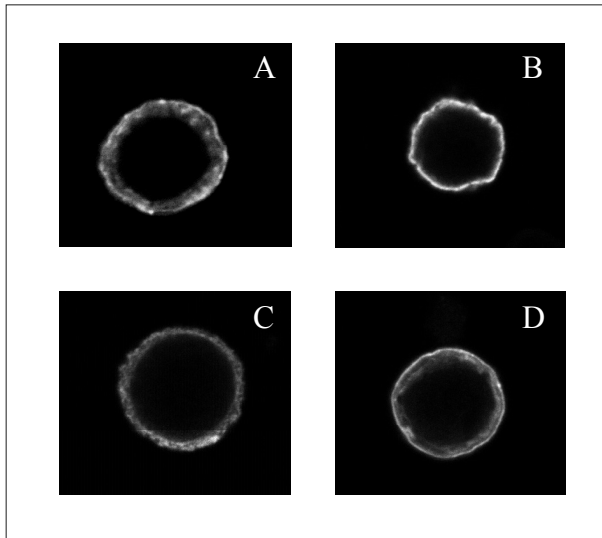


Fig. 5: Typical patterns observed for intracellular localization of wt and mutant rhodopsins in Sf9 cells analyzed by confocal immunofluorescence microscopy. Cells (10^5) were seeded on coverslips and infected with recombinant baculovirus. As primary antibody the polyclonal CERN858 was used in 1:1000 dilution. (A) C222R, (B) C167R, (C) C264del and (D) wt opsin. The immunopositive shell evident in (A) and (D) represents staining of the plasma membrane. Similar staining is never observed in condition (B) and (C). The dense perinuclear staining in (B) is typical for ER localization. Intracellular staining in (C) is always more diffuse than in (B).

was a truncated product with an apparent molecular weight of about 27 kDa (Fig. 3.a) that still contained the i_3 -loop (Fig. 3.c), but considering its molecular weight should lack the C-terminus, TM VII and probably most of TM VI, and indeed did not react with the C-terminal antibody (Fig. 3.b). This fragment was largely present as the unglycosylated species (Fig. 3.a). Also, the intracellular distribution was more diffuse than that of C167R (Fig. 5.c) and suggests its presence in a variety of intracellular structures. Truncation does not seem to be the result of direct proteolytic cleavage of a misfolded mature protein, since no trace of intact protein was observed in the presence of protease inhibitors either even very early after infection of the cells with baculovirus (1-2 days, not shown). In fact, proteolytically highly susceptible sites reside *within* the i_3 -loop [39].

In our view, the most straightforward interpretation of this phenomenon is mutation-induced translational stalling with subsequent abortive release of the ribosome. In this view the deletion, which would twist the face of the extracellular half of TM VI, interferes with the function of a transfer signal and blocks further translocation by the TRAM complex. The cell has several mechanisms to rescue stalled ribosomes by aborting the unfinished bound protein chain [40]. The resulting translational abortion could also explain the low extent of glycosylation.

Hence, we propose to classify this mutation with the biochemical phenotype class III: no photopigment formation, intracellular retention, and no apparent formation of intact protein. The RP-genic character may again result from an overload of synthetic and degradative pathways in the photoreceptor cell. This phenotype further demonstrated that truncated proteins can also be generated in the absence of premature stop codons.

6.3.4 Conclusions

We have studied the biochemical properties of mutants of three transmembrane-located cysteine residues (C167R, C222R, and C264del) that are involved in ADRP. The corresponding C→S mutants produced fully functional, wild-type-like protein. This demonstrates that mutation of these residues per se does not lead to an ADRP phenotype. The ADRP mutations C167R, C222R, and C264del represent three biochemically different phenotypes. Our results clearly indicate that C222R is a class I mutant. C222R resembles wild type in every aspect testable, but nevertheless is RP-genic. We confirmed the classification of C167R as a class IIa mutant. C167R is known to cause type 1 ADRP [37]. C264del resembles the C167R mutation with respect to lack of regeneration with 11-cis retinal and of targeting to the plasma membrane. However, unlike class IIa a truncated product was formed and the mutant represents therefore a new biochemical phenotype that we propose to call class III. Different mutations in rhodopsin lead to different clinical parameters that correspond to a variation in severity of ADRP [41]. Mutations that share the same biochemical classification do not necessarily give rise to the same ADRP phenotype. Among class I mutations, for example, some mutations cause type 1 ADRP where other mutations give rise to type 2 ADRP. About two-third of the class IIa mutants of which both the biochemical and the clinical phenotype have been established are known to cause type 1 ADRP [17]. Type IIb mutations on the other hand cause type 2 ADRP or are described as relatively mild [9,17]. It is therefore hard to predict the severity of the disease outcome solely from biochemical data. Insight into the relationship between biochemical features and disease

outcome would be very welcome, but does need a large body of additional biochemical and clinical data.

References

- Hargrave, P. A. and McDowell, J. H. (1992). Rhodopsin and phototransduction - A model system for G-protein-linked receptors. *FASEB J.*, 6, 2323 - 2331.
- Okada, T., Ernst, O. P., Palczewski, K., and Hofmann, K. P. (2001). Activation of rhodopsin: New insights from structural and biochemical studies. *Trends Biochem. Sci.*, 26, 318 - 324.
- Palczewski, K., Kumasaka, T., Hori, T., Behnke, C. A., Motoshima, H., Fox, B. A., LeTrong, I., Teller, D. C., Okada, T., Stenkamp, R. E., Yamamoto, M., and Miyano, M. (2000). Crystal structure of rhodopsin: A G protein-coupled receptor. *Science*, 289, 739 - 745.
- Lem, J., Krasnoperova, N. V., Calvert, P. D., Kosaras, B., Cameron, D. A., Nicolò, M., Makino, C. L., and Sidman, R. L. (1999). Morphological, physiological, and biochemical changes in rhodopsin knockout mice. *Proc. Nat. Acad. Sci. USA*, 96, 736 - 741.
- Heckenlively, J. R. (1988). *Retinitis pigmentosa* (Lippencott, Philadelphia, USA).
- VanSoest, S., Westerveld, A., DeJong, P. T., Bleeker-Wagemakers, E. M., and Bergen, A. A. B. (1999). Retinitis pigmentosa: defined from a molecular point of view. *Surv. Ophthalmol.*, 43, 321 - 334.
- Al-Magtheth, M., Gregory, C. Y., Inglehearn, C. F., Hardcastle, A. J., and Bhattacharya, S. S. (1993). Rhodopsin mutations in autosomal dominant retinitis pigmentosa. *Hum. Mutat.*, 2, 249 - 255.
- Gal, A., Apfelstedt-Sylla, E., Janecke, A. R., and Zrenner, E. (1997). Rhodopsin mutations in inherited retinal dystrophies and dysfunctions. *Prog. Retin. Eye Res.*, 16, 51 - 79.
- Daiger, S. P., Sullivan, L. S., and Rodriguez, J. A. (1995). Correlation of phenotype with genotype in inherited retinal degeneration. *Behav. Brain Sci.*, 18, 452 - 467.
- Bunge, S., Wedemann, H., David, D., Terwilliger, D. J., VanDenBorn, L. I., Aulehla-Scholz, C., Samanns, C., Horn, M., Ott, J., Schwinger, E., Schinzel, A., Denton, M. J., and Gal, A. (1993). Molecular analysis and genetic mapping of the rhodopsin gene in families with autosomal dominant retinitis pigmentosa. *Genomics*, 17, 230 - 233.
- Inglehearn, C. F., Lester, D. H., Bashir, R., Atif, U., Keen, T. J., Sertedaki, A., Lindsey, J., Jay, M. R., Bird, A. C., Farrar, G. J., Humphries, P., and Bhattacharya, S. S. (1992). Recombination between rhodopsin and locus D3S47 (C17) in rhodopsin retinitis pigmentosa families. *Amer. J. Hum. Genet.*, 50, 590 - 597.
- Dryja, T. P., Hahn, L. B., Cowley, G. S., McGee, T. L., and Berson, E. L. (1991). Mutation spectrum of the rhodopsin gene among patients with autosomal dominant retinitis pigmentosa. *Proc. Nat. Acad. Sci. USA*, 88, 9370 - 9374.
- Sung, C.-H., Schneider, B. G., Agarwal, N., Papermaster, D. S., and Nathans, J. (1991). Functional heterogeneity of mutant rhodopsins responsible for autosomal dominant retinitis-pigmentosa. *Proc. Nat. Acad. Sci. USA*, 88, 8840 - 8844.
- Macke, J. P., Davenport, C. M., Jacobson, S. G., Hennessey, J. C., Gonzalez-Fernandez, F., Conway, B. P., Heckenlively, J. R., Palmer, R. M. J., Maumenee, I. H., Sieving, P. A., Gouras, P., Good, W., and Nathans, J. (1993). Identification of novel rhodopsin mutations responsible for retinitis pigmentosa: Implications for the structure and function of rhodopsin. *Amer. J. Hum. Genet.*, 53, 80 - 89.
- Vaithinathan, R., Berson, E. L., and Dryja, T. P. (1994). Further screening of the rhodopsin gene in patients with autosomal dominant retinitis pigmentosa. *Genomics*, 21, 461 - 463.
- Sung, C.-H., Davenport, C. M., and Nathans, J. (1993). Rhodopsin mutations responsible for autosomal dominant retinitis pigmentosa - Clustering of functional classes along the polypeptide chain. *J. Biol. Chem.*, 268, 26645 - 26649.
- Kaushal, S. and Khorana, H. G. (1994). Structure and function in rhodopsin. 7. Point mutations associated with autosomal dominant retinitis pigmentosa. *Biochemistry-USA*, 33, 6121 - 6128.
- Kunkel, T. A. (1985). Rapid and efficient site-specific mutagenesis without phenotypic selection. *Proc. Nat. Acad. Sci. USA*, 82, 488 - 492.
- Summers, M. D. and Smith, G. E. (1987). *A manual of methods for baculovirus vectors and insect culture procedures*. Texas Exp. Station Bulletin, no.1555.
- DeCaluwé, G. L. J., VanOostrum, J., Janssen, J. J. M., and DeGrip, W. J. (1993). In vitro synthesis of bovine rhodopsin using recombinant baculovirus. *Meth. Neurosci.*, 15, 307 - 321.
- Klaassen, C. H. W., Bovee-Geurts, P. H. M., DeCaluwé, G. L. J., and DeGrip, W. J. (1999). Large-scale production and purification of functional recombinant bovine rhodopsin using the baculovirus expression system. *Biochem. J.*, 342, 293 - 300.

22. Klaassen, C. H. W. and DeGrip, W. J. (2000). Baculovirus expression system for expression and characterization of functional recombinant visual pigments. *Meth. Enzymology*, 315, 12 - 29.
23. Janssen, J. W. H., Bovee-Geurts, P. H. M., Peeters, A. P. A., Bowmaker, J. K., Cooper, H. M., David-Gray, Z. K., Nevo, E., and DeGrip, W. J. (2000). A fully functional rod visual pigment in a blind mammal - A case for adaptive functional reorganization ? *J. Biol. Chem.*, 275, 38674 - 38679.
24. Vissers, P. M. A. M. and DeGrip, W. J. (1996). Functional expression of human cone pigments using recombinant baculovirus: Compatibility with histidine tagging and evidence for N-glycosylation. *FEBS Lett.*, 396, 26 - 30.
25. DeGrip, W. J. (1985). Immunochemistry of rhodopsin. *Prog. Retin. Res.*, 4, 137 - 180.
26. Adamus, G., Zam, Z. S., Arendt, A., Palczewski, K., McDowell, J. H., and Hargrave, P. A. (1991). Anti-rhodopsin monoclonal antibodies of defined specificity: Characterization and application. *Vision Res.*, 31, 17 - 31.
27. Adamus, G., Arendt, A., Zam, Z. S., McDowell, J. H., and Hargrave, P. A. (1988). Use of peptides to select for anti-rhodopsin antibodies with desired amino acid sequence specificities. *Pept. Res.*, 1, 42 - 47.
28. Pierce, E. A. (2001). Pathways to photoreceptor cell death in inherited retinal degenerations. *BioEssays*, 23, 605 - 618.
29. Rath, P., Bovee-Geurts, P. H. M., DeGrip, W. J., and Rothschild, K. J. (1994). Photoactivation of rhodopsin involves alterations in cysteine side chains: Detection of an S-H band in the meta I -> meta II FTIR difference spectrum. *Biophys. J.*, 66, 2085 - 2091.
30. Breikers, G., Bovee-Geurts, P. H. M., DeCaluwé, G. L. J., and DeGrip, W. J. (2001). A structural role for Asp83 in the photoactivation of rhodopsin. *Biol. Chem.*, 382, 1263 - 1270.
31. Janssen, J. J. M., VanDeVen, W. J. M., VanGroningen-Luyben, W. A. H. M., Roosien, J., Vlak, J. M., and DeGrip, W. J. (1988). Synthesis of functional bovine opsin in insect cells under control of the baculovirus polyhedrin promoter. *Mol. Biol. Rep.*, 13, 65 - 71.
32. Karnik, S. S., Sakmar, T. P., Chen, H.-B., and Khorana, H. G. (1988). Cysteine residues 110 and 187 are essential for the formation of correct structure in bovine rhodopsin. *Proc. Nat. Acad. Sci. USA*, 85, 8459 - 8463.
33. Janssen, J. J. M., Mulder, W. R., DeCaluwé, G. L. J., Vlak, J. M., and DeGrip, W. J. (1991). In vitro expression of bovine opsin using recombinant baculovirus: The role of glutamic acid (134) in opsin biosynthesis and glycosylation. *Biochim. Biophys. Acta*, 1089, 68 - 76.
34. Teller, D. C., Okada, T., Behnke, C. A., Palczewski, K., and Stenkamp, R. E. (2001). Advances in determination of a high-resolution three-dimensional structure of rhodopsin, a model of G-protein-coupled receptors (GPCRs). *Biochemistry-USA*, 40, 7761 - 7772.
35. Deretic, D., Schmerl, S., Hargrave, P. A., Arendt, A., and McDowell, J. H. (1998). Regulation of sorting and post-Golgi trafficking of rhodopsin by its C-terminal sequence QVS(A)PA. *Proc. Nat. Acad. Sci. USA*, 95, 10620 - 10625.
36. Acharya, S. and Karnik, S. S. (1996). Modulation of GDP release from transducin by the conserved Glu134-Arg135 sequence in rhodopsin. *J. Biol. Chem.*, 271, 25406 - 25411.
37. Simonelli, F., Rinaldi, M., Nesti, A., Testa, F., Rinaldi, E., Ciccodicola, A., Flagiello, L., Miano, M. G., Ventruto, V., and D'Urso, M. (1998). Ocular signs associated with a rhodopsin mutation (Cys-167->Arg) in a family with autosomal dominant retinitis pigmentosa. *Brit. J. Ophthalmol.*, 82, 709 - 709.
38. Kwar, Z. and Jarvis, D. L. (2001). Biosynthesis and subcellular localization of a lepidopteran insect alpha 1,2-mannosidase. *Insect Biochem. Molec. Biol.*, 31, 289 - 297.
39. Ovchinnikov, Y. A. (1987). Probing the folding of membrane proteins. *Trends Biochem. Sci.*, 12, 434 - 438.
40. Ibba, M. and Söll, D. (2002). Quality control mechanisms during translation. *Science*, 286, 1893 - 1897.
41. Fitzke, F. W., Owens, S., Moore, A. T., Jay, M., Inglehearn, C. F., Bhattacharya, S., and Bird, A. C. (1991). Comparison of functional characteristics of autosomal dominant retinitis pigmentosa with different amino acid changes in the rhodopsin molecule. *Invest. Ophthalmol. Visual Sci. Suppl.*, 32, 1200 -



Chapter 7

Summary and general discussion

Signal transduction mediated by visual pigments has been extensively studied during the last 45 years and in this period the visual pigments have evolved into a model system for the G protein-coupled receptor family. This family contains receptors involved in all major signaling processes in the human body and represents a major target for pharmacological intervention. Detailed knowledge has meanwhile been obtained on the cell biology of the signaling pathways but much less is known about the structural details of signal generation by the receptors. The recent description of a crystal structure of bovine rhodopsin strengthens its position as the model protein for the GPCR family and provides the first atomic insight into the structure and activation mechanism of rhodopsin and GPCRs in general.

As described in **Chapter 1**, rhodopsin is a membrane-spanning protein containing seven transmembrane segments, which undergoes posttranslational modification (disulfide bridge formation, thiopalmitoylation, glycosylation) and is subsequently targeted to the rod outer segment membrane to take up its cellular function. Rhodopsin is a unique member of the family of G protein-coupled receptors because its ligand, 11-*cis* retinal, is covalently bound to the protein, opsin. The visual process begins with the absorption of light inducing *cis/trans* isomerization of the ligand after which photo-excited rhodopsin relaxes via a series of transient photointermediates (Rhodopsin → Bathorhodopsin (Batho) ↔ Blue-shifted-intermediate (BSI) → Lumirhodopsin (Lumi) → Metarhodopsin I (Meta I) ↔ Metarhodopsin II (Meta II) → Metarhodopsin III (Meta III)), that within milliseconds leads to the generation of the active state (Meta II), which binds and activates the G protein transducin (G_T).

The 3D-crystal structure of ground-state rhodopsin (2.6 Å resolution) gives detailed information on the three-dimensional structure of rhodopsin. Rhodopsin can be divided into three topologically distinct domains: 1) the transmembrane domain consisting of helix I – VII that accommodates 11-*cis*-retinal, 2) the extracellular region and 3) the cytoplasmic region where interaction with transducin occurs. Results from earlier experiments indicate that the second transmembrane domain (TM II) of rhodopsin undergoes structural changes during photoactivation [1-5]. Helix II runs from residue 71 to 100 and is kinked around Gly89 and Gly90 placing Gly90 close to Glu113, the residue that interacts with the protonated Schiff base. Helix II displays hydrophobic interactions with other helices to stabilize the dark state of rhodopsin. In spite of our detailed knowledge about the three-dimensional structure of rhodopsin, the role of individual protein residues in the photoactivation cannot be deduced from this structural model since the crystal structure was obtained in the dark configuration and is difficult to extrapolate to rhodopsin in the activated state. We chose to study the structural and functional role of individual residues in the photoactivation of rhodopsin using cysteine scanning mutagenesis in combination with Fourier Transform-Infrared (FT-IR) difference spectroscopy. Cysteine scanning mutagenesis is a technique which uses cysteines as a reporter group to study the structural and functional properties of a protein. Single amino acids are replaced by a unique cysteine residue and analysed by FT-IR difference spectroscopy. This is a very sensitive technique that can measure small structural changes and can directly probe the cysteine sulfhydryl group without requiring additional modification. The –SH group of cysteine is very sensitive to changes in local structure and polarity and vibrational changes can be detected in an isolated region of the FT-IR difference spectrum where there is no interference from other biomembrane components.

Evidence has been presented that Asp83 located in the second transmembrane domain of rhodopsin is active during formation of Meta II and undergoes a change in H-

bonding. Our first target was therefore to study the structural and functional role of residues located in the second transmembrane domain in the photoactivation of rhodopsin using cysteine scanning mutagenesis in combination with FT-IR difference spectroscopy. In **Chapter 2** the contribution of Asp83 to the structure and function of rhodopsin was investigated in more detail, using mutants D83N and D83C. The mutation D83C was selected to test the potential of the combination of cysteine-scanning with FT-IR difference spectroscopy. FT-IR difference spectra show that these Asp83 mutations do not cause long-range structural perturbations. The absorbance bands of D83C and D83N display a small blue-shift relative to wild-type rhodopsin that is smaller in D83C than in D83N, showing that substitution of Asp83 by Cys causes little structural and electronic perturbation of the chromophore. Comparison of the photochemical properties of these species indicates that Asp83 participates in a H-bonded network that contributes to spectral tuning and setting of the pKa of the Meta I \leftrightarrow Meta II equilibrium. Our conclusion is that the proton-donating capacity of the aspartic carboxyl group forms an important supplement to its H-bonding capacity. Since FT-IR difference spectroscopy studies show that the carboxyl group of Asp83 reports local changes upon Meta II formation, we would expect that these changes would also be reflected in the D83C sulfhydryl vibration. Mutant D83C indeed shows a significant increase in the sulfhydryl peak, showing that the -SH peak can be exploited as a very sensitive reporter group for the analysis of local structural changes using FT-IR difference spectroscopy.

This cysteine peak was observed on a background of native cysteines, however. To prevent a large background in the introduced signal by native cysteines and possible reciprocal interactions of introduced cysteines with native cysteine residues, we aimed in **Chapter 3** at creating a base-mutant in which all potentially active cysteine residues are substituted. We started with SOH Δ C in which all potentially reactive cysteines were replaced by a serine except for cysteines 110 and 187 that form the disulfide bridge. Unfortunately, SOH Δ C produced significantly less functional protein than wild type rhodopsin. We attempted to increase the amount of functional base-mutant by alternative cysteine substitutions. Since previous single mutation of Cys167 and Cys264 into a serine on a wild-type background resulted in lower functional yields and a decrease in stability, we tested whether substitution of cysteine 167 and 264 by alanine or methionine would improve base-mutant expression. However, the production levels of functional recombinant protein were even lower than that of SOH Δ C. Since the highest functional expression levels of cysteine-free rhodopsins were still obtained for SOH Δ C and this species could be purified with reasonable recoveries, showed no significant free sulfhydryl activity and retained wild type-level functional activity, we decided to use SOH Δ C as a base-mutant for our cysteine scanning mutagenesis studies. Now that we had developed a cysteine-free base-mutant (Chapter 3) and a probe to study local structural changes (Chapter 2) we aimed in **Chapter 4** to study the role of the residues of the second transmembrane domain of rhodopsin in the photoactivation using cysteine scanning mutagenesis in combination with FT-IR difference spectroscopy. Unfortunately, the majority of the single rhodopsin mutants based upon SOH Δ C produced little or no functional protein, showed poor glycosylation and was retained intracellularly, suggesting folding and/or transport defects. Single substitution of Cys167 and Cys264, both structurally active during the photoactivation, on a wild type background is known to reduce the amount of correctly folded protein and this was aggravated by most mutations. On the other hand some mutations partially rescued the

corresponding mutant from incorrect folding. This is a very intriguing phenomenon. Residues that play an important role in protein structure and/or function are in general well conserved. The native residues of the rescuing mutations L77C, F85C, F88C and G89C, show a maximum conservation of 30% in the family of G protein-coupled receptors, indicating that these residues probably are not very important for structure and function of rhodopsin and substitution of these residues might therefore show no adverse effects. Enhanced structural ability of the functional species might improve the chance that upon translation a protein proceeds to the correctly folded state. We consider it unlikely that the single substitutions mentioned above would make such a major difference, and other factors, like chaperone-mediated processes, are likely to play a role as well. Until now, only base-mutant SOH Δ C and mutant SOH Δ C/L77C have been analysed for several structural and functional properties by UV/VIS spectroscopy, FT-IR difference spectroscopy and the G_T activation assay. We conclude that residue Leu77 is not involved in structural or enzymatical changes underlying rhodopsin activation. Indeed, residue L77 is located in the lipid face of TM II and hence probably inserted in the lipid matrix, which makes it plausible that this residue does not participate in the photoactivation of rhodopsin. We could not yet determine the thermal stabilities of these mutants, but the higher recovery of SOH Δ C/L77C after purification by IMAC indicates that mutant L77C is more stable than the base-mutant.

Since the SOH Δ C-mutants produced very low amounts of functional protein we searched for an alternative approach. In Chapter 2 of this thesis we showed that a change in the vibrational properties of a single cysteine sulfhydryl group can be measured on the background of native cysteines. We decided to risk possible interference of this large background in the introduced signal by native cysteines and proceeded to study the residues of the second transmembrane domain of rhodopsin by cysteine scanning mutagenesis on a wild type background.

The first results of this approach are described in **Chapter 5**. Most wild type-based single cysteine mutants produced total levels of recombinant protein equal to wild type rhodopsin, and most mutants also produced amounts of glycosylated protein similar to wild type. All mutants produced amounts of functional protein that were sufficient for purification by IMAC and for further analysis. However, due to technical problems most mutants could not yet be produced in sufficient quantities to allow a comprehensive analysis. Until now, mutants L76C, L79C, V81C, D83C, F85C, F88C, G89C and G90C have been partially analyzed. Asp83 was already extensively discussed in Chapter 2, where it was shown that this residue does not play an essential role in the signal transduction of rhodopsin, but that it contributes to the structure and the photochemistry by interaction with H-bonded networks. Residues Leu76, Val81 and Phe85 so far do not seem to be essential for signaling, whereas mutants F88C, G90C and probably G89C show a reduced G protein activation rate. Nevertheless, the latter three mutants display a wild type-like photocascade, although the kinetics could not be firmly established yet. In addition, the results so far indicate that the pKa of the Meta I – II transition is close to that of wild type. Global properties of rhodopsin therefore do not seem to be affected. On the other hand, the reduced –SH peak area in the Meta II FT-IR difference spectrum of F88C and G89C suggests either an indirect negative effect of these mutations on the wild type –SH activity or a direct participation of the extra cysteine that is reflected in a negative peak in the difference spectrum and is thus observed as a decrease in the wild type –SH peak area. In our view, this justifies the conclusion that residues Phe88, Gly89 and Gly90 directly participate in Meta II formation and receptor activation, which could explain the lower activity upon

substitution of these residues. Upon photoactivation vectorial conformational changes occur, resulting in helix II moving away from C-IV and towards helix IV. Probably this is facilitated by backbone rotations at the Gly89/Gly90 pair [6], and it is expected that substitution of either of these residues by the cysteine side chain will affect the kinetics of the rotational outward movement. Unfortunately, different from the D83C mutant which shows a considerable increase in -SH peak area, the -SH peak region of the FT-IR difference spectrum of these mutants is difficult to interpret. This is partly due to a relatively high noise level which needs to be reduced by averaging a set of independent experiments. Even then, the presence of a background of active native cysteine residues will seriously complicate the interpretation of the -SH vibration data. We conclude that effective cysteine scanning mutagenesis is better performed on a background free of endogenous cysteine activity. Hereto production of functional cysteine-free rhodopsin will have to be improved.

Correct protein folding is necessary for proper functioning of rhodopsin. In the course of our studies on the contribution of membrane-located residues to structure and function of rhodopsin, our attention was drawn by clinical genetic studies linking a single mutation in a cysteine residue of rhodopsin to autosomal dominant retinitis pigmentosa (ADRP). In **Chapter 6** we analyzed the biochemical phenotype of mutants of three transmembrane-located cysteine residues (C167R, C222R and C264del) that are involved in ADRP. ADRP can be divided into two clinical subtypes: type 1 and 2. Type 1 represents a more severe phenotype and is characterized by earlier onset, diffuse localization, and/or rapid progression. Type 2 is characterized by more regional occurrence and/or slow progression. Biochemically, the mutations have been classified into three classes based upon heterologous expression: class I mutants resemble wild type rhodopsin in folding, targeting to the cell membrane and formation of photosensitive pigment, class IIa mutants do not fold correctly, are retained in the endoplasmic reticulum and do not form a photosensitive pigment and class IIb mutants show less severe folding defects as IIa and produce varying extents of folded protein capable of forming a functional photopigment. The corresponding C → S mutations of residue Cys167, Cys222 and Cys264 produce fully functional, wild type-like protein demonstrating that mutation of these residues per se does not lead to an ADRP phenotype. Our results indicate that the ADRP mutations C167R, C222R and C264del represent three different biochemical phenotypes. C222R is classified as class I: it resembles wild type rhodopsin in every aspect tested. Its RP-genic nature clearly is not expressed in a heterologous system. C167R is classified as class IIa in agreement with results described before in another expression system. Mutant C264del represents a new biochemical class that we propose to call class III and is described by class II-like characteristics (lack of formation of functional pigment and no targeting to the plasma membrane) but a truncated protein was formed. In general, the various mutations in rhodopsin lead to a variety of clinical parameters with variable severity of ADRP. Mutations that share the same biochemical classification do not necessarily give rise to the same ADRP phenotype. It is therefore hard to predict disease outcome solely from biochemical data on recombinant proteins. These results point at a similar phenomenon observed in our cysteine-scanning studies: subtle mutations in rhodopsin can have profound effects on the expression level of functional recombinant protein. Our present data are still very scattered and our insight in the mechanisms of membrane protein folding is still too limited to allow even a preliminary interpretation.

The work presented in this thesis shows that cysteine scanning mutagenesis in combination with FT-IR difference spectroscopy could be a promising, non-invasive technique to study individual, transmembrane-located residues. However, in the case of rhodopsin, the total amounts of recombinant protein produced did not differ much from wild type, but the cysteine-free base-mutant produced strongly reduced quantities of functional protein. Additional substitution of a single residue by a cysteine further reduced the production of functional protein in the majority of the mutants to such a level, that no adequate purification by IMAC, a prerequisite for further analysis, was achieved. The question remains why the SOH Δ C-based mutants showed such a strong reduction in functional protein production. Trouble-makers probably are residues Cys167 and Cys264 that are structurally active during photoactivation (DeGrip et al., unpublished results). Single mutants C167S and C264S on a wild type background already produced lower levels of functional protein and reduced stability during purification (M.J.M. Portier-VandeLuytgaarden, unpublished results). These effects seem to be aggravated in the cysteine-free base mutant (SOH Δ C). N-linked glycosylation is thought to accompany and improve protein folding and prevent aggregation of intermediate folding products [7]. SOH Δ C showed higher amounts of non-glycosylated protein than wild type rhodopsin. This indicates the presence of large quantities of incorrectly folded protein and agrees with the lower level of functional protein compared to wild type. Since conformational stability is considered to be a positive factor in the protein folding process [8], reduced stability might impair correct protein folding of the base-mutant under overexpression conditions. However, additional substitution of a residue of the second transmembrane domain of rhodopsin by a cysteine even further reduced the quantity of functional recombinant rhodopsin produced in the majority of the SOH Δ C-based mutants. This would suggest that a large number of residues in helix II fulfil an important structural or functional role. Indeed, helix I and II form a tight complex by ion pairs and multiple hydrophobic contacts and this combination is believed to play a structural and functional role in rhodopsin and as well as in other GPCRs [9,10]. In addition, residue Tyr74 and Asn78 link these helices with helices III, IV, VII and VIII by a more extended hydrogen bonded network [1]. Substitution of the residues of TM II by a cysteine might perturb interhelical contacts and/or hydrogen bonded networks and as a consequence decrease the stability of the apoprotein. Upon overexpression, the mutant rhodopsins thus might give lower amounts of correctly folded, functional protein at the time of harvesting because the folding rate of the mutants is much lower than that of wild type resulting in overload of the ER folding machinery and accumulation of incompletely or aberrantly folded protein. The observation that this is partially rescued by certain cys-substitutions is very intriguing. The residues exhibiting rescuing potential (L77, F85, F88 and G89) are not restricted to either the lipid or the protein face of helix II (Table 1). Hence, it is likely that apart from a possible positive influence on protein stability also other factors such as effects on pathway selection or kinetics in protein folding or on interaction with folding intermediates play a role.

Because the D83C mutation on a wild type background showed that a change in cysteine sulfhydryl peak vibration can be observed on the background of native cysteines, we tried to study the residues of the second transmembrane domain by cysteine scanning mutagenesis on a background of wild type cysteines. On this background the mutants still produced sufficient amounts of functional protein to allow purification and further analysis. This demonstrates that the cysteine mutations do not interfere with chromophore binding. However, the noise level in the 2600-2500 cm^{-1}

region of the FT-IR difference spectra we were able to record was quite substantial. The change in vibrational activity of the additional cysteine could therefore not be determined reliably, unless the change in peak height is considerable as was observed for the D83C mutant. The noise level can be improved by averaging a reasonable number of independent spectra, but even then the activity of the substituted cysteine residue would be difficult to interpret on a background of native cysteines. It therefore seems essential to perform cysteine scanning mutagenesis on a cysteine-free background. This requires development of a cysteine-free base-mutant that upon single cysteine substitutions still produces sufficient amounts of functional protein for purification and further analysis. One option would be to analyse additional mutations at “rescuing positions”. Preliminary tests with the L77A mutant however gave no indications for a “rescuing effect”. Another option would be to investigate the double mutant reported by Xie et al. [11] in which residue Asn2 and Asp282 were substituted by a cysteine to form a second disulfide bond. The thermal stability of this mutant improved substantially without significant effects on its signaling activity. As was discussed earlier this chapter, the thermal stability of the mutant protein is considered an important factor in protein folding. An additional disulfide bridge might improve the stability of the cysteine-free base-mutant and increase production of functional protein. Because the introduced cysteines form a disulfide bridge, they are expected not to interfere with the introduced cysteines in cysteine scanning mutagenesis. A third option would be to create a base-mutant in which only the cysteines that are active during the photoactivation are substituted. Although single substitution of the active cysteines 167 and 264 reduced the stability of the protein on a wild type background, sufficient amounts of functional protein could still be obtained for purification and further analysis. However, this case has the major drawback that interactions between native and introduced cysteine residues cannot be excluded.

The combined first results from our cysteine scanning mutagenesis studies are summarized in Table 1. We think that helix II can be roughly divided into an intracellular (residue 71 – 83) and an extracellular half (residue 84-100) based on the structural and functional properties of their residues. Our analysis of some of the intracellular located residues (L76, L77, L79, V81 and D83) gave no indications that these residues display any significant structural and/or functional role in the photoactivation of rhodopsin, except for Asp83 that plays a more general structural role [5]. However, previous studies have shown that Tyr74 and Asn78 hydrogen bond with residues located in TM I, III, and IV [1,12]. Because they participate in an extended H-bonded network, mutation of these residues could induce long range effects [4]. In addition, residues Ile75, Leu76, Asn78 and leu79 are considered to be generically important in the GPCR family because of their high conservation, and are thought to be involved in stabilizing transmembrane interactions and folding [13]. In addition, certain substitutions of residues Ile75, Leu76, Asn78 and Leu79 give a constitutively active protein [13]. Together, these results support the view that residues of the intracellular half of helix II in general play a role in establishing a correct protein structure. Our analyses of the residues of the extracellular half of helix II indicate that Phe88, Gly89 and Gly90 participate in Meta II formation and receptor activation. Helix II is kinked around Gly89-Gly90 and brings the extracellular part of this helix, in particular Gly90, closer to helix III in which Glu113, the counterion for the protonated Schiff base, is located [1]. Mutations of Gly89 are observed in retinitis pigmentosa patients [14,15] while the Gly90 mutation is associated with congenital night blindness [16], confirming

	% conservation		Localization: L(lipid face) P(protein face)	$\Delta \lambda_{\max}$ (nm)	G_T activation rate	pKa MI/II transition	structural effects		-SH peak area
	R	C					local	long range	
L76C	37	85	P	↓ 3	=	=	↑	=	=
L77C	31	48	L	=	↑	↓	=	=	=
L79C	91	98	P	=	-	-	-	-	-
V81C	30	40	L	=	=	-	-	-	-
D83C	94	95	P	↓ 3	=	=	=	=	↑
F85C	7	77	L	=	=	=	↑	=	=
F88C	7	58	L	=	↓	=	↑	=	↓
G89C	5	18	P	=	↓	=	↑	=	↓
G90C	3	22	P	↓ 9	↓	=	-	-	-

Table 1: This table summarizes the biochemical and structural data described in this thesis for the mutants Y74C to G90C. The results described in this overview were obtained from single cysteine substitutions on a background of native cysteines except for L77C which was studied on a cysteine-free background. =; not significantly different from wild type, ↑ or ↓; increased or decreased compared to wild type. % conservation: the percentage conservation within the GPCR family; R (Residue); percentage absolute conservation of a residue within the GPCR family, C (Class); % percentage conservation within the same residue subclass within the GPCR family. Classification of subclasses of residues: apolar, large: Y/L/I/F/M, apolar, small: A/G/V/P, polar, non-charged: S/T/N/P/Q/H, polar, charged: D/E/K/R. Localization; localization of the amino acid residue in either the lipid face (L) or protein face (P) of helix II, based upon the crystal structure [1,4,17]. G_T ; G protein activation rate compared to wild type, Δ structure; structural changes observed by FT-IR difference spectroscopy, -; not yet determined.

the importance of these residues for rhodopsin. Bioinformatical studies propose that residues Phe85, Met86, Val87 and Phe91 are generally important in the GPCR receptor family. Mutation of these residues affects ligand binding, showing that these residues are of functional importance to rhodopsin [13]. However, in our experiments we found no effect of Phe85 mutation on the G protein activation capacity. So far, we can not explain this discrepancy. Phe91 forms part of a H-bonded network that lies at the extracellular side of the chromophore-binding site, and mutation of this residue might cause long range effects on the spectral properties of rhodopsin [4]. Together, these results suggest that the extracellular region of helix II plays a significant role both in structure and in function of rhodopsin.

Until now, too little information is available to give a complete detailed description of helix II, both structurally and functionally. However, considering the nature of the information obtained from our preliminary results, we think that in principle cysteine scanning mutagenesis of rhodopsin in combination with FT-IR difference spectroscopy and functional studies should be able to provide detailed diagnostic information on involvement of particular residues in structure and/or receptor activation.

References

1. Palczewski, K., Kumasaka, T., Hori, T., Behnke, C. A., Motoshima, H., Fox, B. A., LeTrong, I., Teller, D. C., Okada, T., Stenkamp, R. E., Yamamoto, M., and Miyano, M. (2000). Crystal structure of rhodopsin: A G protein-coupled receptor. *Science*, 289, 739 - 745.
2. Fahmy, K., Jäger, F., Beck, M., Zvyaga, T. A., Sakmar, T. P., and Siebert, F. (1993). Protonation states of membrane-embedded carboxylic acid groups in rhodopsin and metarhodopsin II: A Fourier-transform infrared spectroscopy study of site-directed mutants. *Proc. Nat. Acad. Sci. USA*, 90, 10206 - 10210.

3. Rath, P., DeCaluwé, G. L. J., Bovee-Geurts, P. H. M., DeGrip, W. J., and Rothschild, K. J. (1993). Fourier transform infrared difference spectroscopy of rhodopsin mutants: Light activation of rhodopsin causes hydrogen-bonding changes in residue aspartic acid-83 during meta II formation. *Biochemistry-USA*, 32, 10277 - 10282.
4. Okada, T., Fujiyoshi, Y., Silow, M., Navarro, J., Landau, E. M., and Shichida, Y. (2002). Functional role of internal water molecules in rhodopsin revealed by x-ray crystallography. *Proc. Nat. Acad. Sci. USA*, 99, 5982 - 5987.
5. Breikers, G., Bovee-Geurts, P. H. M., DeCaluwé, G. L. J., and DeGrip, W. J. (2001). A structural role for Asp83 in the photoactivation of rhodopsin. *Biol. Chem.*, 382, 1263 - 1270.
6. Altenbach, C. A., Klein-Seetharaman, J., Cai, K. W., Khorana, H. G., and Hubbell, W. L. (2001). Structure and function in rhodopsin: Mapping light-dependent changes in distance between residue 316 in helix 8 and residues in the sequence 60-75, covering the cytoplasmic end of helices TM1 and TM2 and their connection loop CL1. *Biochemistry-USA*, 40, 15493 - 15500.
7. Helenius, A. (1994). How N-linked oligosaccharides affect glycoprotein folding in the endoplasmic reticulum. *Mol. Biol. Cell*, 5, 253 - 265.
8. Conn, P. M., Leaños, M. A., and Janovick, J. A. (2002). Protein origami: Therapeutic rescue of misfolding gene products. *Mol. Interv.*, 2, 308 - 316.
9. Abdulaev, N. G. (2003). Building a stage for interhelical play in rhodopsin. *Trends Biochem. Sci.*, 28, 399 - 402.
10. Okada, T. and Palczewski, K. (2001). Crystal structure of rhodopsin: Implications for vision and beyond. *Curr. Opin. Struct. Biol.*, 11, 420 - 426.
11. Xie, G. F., Gross, A. K., and Oprian, D. D. (2003). An opsin mutant with increased thermal stability. *Biochemistry-USA*, 42, 1995 - 2001.
12. Teller, D. C., Okada, T., Behnke, C. A., Palczewski, K., and Stenkamp, R. E. (2001). Advances in determination of a high-resolution three-dimensional structure of rhodopsin, a model of G-protein-coupled receptors (GPCRs). *Biochemistry-USA*, 40, 7761 - 7772.
13. Madabushi, S., Gross, A. K., Philippi, A., Meng, E. C., Wensel, T. G., and Lichtarge, O. (2004). Evolutionary trace of G protein-coupled receptors reveals clusters of residues that determine global and class-specific functions. *J. Biol. Chem.*, 279, 8126 - 8132.
14. Dryja, T. P., Hahn, L. B., Cowley, G. S., McGee, T. L., and Berson, E. L. (1991). Mutation spectrum of the rhodopsin gene among patients with autosomal dominant retinitis pigmentosa. *Proc. Nat. Acad. Sci. USA*, 88, 9370 - 9374.
15. Sung, C.-H., Davenport, C. M., Hennessey, J. C., Maumenee, I. H., Jacobson, S. G., Heckenlively, J. R., Nowakowski, R., Fishman, G. A., Gouras, P., and Nathans, J. (1991). Rhodopsin mutations in autosomal dominant retinitis-pigmentosa. *Proc. Nat. Acad. Sci. USA*, 88, 6481 - 6485.
16. Rao, V. R., Cohen, G. B., and Oprian, D. D. (1994). Rhodopsin mutation G90D and a molecular mechanism for congenital night blindness. *Nature*, 367, 639 - 642.
17. Okada, T., Ernst, O. P., Palczewski, K., and Hofmann, K. P. (2001). Activation of rhodopsin: New insights from structural and biochemical studies. *Trends Biochem. Sci.*, 26, 318 - 324.

Samenvatting

Het signaaltransductie pad geïnitieerd door visuele pigmenten is gedurende de laatste 45 jaar uitgebreid bestudeerd en in deze periode hebben de visuele pigmenten zich ontwikkeld tot een modelsysteem voor de familie van G-eiwit gekoppelde receptoren. Deze familie omvat receptoren die betrokken zijn bij alle belangrijke signaal transductie processen in het menselijk lichaam en vertegenwoordigen een belangrijke doelgroep voor farmacologische interventie. Inmiddels zijn veel details bekend geworden van celbiologische aspecten van dit signaal transductiepad maar over de structurele principes achter de signaal transductie door de receptoren is nog weinig bekend. De recente publicatie van de eerste kristal structuur van runder rhodopsine heeft de positie van rhodopsine als model voor de familie van G-eiwit gekoppelde receptoren verder versterkt en de eerste inzichten op atomair niveau verschaft in structuur en activatie mechanismen van rhodopsine en G-eiwit gekoppelde receptoren in het algemeen.

Hoofdstuk 1 beschrijft de belangrijkste eigenschappen van rhodopsine. Het is een membraaneiwit bestaande uit zeven transmembraan segmenten, dat posttranslationele modificatie ondergaat (disulfide brug, palmitoylering, glycosylering) en vervolgens naar het buitensegment van het staafje wordt getransporteerd om zijn cellulaire functie uit te oefenen. Rhodopsine is een uniek lid van de familie van G-eiwit gekoppelde receptoren omdat zijn ligand, 11-*cis* retinal, covalent gebonden is aan het eiwit, opsine. Het proces van het zien begint met de absorptie van lichtenergie waardoor er *cis/trans* isomerisatie van de ligand plaatsvindt waarna het geactiveerde rhodopsine via een aantal conformationele veranderingen (Rhodopsine (Rho) → Bathorhodopsine (Batho) ↔ Blue-shifted intermediate (BSI) → Lumirhodopsine (Lumi) → Metarhodopsine I (Meta I) ↔ Metharhodopsine II (Meta II) → Metarhodopsine III (Meta III)) binnen een tijdsbestek van milliseconden de actieve vorm (Metarhodopsine II) aanneemt die het G-eiwit transducine bindt en activeert.

De kristalstructuur van rhodopsine in de grondtoestand (resolutie 2.6 Å) geeft gedetailleerde informatie over de driedimensionale structuur. Het rhodopsine kan worden onderverdeeld in drie verschillende domeinen: 1) het transmembraandomein bestaande uit helix I – VII waarbinnen het 11-*cis* retinal zich bevindt, 2) het extracellulaire domein en 3) het intracellulaire domein waar de interactie met het G-eiwit transducine plaatsvindt. Resultaten van voorgaande experimenten duiden er op dat het tweede transmembraansegment (TM II of Helix II) van rhodopsine een structurele verandering ondergaat tijdens de fotoactivatie [1-5]. Helix II loopt van residu 71 tot 100 en vertoont een knik ter hoogte van Gly89 en Gly90 waardoor Gly90 in de buurt van Glu113 komt, het residu dat een interactie aangaat met de geprotoneerde Schiffse base. Helix II staat in verbinding met andere helices via hydrofobe en H-brug interacties waarmee de grondtoestand van rhodopsine wordt gestabiliseerd. Ondanks onze gedetailleerde kennis van de driedimensionale structuur van rhodopsine kan de rol van de individuele eiwitresiduen in de fotoactivatie van rhodopsine niet afgeleid worden van dit structurele model, aangezien de kristalstructuur verkregen is in de grondtoestand en het zeer moeilijk is om dit te extrapoleren naar de geactiveerde toestand. Wij hebben er voor gekozen om de structurele en functionele rol van individuele residuen in de fotoactivatie van rhodopsine te bestuderen met behulp van cysteine-scanning mutagenese in combinatie met Fourier transform-infrarood (FT-IR) verschilspectroscopie. Cysteïne scanning mutagenese is een techniek waarbij cysteïnes worden gebruikt als reporter groep om de structurele en functionele eigenschappen van

een eiwit te bestuderen. Individuele aminozuren worden vervangen door een uniek cysteïne residu en geanalyseerd door middel van FT-IR verschillingspectroscopie. Dit is een zeer gevoelige techniek die kleine structurele veranderingen direct aan de -SH groep van het cysteïne residu kan meten zonder dat extra modificaties nodig zijn. De -SH groep van cysteïne is erg gevoelig voor veranderingen in lokale structuur, polariteit en corresponderende veranderingen in vibratie frequentie kunnen worden gedetecteerd in een geïsoleerd gebied van het FT-IR verschillingspectrum waar er geen verstoring optreedt door andere biomembraan componenten.

Het is aangetoond dat Asp83, gelegen in het tweede transmembraandomein van rhodopsine, actief is tijdens de vorming van Meta II en een verandering ondergaat in H-brug interactie (2,3,5). Ons eerste doel was derhalve om met behulp van cysteïne-scanning mutagenese in combinatie met FT-IR verschillingspectroscopie de structurele en functionele rol te bestuderen van residuen die gelegen zijn in het tweede transmembraandomein van rhodopsine. In **Hoofdstuk 2** wordt de bijdrage van Asp83 aan de structuur en functie van rhodopsine in meer detail bestudeerd met behulp van de mutanten D83N en D83C. De mutatie D83C was gekozen om de mogelijkheden van een combinatie van cysteïne scanning met FT-IR verschillingspectroscopie te testen. FT-IR verschillingspectra laten zien dat deze Asp83-mutaties geen “long-range” structuur veranderingen veroorzaken. De absorptie spectra van D83C en D83N vertonen een kleine blauw-verschuiving ten opzichte van wild-type rhodopsine die kleiner is in D83C dan in D83N, daarmee aantonend dat substitutie van Asp83 door cysteïne zeer beperkte structurele en elektronische verstoring van de chromofoor veroorzaakt. Vergelijking van de fotochemische eigenschappen van de mutanten duidt er op dat Asp83 participeert in een netwerk van H-bruggen dat bijdraagt aan golflengte regulatie en de pKa van het Meta I ↔ Meta II evenwicht. Onze conclusie is dat hiervoor de proton donerende capaciteit van de carboxyl groep van asparaginezuur 83 een belangrijke aanvulling vormt op zijn H-brug vormende capaciteit. Aangezien FT-IR verschillingspectroscopie laat zien dat de carboxyl groep van Asp83 reageert op lokale veranderingen bij Meta II vorming, zouden we verwachten dat deze veranderingen ook zichtbaar zijn in de -SH vibratie van D83C. Mutant D83C laat inderdaad een significante toename zien in de -SH piek, daarmee aantonend dat de -SH piek gebruikt kan worden als een zeer gevoelige reporter groep voor de analyse van lokale structurele veranderingen door middel van FT-IR verschillingspectroscopie.

Deze cysteïne piek werd echter waargenomen op een achtergrond van natieve cysteïnes. Om een hoge achtergrond door natieve cysteïnes in het geïntroduceerde signaal en mogelijke wederzijdse interacties van geïntroduceerde cysteïnes met natieve cysteïne residuen te voorkomen, wordt in **Hoofdstuk 3** de constructie van een basismutant beschreven waarin alle mogelijkerwijs reactieve cysteïnes zijn vervangen. Gestart is met het SOH ΔC construct waarin alle potentieel reactieve cysteïnes zijn vervangen door een serine, uitgezonderd cysteïne 110 en 187 die de disulfide brug vormen. Helaas produceerde deze SOH ΔC mutant beduidend minder functioneel eiwit dan wild-type rhodopsine. Geprobeerd is om de hoeveelheid functionele basismutant te verhogen door alternatieve cysteïne-substituties. Gezien eerdere ervaringen met enkelvoudige mutaties van Cys167 en Cys264 naar een serine op een wild-type achtergrond, die duiden op lagere hoeveelheden functioneel eiwit met een verminderde stabiliteit, is getest of substitutie van Cys167 en Cys264 door alanine of methionine een basismutant met betere functionele expressie verkregen kon worden. Echter, de productie niveaus van functioneel eiwit lagen zelfs lager dan die van SOHΔC. Daarom is SOHΔC verder onderzocht op geschiktheid als basismutant. Hieruit bleek dat deze mutant gezuiverd

kon worden met een redelijke opbrengst, geen noemenswaardige vrije –SH activiteit liet zien en, op basis van FI-IR analyse, met wild-type vergelijkbare functionele activiteit behield. Op grond van deze resultaten is SOH Δ C geselecteerd als basismutant voor de cysteïne scanning mutagenese studies.

Aangezien een cysteïne-vrije basismutant was ontwikkeld (hoofdstuk 3) en een methode beschikbaar was om non-invasief lokale structurele veranderingen te bestuderen (hoofdstuk 2) wordt in **Hoofdstuk 4** de toepassing hiervan beschreven in onderzoek naar de rol van de residuen in het tweede transmembraandomein van rhodopsine in de fotoactivatie, gebruik makend van cysteïne scanning mutagenese gecombineerd met FT-IR verschillenspectroscopie. Hierbij kwam het grote probleem naar boven dat de meerderheid van de enkelvoudige rhodopsine mutanten gebaseerd op SOH Δ C nauwelijks of geen functioneel eiwit genereerde. Het geproduceerde recombinante eiwit was nauwelijks geglycosyleerd en werd intracellulair vastgehouden, hetgeen duidt op vouwings- en/of transport defecten. Enkelvoudige substitutie, op een wild-type achtergrond, van Cys167 en Cys264, beide structureel actief tijdens de fotoactivatie, leidt al tot een verminderde hoeveelheid correct gevouwen eiwit en dit werd in de meeste gevallen verergerd door de additionele mutatie. Opmerkelijk was dat sommige mutaties juist de corresponderende mutant gedeeltelijk beschermden tegen onjuiste vouwing. Dit is een zeer intrigerend fenomeen. Residuen die een belangrijke rol spelen in eiwit structuur en/of functie zijn in het algemeen door de evolutie heen goed geconserveerd. De natieve residuen van de “beschermende” mutaties L77C, F85C, F88C en G89C zijn in maximaal 30% van de familie van G-eiwit gekoppelde receptoren geconserveerd, een aanwijzing dat deze residuen waarschijnlijk niet van groot belang zijn voor de stabiliteit van rhodopsine en dat substitutie van deze residuen daarom mogelijk geen negatieve effecten laat zien. Een verhoogde stabiliteit van de mutant zou de kans kunnen vergroten dat na translatie het eiwit correct wordt gevouwen. Hoewel de thermische stabiliteit van deze mutanten nog niet kon worden bepaald, zou de hogere opbrengst van SOH Δ C/L77C na zuivering door middel van IMAC (immobilized metal affinity chromatography) er op kunnen wijzen dat deze mutant stabiel is dan de basismutant. Het lijkt echter niet waarschijnlijk dat de enkelvoudige substituties zoals hierboven genoemd een belangrijk verschil in stabiliteit zouden kunnen leveren. Andere factoren, zoals chaperone-gemedieerde processen, zullen waarschijnlijk een grotere rol spelen. Tot nog toe zijn alleen basismutant SOH Δ C en mutant SOH Δ C/L77C geanalyseerd op een aantal structurele en functionele eigenschappen door middel van UV-VIS spectroscopie, FT-IR verschillenspectroscopie en de G-eiwit activerings bepaling. Hieruit blijkt dat residu Leu77 niet betrokken is bij structurele of katalytische veranderingen die ten grondslag liggen aan rhodopsine activatie. Daarbij komt dat volgens de kristalstructuur residu Leu77 is gelocaliseerd in de lipide matrix, hetgeen het plausibel maakt dat dit residu niet deelneemt aan de fotoactivatie van rhodopsine.

Aangezien de meeste SOH Δ C-mutanten zeer lage hoeveelheden functioneel eiwit produceerden is naar een alternatieve benadering gezocht. In Hoofdstuk 2 van dit proefschrift werd aangetoond dat een verandering in vibratie-eigenschappen van een enkele cysteïne –SH groep gemeten kan worden op een achtergrond van natieve cysteïnes. Niettemin is er een reëel risico op interferentie met het geïntroduceerde signaal door de hoge achtergrond van natieve cysteïnes. Gezien de beschikbare gegevens leek het desondanks verantwoord cysteïne scanning mutagenese uit te voeren op een wild-type achtergrond.

De eerste resultaten van deze benadering zijn beschreven in **Hoofdstuk 5**. De meeste op wild-type rhodopsine gebaseerde mutanten produceerden hoeveelheden eiwit gelijk aan die van wild-type rhodopsine en eveneens vergelijkbare niveaus van glycosylering. Alle mutanten produceerden voldoende hoeveelheden functioneel eiwit om zuivering door middel van IMAC en verdere analyse mogelijk te maken. Door technische problemen konden de meeste mutanten echter niet in voldoende grote hoeveelheid geproduceerd worden om alle geplande studies uit te voeren. Tot nu toe konden de mutanten L76C, L79C, V81C, D83C, F85C, F88C, G89C en G90C op zijn minst gedeeltelijk worden geanalyseerd. Asp83 is al uitgebreid besproken in Hoofdstuk 2 waar werd aangetoond dat dit residu geen directe rol speelt in de signaal transductie van rhodopsine maar een bijdrage levert aan de structuur en de fotochemie door interactie met op H-bridgen gebaseerde netwerken. Onze gegevens tot nu toe wijzen niet op een belangrijke rol voor residuen Leu76, Val81 en Phe85 in fotoactivering en signaaltransductie van rhodopsine. De mutanten F88C, G89C en G90C vertonen een vertraagde G-eiwit activatie. De laatste drie mutanten lijken niettemin een wild-type-achtige fotocascade te vertonen, hoewel de kinetiek nog niet eenduidig kon worden vastgesteld. Tevens duiden de resultaten er tot nog toe op dat voor alle mutanten de pKa van de Meta I → Meta II overgang niet veel verschilt van die van wild-type rhodopsine. De fotochemische eigenschappen van rhodopsine lijken daarom door deze enkelvoudige mutaties niet significant te zijn veranderd. Het Meta II FT-IR verschilspectrum van F88C en G89C vertoont wel een gereduceerd piekoppervlak van de –SH vibratie, hetgeen suggereert dat deze mutaties ofwel een indirect negatief effect hebben op de wild-type –SH activiteit of dat directe participatie van de extra cysteïne zichzelf weerspiegelt in een negatieve piek in het verschilspectrum en dus wordt waargenomen als een afname van het wild-type –SH piek oppervlak. Dit rechtvaardigt mijns inziens de conclusie dat de residuen Phe88, Gly89 en Gly90 direct bijdragen aan de vorming van Meta II en receptoractivatie, wat een verklaring zou kunnen zijn voor de lagere activiteit na substitutie van deze residuen door cysteïne. Na fotoactivatie treden er vectoriële conformatie veranderingen op die er in resulteren dat Helix II zich verwijderd van de cytoplasmatische lus IV en dichter naar helix IV toe beweegt. Dit wordt mogelijk vergemakkelijkt door aanpassingen in de eiwitketen via een rotatie rond het Gly89/Gly90 paar [6] en het is te verwachten dat substitutie van een van deze residuen door een cysteïne zijketen de kinetiek van de roterende uitwaartse beweging zal beïnvloeden. Helaas is, behalve voor de D83C mutant die een aanzienlijke toename in –SH piekoppervlakte laat zien, het –SH gebied van het FT-IR verschilspectrum van deze mutanten lastig te interpreteren. Dit wordt deels veroorzaakt door een relatief hoge ruis die gereduceerd zal kunnen worden door een behoorlijke set van onafhankelijke experimenten te middelen. Zelfs dan zal de aanwezigheid van de achtergrond van native cysteïnes de interpretatie van de –SH vibratie data ernstig bemoeilijken. Onze conclusie is dat effectieve cysteïne scanning mutagenese het beste uitgevoerd kan worden op een achtergrond die vrij is van endogene cysteïne activiteit. Om dit te bereiken zal onderzocht moeten worden hoe de productie van functioneel cysteïne-vrij rhodopsine verbeterd kan worden.

Een correcte eiwitvouwing is noodzakelijk voor rhodopsine om correct te kunnen functioneren. Gedurende mijn onderzoek naar de bijdrage van membraan-gelocaliseerde residuen aan structuur en functie van rhodopsine bleek uit klinisch-genetische studies dat enkelvoudige mutaties in cysteïne residuen in het membraan-domein van rhodopsine te koppelen waren aan de autosomaal dominante ziekte retinitis pigmentosa (ADRP). In **Hoofdstuk 6** hebben we het biochemisch fenotype bestudeerd van drie cysteïne

residuen die gelegen zijn in het membraan domein (C167R, C222R en C264del) en die betrokken zijn bij ADRP. ADRP kan onderverdeeld worden in twee klinische subtypes: type 1 en 2. Type 1 heeft een wat ernstiger fenotype en wordt gekarakteriseerd door manifestatie al op jonge leeftijd, diffuse localisatie, en/of een snelle progressie. Type 2 wordt gekarakteriseerd door een meer regionaal voorkomen, en/of langzame progressie. Biochemisch gezien zijn de mutaties geïnclassificeerd in drie klassen gebaseerd op heterologe expressie: klasse I mutanten lijken op wild-type met betrekking tot vouwing, gericht transport naar de celmembraan en vorming van een lichtgevoelig pigment na toevoeging van 11-*cis* retinal; klasse IIa mutanten genereren het complete eiwit, maar vouwen niet goed, worden vastgehouden in het endoplasmatisch reticulum en vormen geen lichtgevoelig pigment; klasse IIb mutanten laten minder ernstige vouwingsdefecten zien dan IIa en produceren variabele hoeveelheden correct gevouwen eiwit dat in staat is om een functioneel fotopigment te vormen. De corresponderende C → S mutaties van residu Cys167, Cys222 en Cys264 werden geconstrueerd als controle en blijken volledig functioneel, wild-type-achtig eiwit te genereren, daarmee aantonend dat mutatie van deze residuen op zichzelf niet leidt tot een ADRP-fenotype. Onze resultaten duiden er op dat de ADRP-mutaties C167R, C222R en C264del representatief zijn voor biochemisch drie verschillende fenotypes. C222R wordt geïnclassificeerd als klasse I: het lijkt in elk getest aspect op wild-type rhodopsine. De eigenschappen, die aanleiding geven tot retinitis pigmentosa komen blijkbaar niet tot expressie in een niet-natieve omgeving.

C167R wordt geïnclassificeerd als klasse IIa in overeenstemming met resultaten reeds eerder beschreven in een ander expressie systeem. Mutant C264del vertegenwoordigt een nieuwe biochemische klasse die klasse III is gedoopt en wordt gekenmerkt door klasse II-eigenschappen (geen vorming van functioneel pigment en geen transport naar de plasma membraan), maar bovendien wordt geen compleet eiwit gegenereerd. In het algemeen leiden ADRP-gecorrleerde mutaties in rhodopsine tot een verscheidenheid aan klinische beelden met variërende ernst van ADRP. Mutaties die eenzelfde biochemische classificatie dragen leiden niet noodzakelijkerwijs tot hetzelfde klinische ADRP-fenotype. Het is daarom nog niet mogelijk om alleen op basis van biochemische data verkregen met recombinante eiwitten de ernst van de ziekte te voorspellen. Deze resultaten duiden op een soortgelijk fenomeen als hetgeen is waargenomen in mijn cysteine-scanning studies: subtiele mutaties in rhodopsine kunnen verstrekende gevolgen hebben voor het vermogen om functioneel recombinant eiwit te genereren. De huidige gegevens zijn nog steeds zeer onvolledig en het inzicht in de mechanismen van membraaneiwit vouwing is nog steeds zeer beperkt, waardoor zelfs een voorlopige interpretatie van deze verschijnselen nog ondoenlijk is.

References

1. Palczewski, K., Kumasaka, T., Hori, T., Behnke, C. A., Motoshima, H., Fox, B. A., LeTrong, I., Teller, D. C., Okada, T., Stenkamp, R. E., Yamamoto, M., and Miyano, M. (2000). Crystal structure of rhodopsin: A G protein-coupled receptor. *Science*, 289, 739 - 745.
2. Fahmy, K., Jäger, F., Beck, M., Zvyaga, T. A., Sakmar, T. P., and Siebert, F. (1993). Protonation states of membrane-embedded carboxylic acid groups in rhodopsin and metarhodopsin II: A Fourier-transform infrared spectroscopy study of site-directed mutants. *Proc. Nat. Acad. Sci. USA*, 90, 10206 - 10210.
3. Rath, P., DeCaluwé, G. L. J., Bovee-Geurts, P. H. M., DeGrip, W. J., and Rothschild, K. J. (1993). Fourier transform infrared difference spectroscopy of rhodopsin mutants: Light activation of rhodopsin causes hydrogen-bonding changes in residue aspartic acid-83 during meta II formation. *Biochemistry-USA*, 32, 10277 - 10282.

Samenvatting

4. Okada, T., Fujiyoshi, Y., Silow, M., Navarro, J., Landau, E. M., and Shichida, Y. (2002). Functional role of internal water molecules in rhodopsin revealed by x-ray crystallography. *Proc. Nat. Acad. Sci. USA*, 99, 5982 - 5987.
5. Breikers, G., Bovee-Geurts, P. H. M., DeCaluwé, G. L. J., and DeGrip, W. J. (2001). A structural role for Asp83 in the photoactivation of rhodopsin. *Biol. Chem.*, 382, 1263 - 1270.
6. Altenbach, C. A., Klein-Seetharaman, J., Cai, K. W., Khorana, H. G., and Hubbell, W. L. (2001). Structure and function in rhodopsin: Mapping light-dependent changes in distance between residue 316 in helix 8 and residues in the sequence 60-75, covering the cytoplasmic end of helices TM1 and TM2 and their connection loop CL1. *Biochemistry-USA*, 40, 15493 - 15500.

List of abbreviations

3D	three dimensional
ADRP	autosomal dominant retinitis pigmentosa
arRP	autosomal recessive retinitis pigmentosa
Batho	Bathorhodopsin
BSA	bovine serum albumin
BSI	Blue-shifted intermediate
cGMP	cyclic GMP
CHAPS	3-[(3-Cholamidopropyl)dimethylammonio]-1-propanesulfonate
C-I	cytoplasmic loop I
C-II	cytoplasmic loop II
C-III	cytoplasmic loop III
C-IV	cytoplasmic loop IV
d.p.i.	days post infection
DOM	Dodecylmaltoside
E.R.	endoplasmic reticulum
EDTA	(ethylene-1,2-diamino)N-tetra-acetic acid
E-I	extracellular loop I
E-II	extracellular loop II
E-III	extracellular loop III
EPR	electron paramagnetic resonance
FCS	Fetal calf serum
FT-IR	Fourier Transform Infrared
G protein	GTP-binding protein
GARPO	Goat anti-Rabbit conjugated to PO
GPCR	G protein-coupled receptor
G _T	transducin
GTP _γ S	guanosine 5'-O-(3-thiotriphosphate)
his-tag	histidine tag
HOOP	hydrogen-out-of plane
IMAC	immobilized metal affinity chromatography
IRBP	interphotoreceptor retinoid-binding protein
LB	Luria-Bertani
LRAT	lecithin:retinol acyltransferase
Lumi	Lumirhodopsin
M.O.I	multiplicity of infection
Me ta I	Metarhodopsin I
Meta II	Metarhodopsin II
Meta III	Metarhodopsin III
NTA	Ni ²⁺ -nitrilotriacetic acid
PBS	Phosphate Buffered Saline
PDE	phosphodiesterase
RGR	retinal G protein-coupled receptor
ROS	rod outer segment
RP	retinitis pigmentosa
RPAP	Rabbit Polyclonal Anti-Porc Ig
SAR(-TRITC)	Swine anti-rabbit Ig (conjugated to rhodamine)

Abbreviations

SDSL	site-directed spin labeling
SDS-PAGE	SDS Polyacrylamide gel electrophoresis
Sf9	Spodoptera frugiperda cell line
-SH	cysteine sulfhydryl group
SOH Δ C	Synthetic Opsin His-tagged cysteine-free bovine opsin
SOH WT	Synthetic Opsin His-tagged bovine opsin
TE	Tris-EDTA
TM	transmembrane segment
wt	wild type
x1RP	X-linked retinitis pigmentosa

Table 1: One and three letter code abbreviations of amino acids

Amino acid	Three letter code	One letter code
Alanine	Ala	A
Arginine	Arg	R
Asparagine	Asn	N
Aspartic acid	Asp	D
Cysteine	Cys	C
Glutamine	Gln	Q
Glutamic acid	Glu	E
Glycine	Gly	G
Histidine	His	H
Isoleucine	Ile	I
Leucine	Leu	L
Lysine	Lys	K
Methionine	Met	M
Phenylalanine	Phe	F
Proline	Pro	P
Serine	Ser	S
Threonine	Thr	T
Tryptophane	Trp	W
Tyrosine	Tyr	Y
Valine	Val	V

Dankwoord

Na een lange weg komt dan nu toch de afronding van mijn proefschrift in zicht. Mijn vader noemde mijn afstudeerscriptie ooit mijn levenswerk. Wisten wij beiden toen veel....

Rest mij nog het bedanken van een aantal mensen. Want, cliché, cliché, promoveren doe je niet alleen. Allereerst natuurlijk mijn promotor prof. Wim de Grip en co-promotor dr. Giel Bosman. Wim, zelf gepromoveerd van co-promotor tot promotor kon je nu mij optimaal begeleiden bij mijn promotie. Jouw eeuwig optimisme en droge humor zorgden er voor dat ik de moed niet opgaf in moeilijke tijden. Op de meest vreemde dagen en tijdstippen maakte je tijd voor mijn proefschrift wat het mij mogelijk maakte om het schrijven van mijn proefschrift en het werken in Maastricht te combineren. Dankjewel voor je geduld met mij. Giel, ik kon altijd op je rekenen met “de celletjes” en achter de confocale was het altijd leerzaam en gezellig. Als “pet”-AIO ben ik meteen ook jouw eerste AIO als co-promotor, spannend voor ons allebei.

Jenny van Oostrum, ook op jou kon ik altijd rekenen met de celkweek en een peptalk als ik het niet meer zo zag zitten. Jenny bedankt, dankzij jou en Giel kon ik in de weekenden gewoon naar huis.

Petra Bovee, onze steun en toeverlaat. Ik ben jou veel dank verschuldigd voor de vele experimenten die jij hebt gedaan en altijd kon ik met mijn vragen bij jou terecht. Bedankt Petra, zonder jou was menige figuur nog blanco.

Arthur Pistorius, jij brengt infrarood tot leven. Zwitserland is ons beider passie, met zijn pieken en dalen (zou het hem daar in zitten?).

Corné Klaassen, jij hebt mij wegwijs gemaakt in het cloneer- en baculoviruswerk. Ik denk dat de meeste beginnende AIO's het zonder zo'n uitgebreide introductie moeten doen. Dankzij jouw basis heb ik menige mutant kunnen maken.

Jannie Janssen, bedankt voor je zorgen als collega-aio toen ik net als groentje binnenkwam. Jij maakt jouw promotietraject vele malen ingewikkelder dan het mijne. Houd vol, jij bent gewoon de volgende!

Micha Ummels en Heidi Willems wil ik bedanken voor hun ondersteunende werkzaamheden. Jullie hebben me een boel geclo(oi)neer uit handen genomen.

Maikel Giesbers, naast aio ook onze computer vraagbaak. Met de kegeltjes heb jij een nog zwaardere klus dan ik met mijn mutanten. Hopelijk lukt het ook jou om een mooi boekje bij elkaar te pipetteren.

En uiteraard wil ik stagiair Zan Peeters bedanken voor zijn bijdrage en voor zijn gezellige tijd op het mini-labje in het Trigon samen met Prasad. Ik wist niet dat mannen zo konden kletsen.

Verder wil ik de collega's van Oogheelkunde bedanken voor de gezellige tijd. Dank voor jullie bijdragen tijdens onze gezamenlijke werkbesprekingen en het introduceren van de thee- c.q. fruitpauze.

Pap en mam, dankzij jullie ben ik kunnen gaan studeren. Jullie hebben me altijd gestimuleerd om er uit te halen wat er in zit en me altijd vrijgelaten en gesteund in mijn keuzes. Dankjewel dat jullie er altijd voor me waren en zijn, ook al hadden jullie vaak misschien geen idee waar ik nou precies mee bezig was.

Last but not least, mien Frenske. Jouw geduld is misschien nog wel het meest op de proef gesteld. Gelukkig heb je altijd in mij geloofd, zodat we dan nu eindelijk een turbulente periode met een mooi feestje kunnen afsluiten.

Publications

Breikers, G., van Breda, S.G.J., Bouwman, F.G., van Herwijnen, M.H.M., Renes, J.W., Mariman, E.C.M., Kleinjans, J. and van Delft, J.H.M. Potential protein markers for nutritional health effects on colon cancer in the mouse as revealed by proteomics analysis. In preparation.

Breikers G., Bovee-Geurts P.H., Van Oostrum J., Bosman, G.J.C.G.M., De Grip W.J. (2003). Importance of residue L77 in the structure and function of rhodopsin. In preparation.

Bosman, G.J.C.M., Van Oostrum, J., Breikers, G., Bovee-Geurts, P.H., Klaassen, C.H.W., De Grip, W.J. (2003). Functional expression of his-tagged rhodopsin in Sf9 insect cells. *Methods Mol. Biol.*, 228, 73-86.

Breikers G., Portier-Van de Luytgaarden M., Bovee-Geurts P., De Grip W. (2002). Retinitis pigmentosa-associated rhodopsin mutations in three membrane-located cysteine residues present three different biochemical phenotypes. *Biochem. Biophys. Res. Commun.*, 297, 847-853.

Breikers G., Bovee-Geurts P.H., De Caluwe G.L., De Grip W.J. (2001). A structural role for Asp83 in the photoactivation of rhodopsin. *Biol. Chem.*, 382, 1263-1270.

den Dekker E., Molin D.G., Breikers G., van Oerle R., Akkerman J.W., van Eys G.J., Heemskerk J.W.. Expression of transient receptor potential mRNA isoforms and Ca(2+) influx in differentiating human stem cells and platelets (2001). *Biochim. Biophys. Acta*, 1539, 243-255.

Heemskerk J.W., Siljander P., Vuist W.M., Breikers G., Reutelingsperger C.P., Barnes M.J., Knight C.G., Lassila R., Farndale R.W. (1999). Function of glycoprotein VI and integrin alpha2beta1 in the procoagulant response of single, collagen-adherent platelets. *Thromb. Haemost.*, 1999, 81, 782-792.

Curriculum vitae

Githa Breikers werd geboren op 9 november 1972 te Geleen. Aan de R.K.S.G. Serviam te Sittard werd in 1992 het Gymnasium diploma behaald waarna zij in hetzelfde jaar begon met de studie Gezondheidswetenschappen aan de Universiteit van Maastricht met als afstudeerrichting Biologische Gezondheidskunde. Haar afstudeerstage werd uitgevoerd bij de vakgroepen Biochemie en Moleculaire Celbiologie van de Universiteit van Maastricht, een tweede stage werd gelopen bij de vakgroep Pathologie van het Academisch Ziekenhuis Maastricht. Het doctoraaldiploma werd behaald in augustus 1997.

Van januari 1998 tot oktober 2002 werkte zij onder leiding van Prof. W.J. de Grip als Onderzoeker in Opleiding aan de Radboud Universiteit Nijmegen op de afdeling Biochemie van de Faculteit der Medische wetenschappen aan een door N.W.O. gefinancierd project dat is beschreven in dit proefschrift. Tijdens deze periode heeft zij geassisteerd bij verscheidene practica voor studenten Geneeskunde en heeft zij een tweetal studenten begeleid tijdens hun stages.

Van 16 april 2003 tot 13 oktober 2004 heeft zij als Universitair docent gewerkt bij de vakgroep Gezondheidsrisico-analyse en Toxicologie van de Universiteit Maastricht waar zij, naast het geven van onderwijs, onderzoek deed met behulp van Proteomics naar het beschermend effect van een groentedieet op dikke darm kanker bij muizen.